Title: As-Run Thermal Analysis of the AGC-3 Experiment

ECAR No.: 3386 Rev. No.: 0 Project No.: 23747 Date: 10/11/2016

	Name	Organization	Signature	Date
Performer:	P. E. Murray	C130		
Checker[1]:	G. L. Hawkes	C130		
Independent Peer Reviewer[2]:	Not Required			
CUI Reviewer:	M. E. Davenport	C020		
Manager[3]:	M. A. Lillo	C130		
Owner[4]:	M. E. Davenport	C020		
ART Technical Development[4]:	W. E. Windes	B120		
Nuclear Safety[4]:	Not Required			
ATR Experiment Engineering Manager[3]:	Not Required			

1. Confirmation of completeness, mathematical accuracy, and correctness of data and appropriateness of assumptions.
2. Concurrence of method or approach. See definition, LWP-10106.
3. Concurrence of procedure compliance. Concurrence with method/approach and conclusion.
4. Concurrence with the document's assumptions and input information. See definition of Acceptance, LWP-10200.

REVISION LOG

Rev.	Date	Affected Pages	Revision Description
0	10/11/2016	All	Initial issue.

Title: As-Run Thermal Analysis of the AGC-3 Experiment

ECAR No.: 3386 Rev. No.: 0 Project No.: 23747 Date: 10/11/2016

1. Quality Level (QL) No.	2	**Professional Engineer's Stamp** N/A See LWP-10010 for requirements.
2. QL Determination No.	RTC-000486	
3. Engineering Job (EJ) No.	N/A	
4. eCR No.	N/A	
5. SSC ID	AGC-3 Experiment	
6. Building	TRA-670	
7. Site Area	ATR Complex	

8. Objective/Purpose:

The third Advanced Graphite Creep (AGC-3) experiment was designed to irradiate various types of graphite specimens at a temperature of 900°C. The specimens were irradiated in an instrumented leadout capsule experiment in the east flux trap of the ATR during cycles 152B, 154B, 155A, and 155B. Temperature was monitored using twelve thermocouples located at various elevations in the reactor core, and a helium-argon gas mixture was used for gas gap temperature control of the specimens.

The purpose of this analysis is to calculate specimen temperature using measured data on reactor power and helium-argon gas flows, and as-run calculations of heating rates and displacement per atom (DPA) in graphite. The accuracy of the model is assessed by comparing measured and calculated thermocouple temperatures. Uncertainty in gas gaps may preclude an accurate temperature calculation. In these cases, adjustments are made to the thermal model in order to reconcile the measured and calculated thermocouple temperature and to ensure the accuracy of the calculated specimen temperature.

9. Conclusions/Recommendations:

A finite element, steady-state heat transfer analysis of the entire AGC-3 test train was performed using ABAQUS. The analysis was performed at three selected days during each cycle, using the measured east source power, measured gas flows, as-run heating rates, and as-run graphite DPA, to obtain best-estimate temperatures of the specimens and thermocouples. The accuracy of the model was assessed by comparing the measured and calculated thermocouple temperatures. The difference between these temperature values was used to estimate the mean and standard deviation of the error. Setting the uncertainty equal to the mean ± two standard deviations corresponding to a 95% confidence interval, the results indicate that the maximum uncertainty in the calculated thermocouple temperature is ±50°C.

The temperature of each creep specimen is desired to be maintained at 900°C ±50°C. However, the results of this analysis show that the temperature of the specimen stacks is outside the desired range at the top of the test train where the temperature is less than the desired temperature due to lower gamma heating at this location. In most cases, the temperature of the center specimen stack is approximately 900°C ±50°C while the temperature of the peripheral specimen stacks is approximately 850°C ±50°C. Moreover, specimen temperature varies with elevation because of the uncertainty in the variable gas gaps used to compensate for the axial heating profile.

CONTENTS

FIGURES

SCOPE OF ANALYSIS AND BRIEF DESCRIPTION

The third Advanced Graphite Creep (AGC-3) experiment was designed to irradiate various types of graphite specimens at a temperature of 900°C. The specimens were irradiated in an instrumented leadout capsule experiment in the east flux trap of the ATR during cycles 152B, 154B, 155A, and 155B. Temperature was monitored using thermocouples, and a helium-argon gas mixture was used for gas gap temperature control of the specimens. A pneumatic piston was used to apply a maximum compressive load of 3000 psi to approximately half the specimens, resulting in corresponding pairs of stressed and unstressed specimens. The dimensional changes of corresponding specimen pairs will be used to determine irradiation-induced creep by distinguishing the separate effects of shrinkage occurring in all specimens and creep occurring in the stressed specimens only.

The purpose of this analysis is to calculate specimen temperature using measured data on reactor power and helium-argon gas flows, and as-run calculations of heating rates and displacement per atom (DPA) in graphite. The AGC-3 experiment contains twelve thermocouples located at various elevations in the reactor core. The accuracy of the model is assessed by comparing measured and calculated thermocouple temperatures. Uncertainty in gas gaps may preclude an accurate temperature calculation. In these cases, adjustments are made to the thermal model in order to reconcile the measured and calculated thermocouple temperature and to ensure the accuracy of the calculated specimen temperature.

DESIGN OR TECHNICAL PARAMETER INPUTS AND SOURCES

The technical and functional requirements for the AGC-3 experiment are given in TFR-791. The quality level of the analysis is “2” (important to safety) per quality level determination RTC-000486.

EXPERIMENT DESCRIPTION AND OTHER BACKGROUND DATA

The AGC-3 experiment is the third in a series of irradiation experiments to obtain data on fine-grained isotropic graphite used in the next generation very high temperature reactor (VHTR). The test train consists of seven stacks of cylindrical graphite specimens 0.5 inches in diameter contained in a graphite holder. The center stack contains unstressed specimens, while the peripheral stacks contain stressed specimens above core mid-plane and unstressed specimens below core mid-plane. The holder is contained in a stainless steel capsule, with a stainless steel heat shield placed between them. The holder has a stepped outside diameter to provide an axially varying temperature control gas gap to compensate for the axial variation in heating. The test train is divided into five temperature control gas zones containing separate helium-argon gas mixtures used for gas gap temperature control of the specimens. All specimens are desired to be irradiated at the same temperature, while corresponding stressed and unstressed specimens are desired to be irradiated to the same DPA. Other capsule internal components include tungsten heaters at the top and bottom of the test train, and a ceramic insulator at the top of the test train. Thermocouples and gas tubing are located in holes and grooves in the holder. Design details are from the drawings listed at the end of this document.

The thermal analysis was performed using a detailed finite element model of the experiment. Data on material properties are obtained from the handbooks and databases listed in the references. Results are given in Appendix A.1. The gas gaps between capsule components, accounting for the change in diameter of the capsule components due to thermal expansion and the change in diameter of graphite due to irradiation-induced shrinkage, are calculated in Appendix A.2. The resulting heat transfer coefficients for the fluence-dependent "hot" gas gaps are computed using various helium-argon gas mixtures and various values of DPA. Results are given in Appendix A.3.

The thermal conductivity of graphite depends on temperature and neutron fluence. Experimental data for NBG-25, IG-110, and H-451 is shown in Fig. 1, along with the temperature and DPA-dependent profiles assumed in this analysis. The calculated profiles show the correct trends observed in irradiated graphite: increasing conductivity with increasing temperature due to annealing of defects, and decreasing conductivity with increasing fluence due to generation of defects. The calculated profiles are the same as those used in previous as-run analyses of AGC experiments (ECAR-2562, ECAR-2322), and are consistent with the data reported in Vreeling, Wouters, and van der Lann, 2008, Maruyama and Harayama, 1992, and Price, 1975.

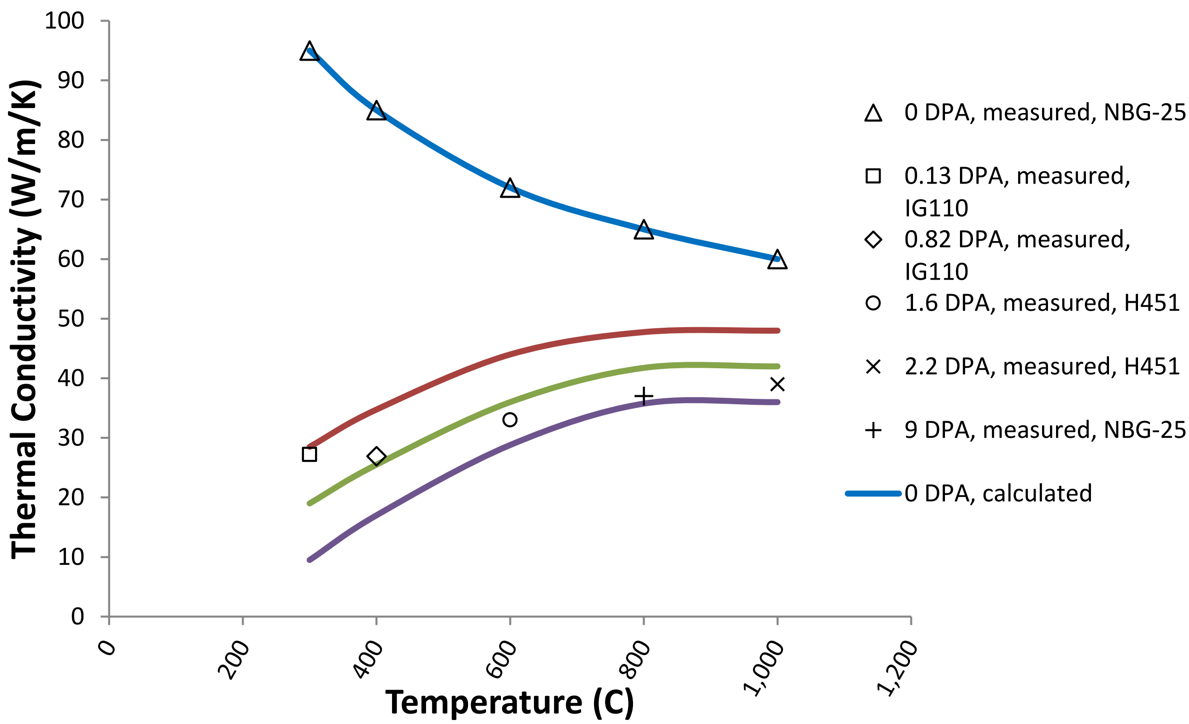

Figure 1. Effect of temperature and DPA on thermal conductivity of graphite.

The size of the temperature control gas gap between the graphite holder and stainless steel heat shield depends on temperature and neutron fluence. The temperature dependence results from thermal expansion, and the fluence dependence results from irradiation-induced shrinkage of graphite. Experimental data for the change in diameter of graphite due to irradiation-induced shrinkage is shown in Fig. 2, along with a linear regression of the data which provides a relation between diameter change and DPA. The data was obtained from measurements of the dimensional change of NBG-25 specimens irradiated in the AGC-1 experiment (Windes, 2012). The graphite in the AGC-3 experiment was irradiated to a peak fast neutron (energy > 0.1 MeV) fluence of approximately 5.0×10^{21} neutrons/cm^2 which corresponds to a peak DPA of approximately 3.6 (ECAR-3051). At this neutron fluence, the diameter reduction is expected to be approximately 0.7%.

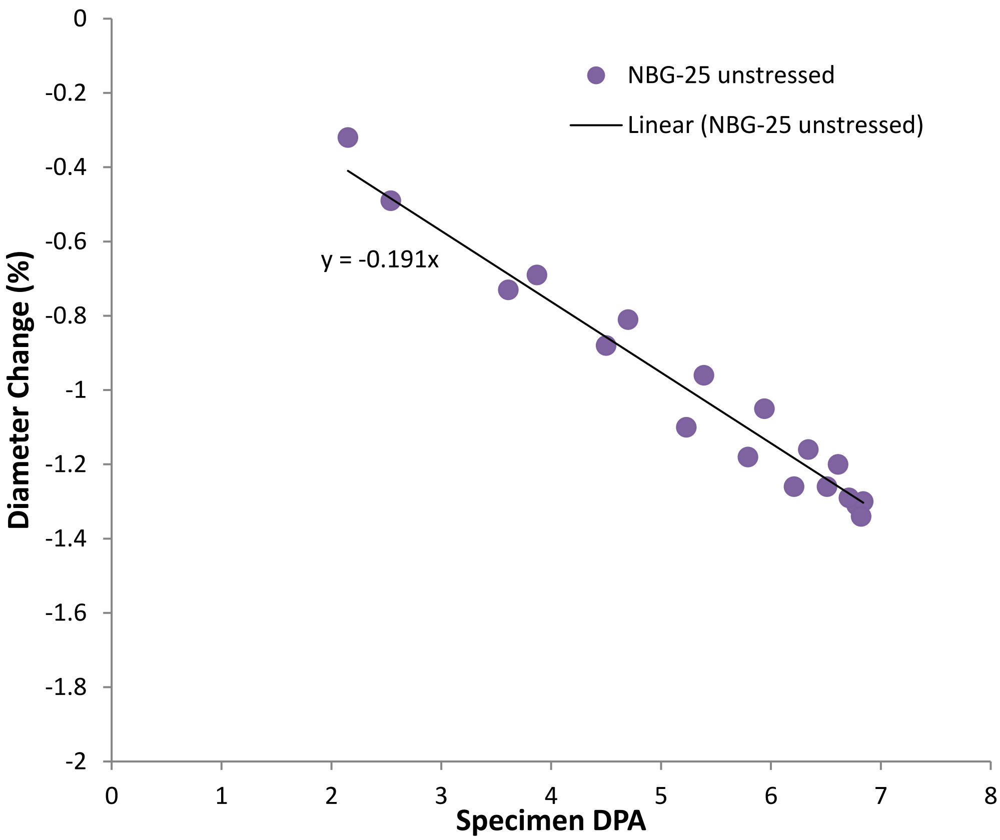

Figure 2. Effect of DPA on diameter of graphite specimens.

The flow of primary coolant in the annular gap between the capsule and chopped dummy in-pile tube is calculated for two-pump operation. Heat transfer coefficients for turbulent forced convection to the primary coolant were obtained from an experimental correlation using the film temperature method to account for fluid property variation. Details are given in Appendix A.4.

The heating rates of the experiment components in the east flux trap at 20.4 MW source power were obtained from the reactor physics analysis (ECAR-3051). Heating rates for each component in the test train were obtained as a function of position with respect to core mid-plane. For the capsule, heat shield, graphite holder and specimens, thermocouples, and primary coolant, a cosine-shaped profile was used to represent the axial variation in heating. The axial profile was split into separate profiles above and below core mid-plane, producing an unsymmetrical profile that preserves total core heating. The unsymmetrical heating profile improves temperature calculations as compared to using a symmetrical profile. Heating rates at a different power are obtained by linear scaling using the nominal operating heating rates provided in ECAR-3051 as a baseline. Details are given in Appendix A.5.

Reactor power, temperature control gas flows, and thermocouple temperatures are obtained from the Nuclear Data Management and Analysis System (NDMAS). Spreadsheets containing data recorded at 10 minute intervals were downloaded from the NDMAS website (https://htgr.inl.gov). Reactor power, temperature control gas flows, and thermocouple temperatures at selected days during each cycle are computed by averaging the data over the entire day. Peak DPA at those days was obtained from the as-run reactor physics analysis (ECAR-3051). The data from NDMAS is given in Appendix A.6.

ASSUMPTIONS

One significant uncertainty is the gap between the heat shield and capsule which can vary from the case where the dimples on the inside surface of the heat shield contact the holder to the case where the dimples on the outside surface of the heat shield contact the capsule. In this analysis, the location of the heat shield is calculated assuming the dimples on the outside surface of the heat shield contact the inside surface of the capsule, leading to a 0.10 inch gap between heat shield and capsule. The resulting temperature control gas gaps are calculated using the assumed location of the heat shield and accounting for thermal expansion and shrinkage of the capsule and holder.

The gas gap between the heat shield and capsule is adjusted to account for uncertainty in the exact location of the heat shield, the increased thermal conductance due to contact between the capsule and dimples on the heat shield, and the uncertainty in the control gas composition due to gas leakage around the rings separating adjacent gas zones. The variable gas gap between the heat shield and capsule was adjusted in order to bring into agreement the measured and calculated thermocouple temperatures. Moreover, the control gases in adjacent gas zones may mix since the seals are not gas-tight. In some cases, an argon-rich mixture in one zone was assumed to mix with a helium-rich mixture in an adjacent zone in order to bring into agreement the measured and calculated thermocouple temperatures. Details are given in Appendix A.6.

Another uncertainty is the gas gap between the graphite specimens and graphite holder which increases during irradiation due to graphite shrinkage. The bore diameter measurements of the irradiated holders showed a significant difference in the dimensional changes occurring in the lower and upper holders (INL/EXT-14-32060), suggesting that compressive loading of the lower holder had affected the measured dimensional change. Moreover, the position of the specimens in the bore channels of the graphite holder is not fixed and the diameter of the stressed specimens is also changing due to creep. These uncertainties preclude an accurate calculation of the gas gap between the specimens and holder. Therefore, the gas gap is set to its nominal design value of 0.010 inch and is assumed not to change during irradiation. A previous analysis of temperature uncertainty in the AGC experiments reported that the uncertainty in the gap between the specimens and holder will add approximately 12°C to the uncertainty in the temperature of the center specimen stack (ECAR-3017).

An additional uncertainty is the gas gap between the thermocouples and graphite holder which may vary due to the loose fit of the thermocouple inside the holder. The gas gap assumed in this analysis is based on the experiments reported in ECAR-2429, and is discussed in the as-run analyses of the AGC-1 and AGC-2 experiments (ECAR-2562, ECAR-2322).

The AGC-3 test train was rotated 180° after the first two cycles of irradiation. The effect of test train rotation on the azimuthal position of the specimens and thermocouples was included in the analysis. For the other components (capsule, heat shield and graphite holder), the heating rate at a particular elevation in the core is computed by averaging the heating rates over azimuthal segments. Sensitivity studies show that azimuthal variations in the heating rates of these components do not have a significant effect on temperature because conduction heat transfer between components tends to equalize the temperature (ECAR-2562, ECAR-2322). Since the gas gaps surrounding the specimens and thermocouples provide resistance to conduction in the azimuthal direction, the effect of test train rotation on the heating rates of the specimens and thermocouples was included in the analysis.

The length of the specimen stacks under axial compression will change during irradiation due to irradiation-induced creep. In this analysis, temperature is evaluated in the undeformed configuration. Therefore, this analysis provides specimen temperature as a function of elevation. For a given specimen, its temperature at a particular time during irradiation may be determined by estimating its location with respect to core mid-plane, including the effect of axial compression, and then using the results of this analysis to obtain the temperature at that location.

SOFTWARE VALIDATION

A finite element heat transfer analysis of the AGC-3 experiment was performed using ABAQUS version 6.14-2 on a SGI ICE X distributed memory cluster with 684 compute nodes (“falcon” on the INL network). The operating system is SLES 11 SP 3, and each compute node has two 12-core 2.5 GHz Intel Xenon (Haswell) processors. ABAQUS is listed in the INL Enterprise Architecture (EA) repository of qualified scientific and engineering analysis software (EA Identifier 238858). ABAQUS has been validated for thermal analysis of ATR experiments by solving several test problems and verifying the results against analytical solutions provided in heat transfer textbooks. A complete description of the validation test problems is given in ECAR-131. Scripts were developed to automate the execution, data collection, and relative error calculation for each test problem. The scripts were run on computer “falcon” and a report file containing the results of validation testing was automatically generated (Appendix B). The test results meet the acceptance criterion that the relative error is less than 3%. Calculations given in the appendices were performed using Mathcad version 15, and verification of the computer-generated results was done during checking.

ANALYSIS RESULTS

A finite element, steady-state heat transfer analysis of the AGC-3 test train, including the capsule and all internal components, was performed using ABAQUS. The 8-node linear brick element was used to model all solid components except the heat shield which was modeled using the 4-node linear shell element. The 8-node forced convection brick element was used to model the primary coolant with a prescribed mass flow rate. The model geometry and finite element mesh of the experiment cross-section at the top of the test train where all thermocouples are visible is shown in Fig. 3. A 3-D cutaway view of the experiment is shown in Fig. 4. In these figures, the capsule is blue, specimen holder is green, specimens are red, and thermocouples are orange. The heat shield is modeled as a thin shell and is not clearly visible in the figure. The primary coolant and chopped dummy in-pile tube are also not shown.

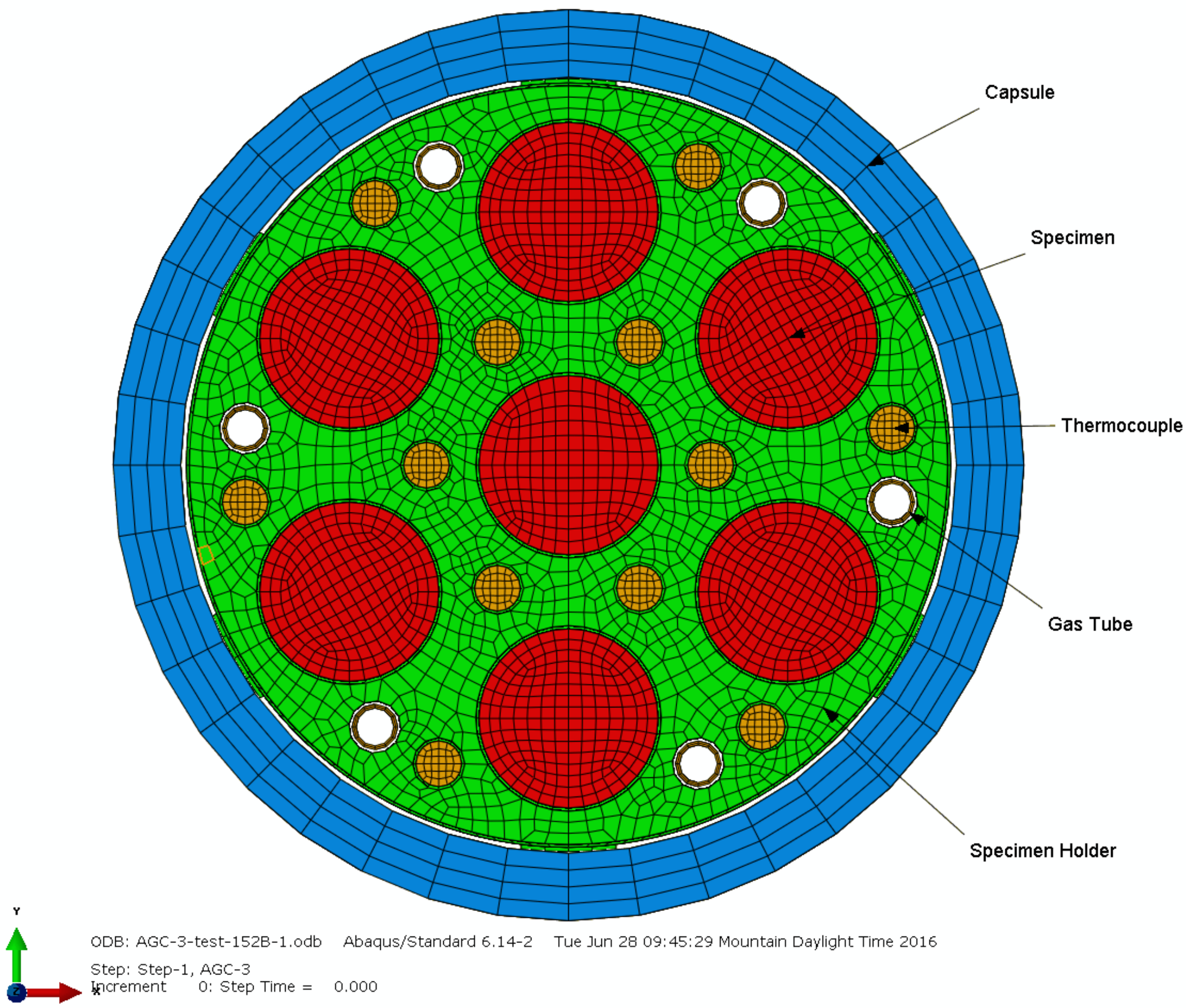

Figure 3. Model geometry and finite element mesh (cross-sectional view of the experiment).

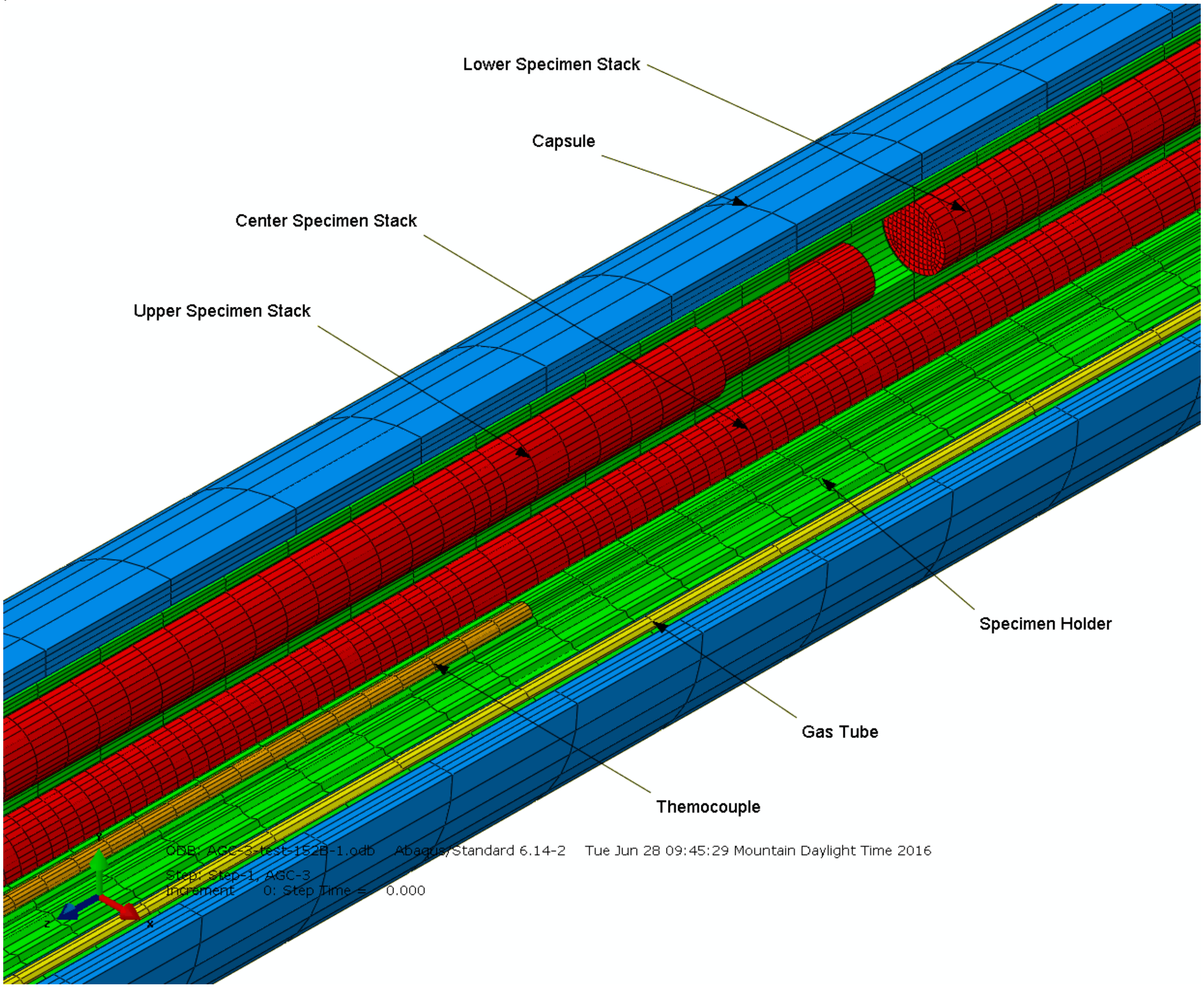

Figure 4. Model geometry and finite element mesh (cutaway view of the experiment).

A thermal analysis was performed at three selected days during each cycle, using the measured east source power, measured gas flows, as-run heating rates, and as-run graphite DPA, to obtain best-estimate temperatures of the test train components. Comparisons of the measured and calculated temperatures (ºC) of each thermocouple in the test train, during all irradiation cycles, are shown in Figs. 5 – 16. The difference between the measured and calculated thermocouple temperature was used to estimate the mean and standard deviation of the error. Setting the uncertainty equal to the mean ± two standard deviations corresponding to a 95% confidence interval, the results indicate that the maximum uncertainty in the calculated thermocouple temperature is ±50°C.

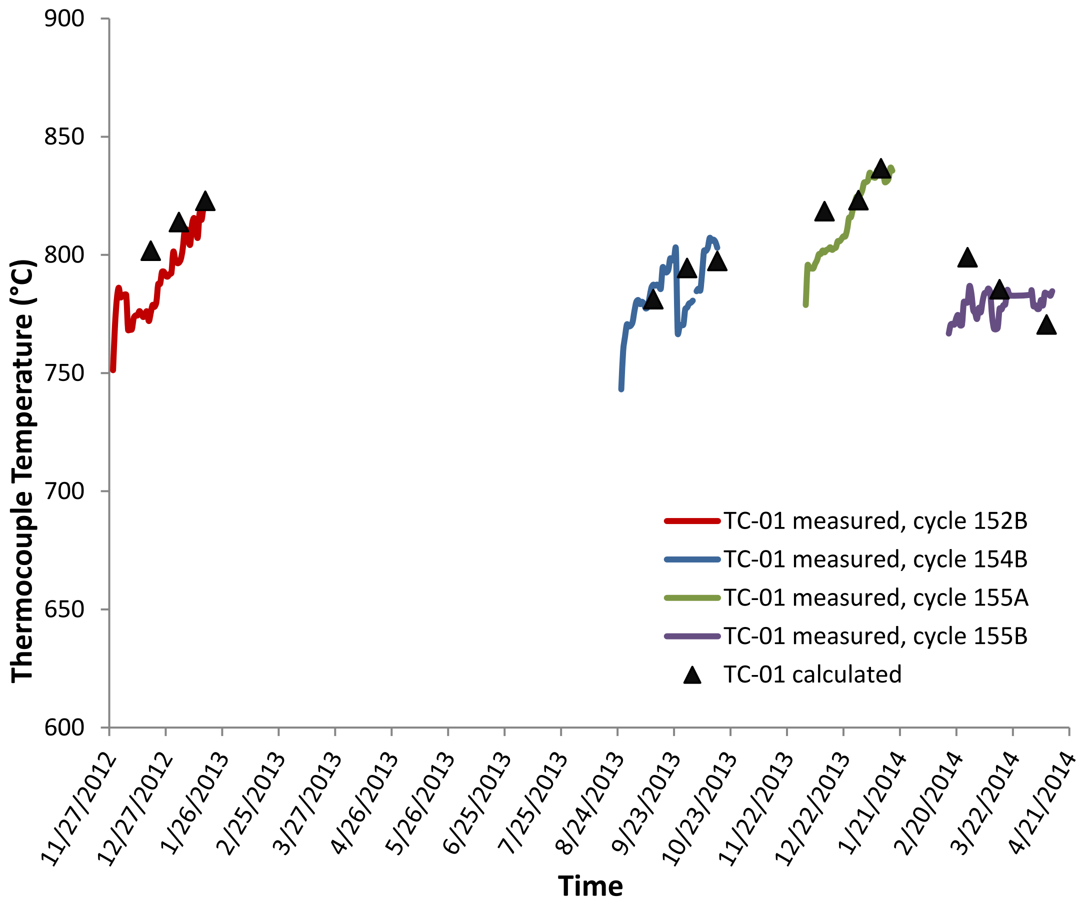

Figure 5. Measured and calculated temperature (°C) of TC-01 (18 inches above core mid-plane) during all irradiation cycles.

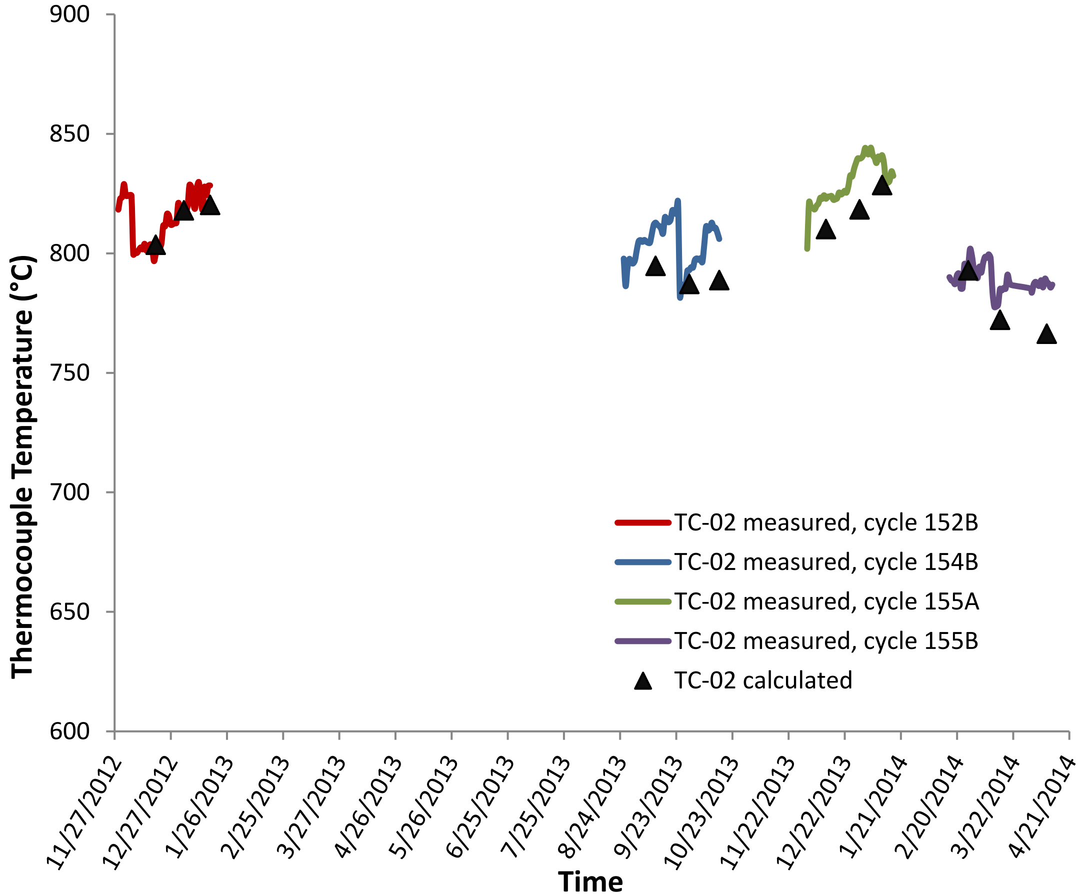

Figure 6. Measured and calculated temperature (°C) of TC-02 (13 inches above core mid-plane) during all irradiation cycles.

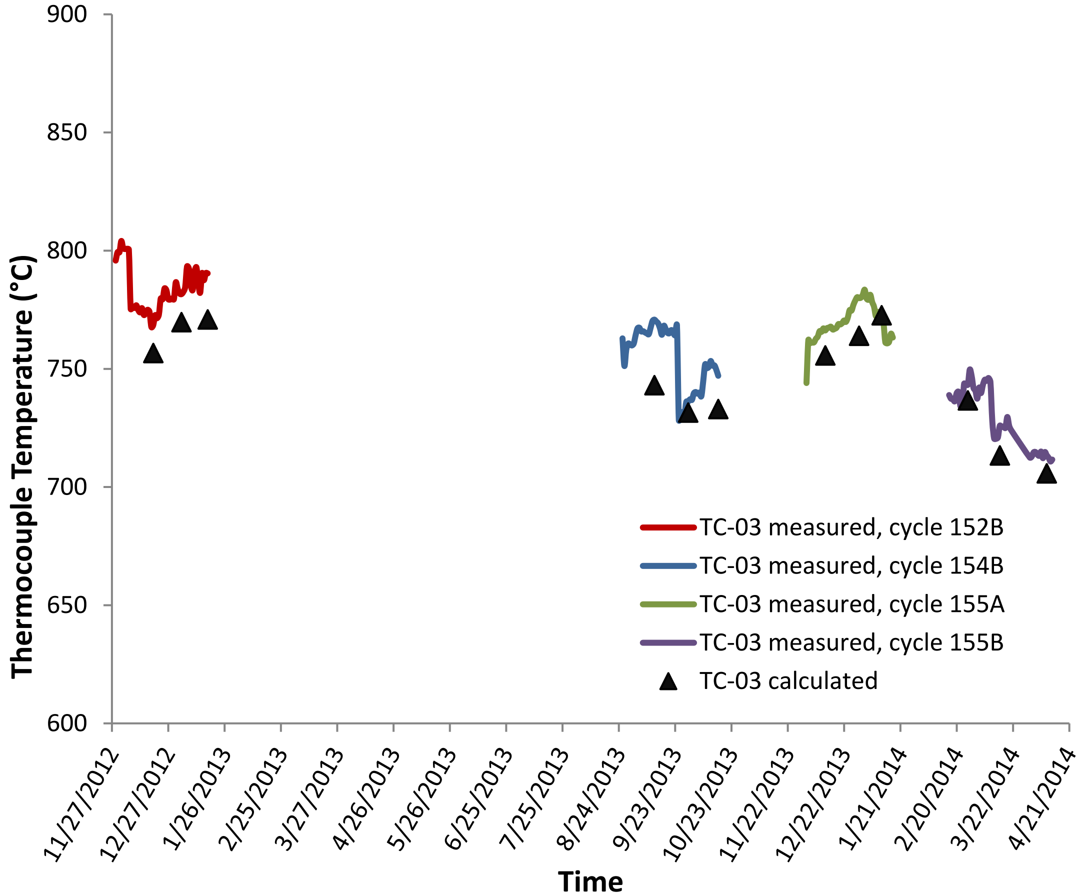

Figure 7. Measured and calculated temperature (°C) of TC-03 (13 inches above core mid-plane) during all irradiation cycles.

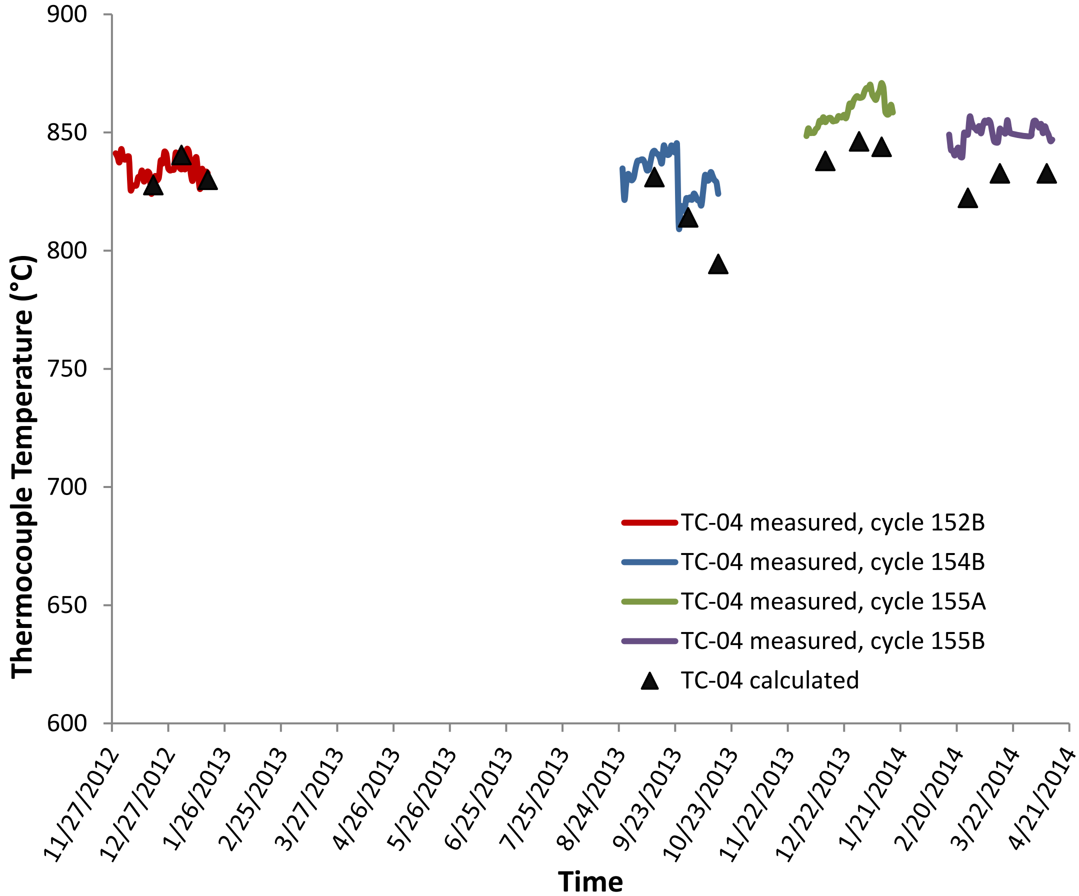

Figure 8. Measured and calculated temperature (°C) of TC-04 (6 inches above core mid-plane) during all irradiation cycles.

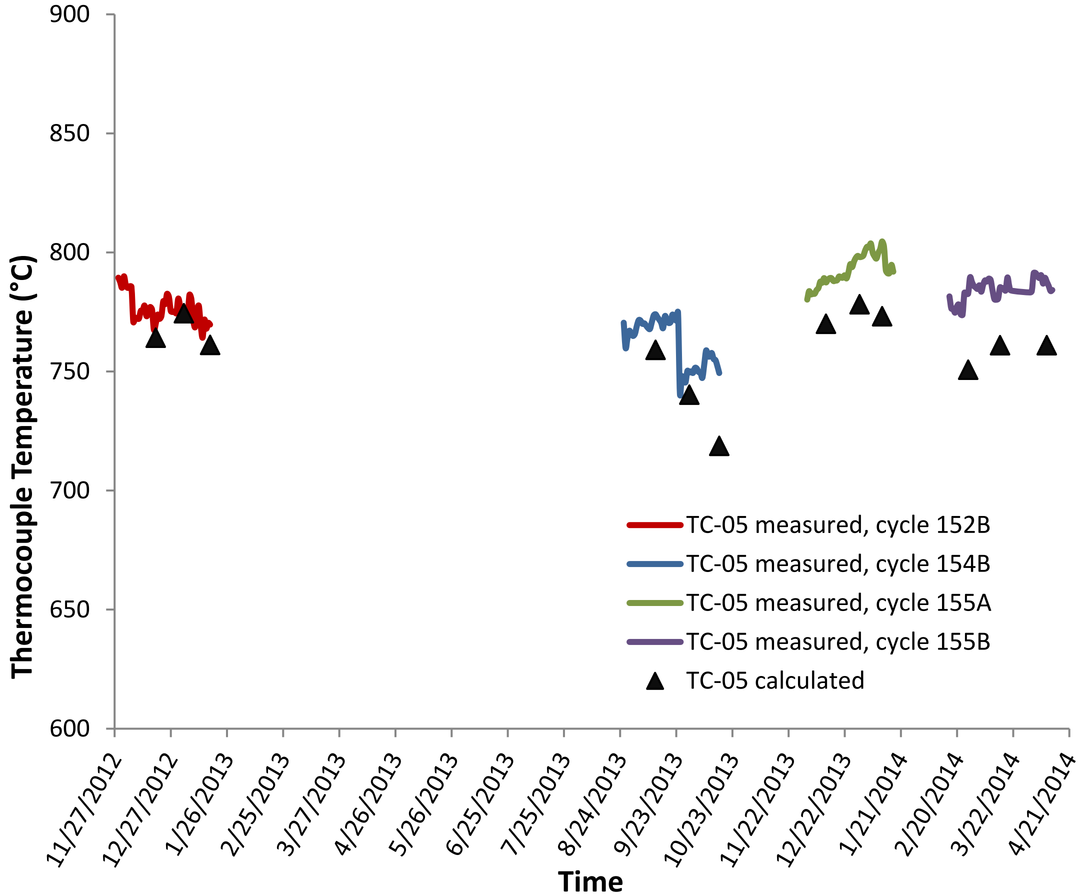

Figure 9. Measured and calculated temperature (°C) of TC-05 (6 inches above core mid-plane) during all irradiation cycles.

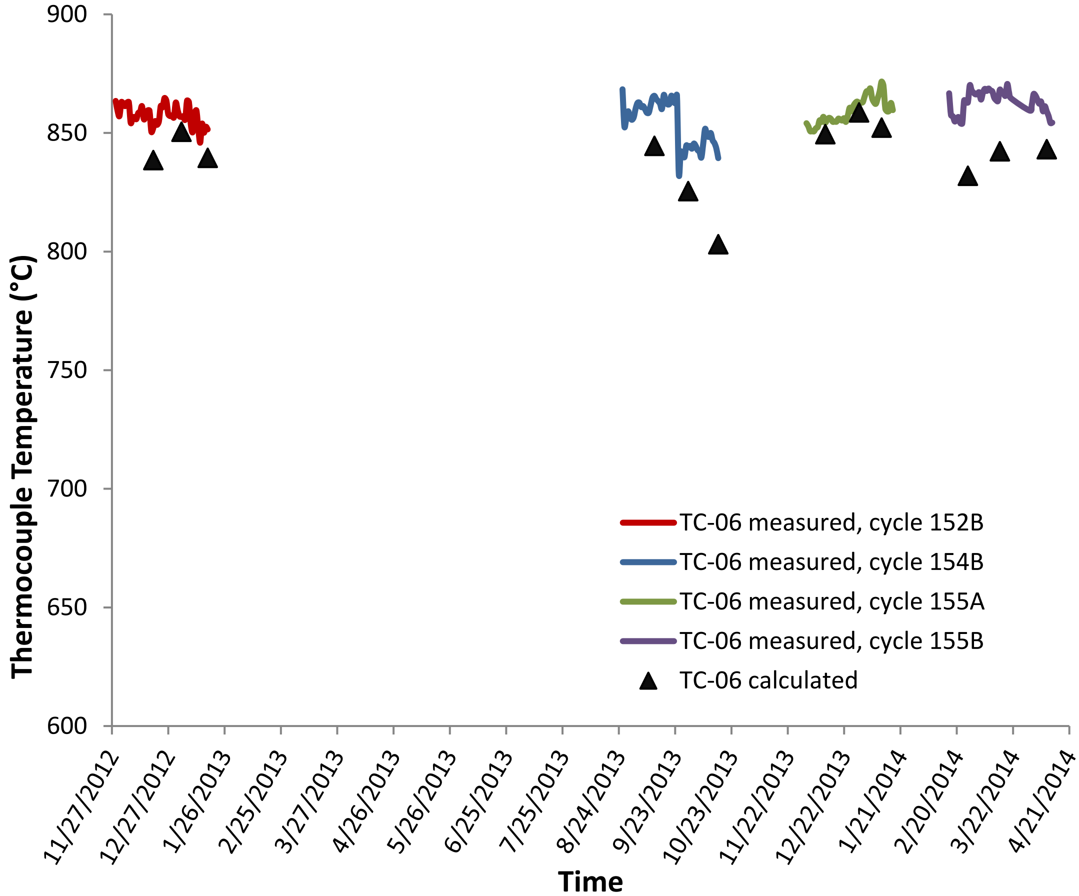

Figure 10. Measured and calculated temperature (°C) of TC-06 (2 inches above core mid-plane) during all irradiation cycles.

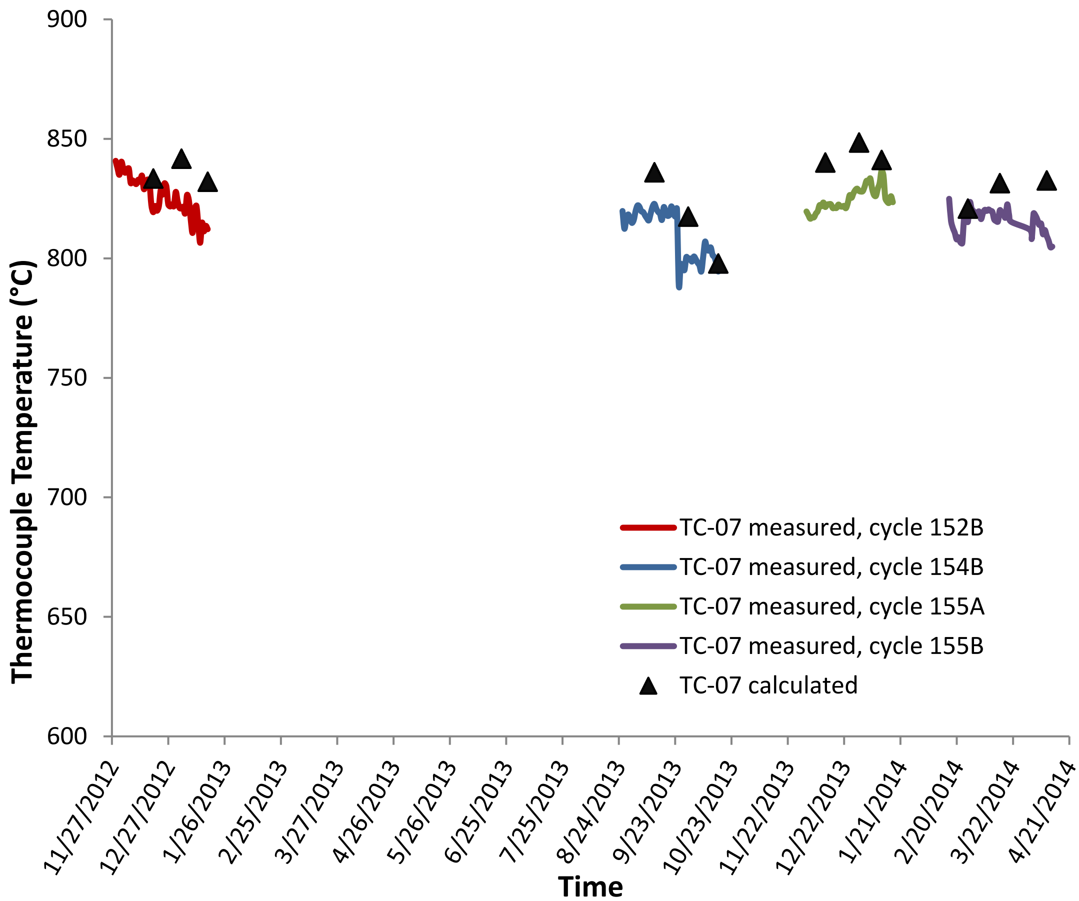

Figure 11. Measured and calculated temperature (°C) of TC-07 (6 inches below core mid-plane) during all irradiation cycles.

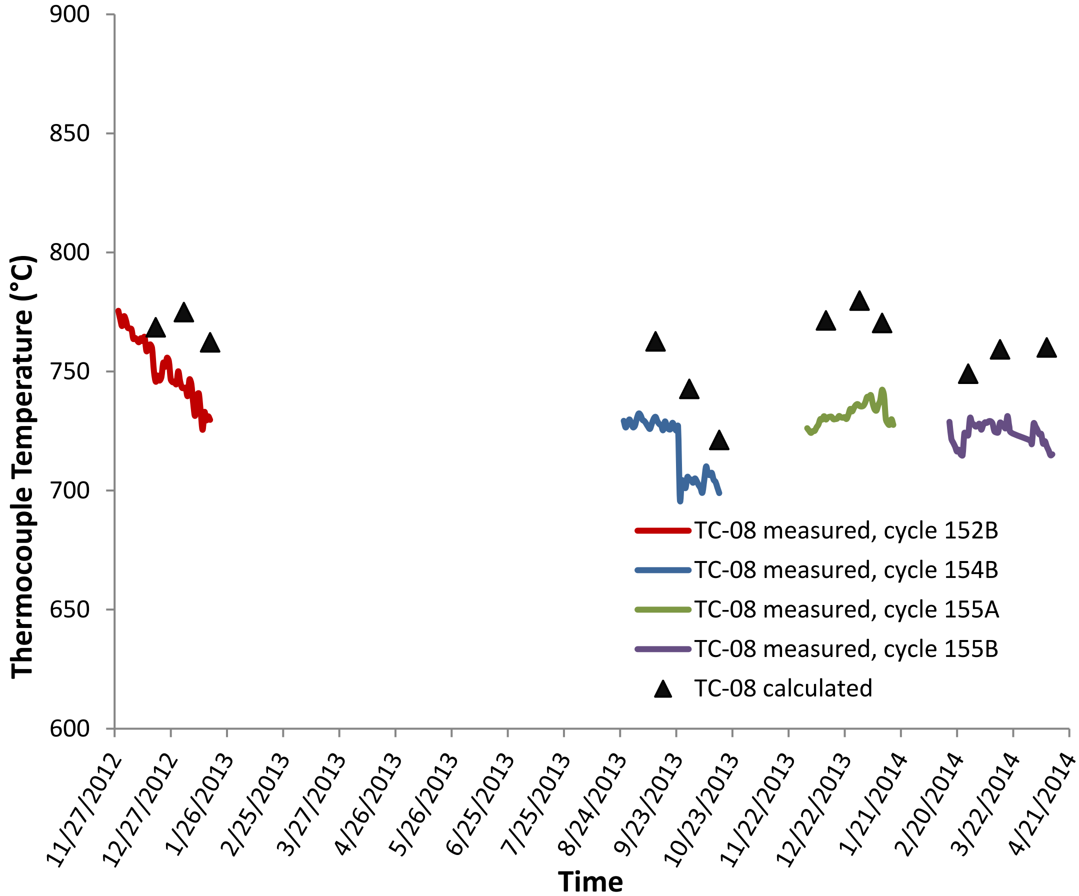

Figure 12. Measured and calculated temperature (°C) of TC-08 (6 inches below core mid-plane) during all irradiation cycles.

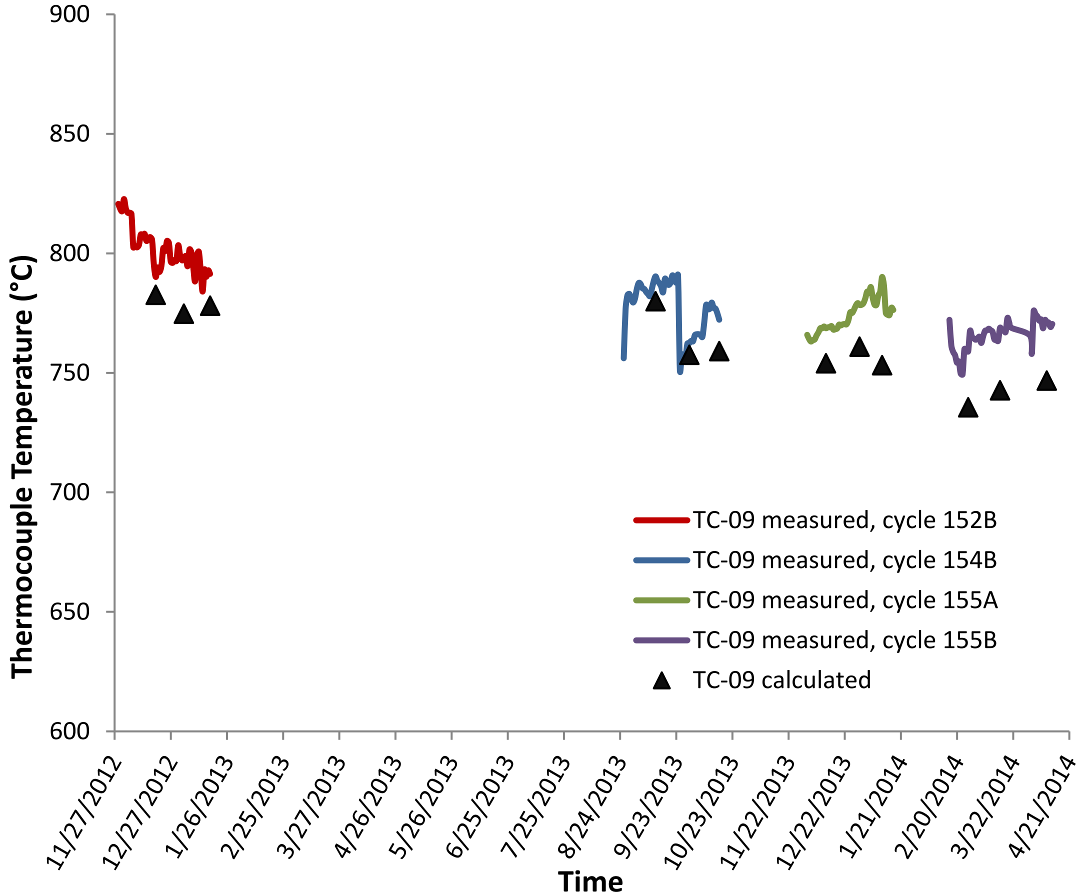

Figure 13. Measured and calculated temperature (°C) of TC-09 (11.25 inches below core mid-plane) during all irradiation cycles.

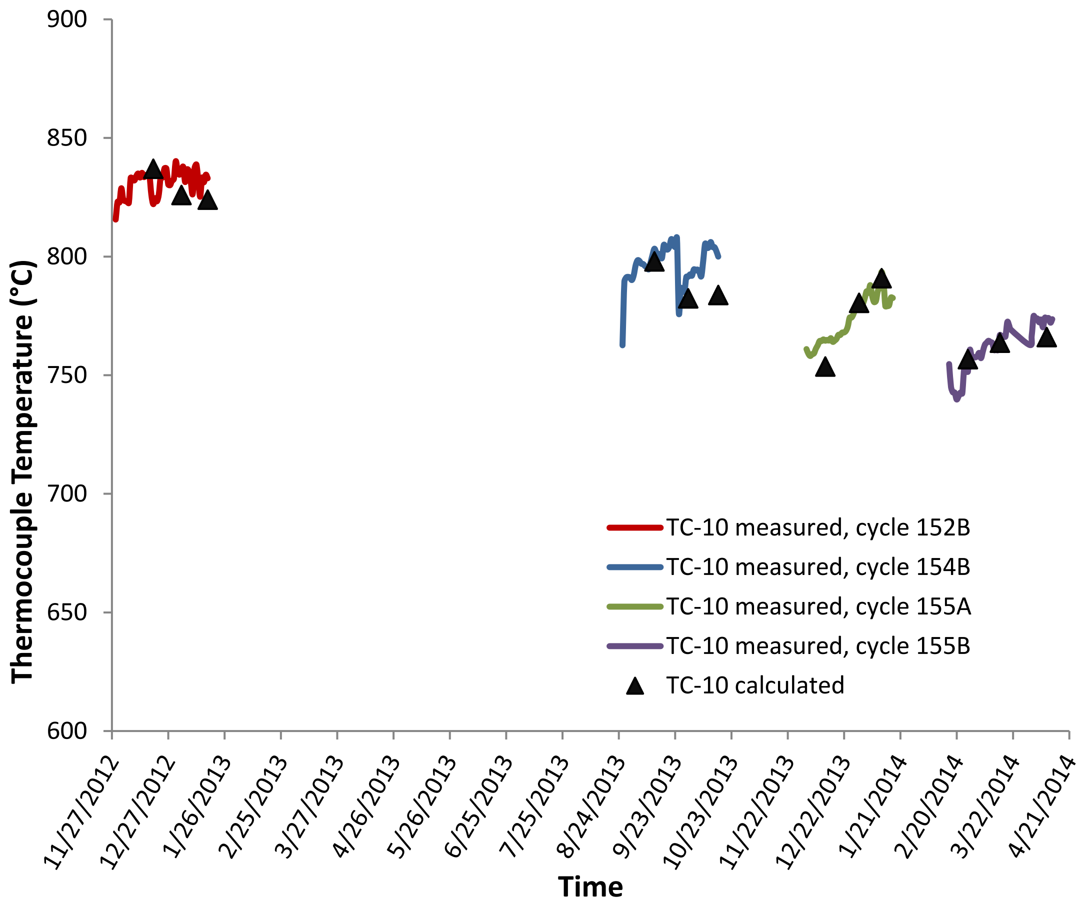

Figure 14. Measured and calculated temperature (°C) of TC-10 (18 inches below core mid-plane) during all irradiation cycles.

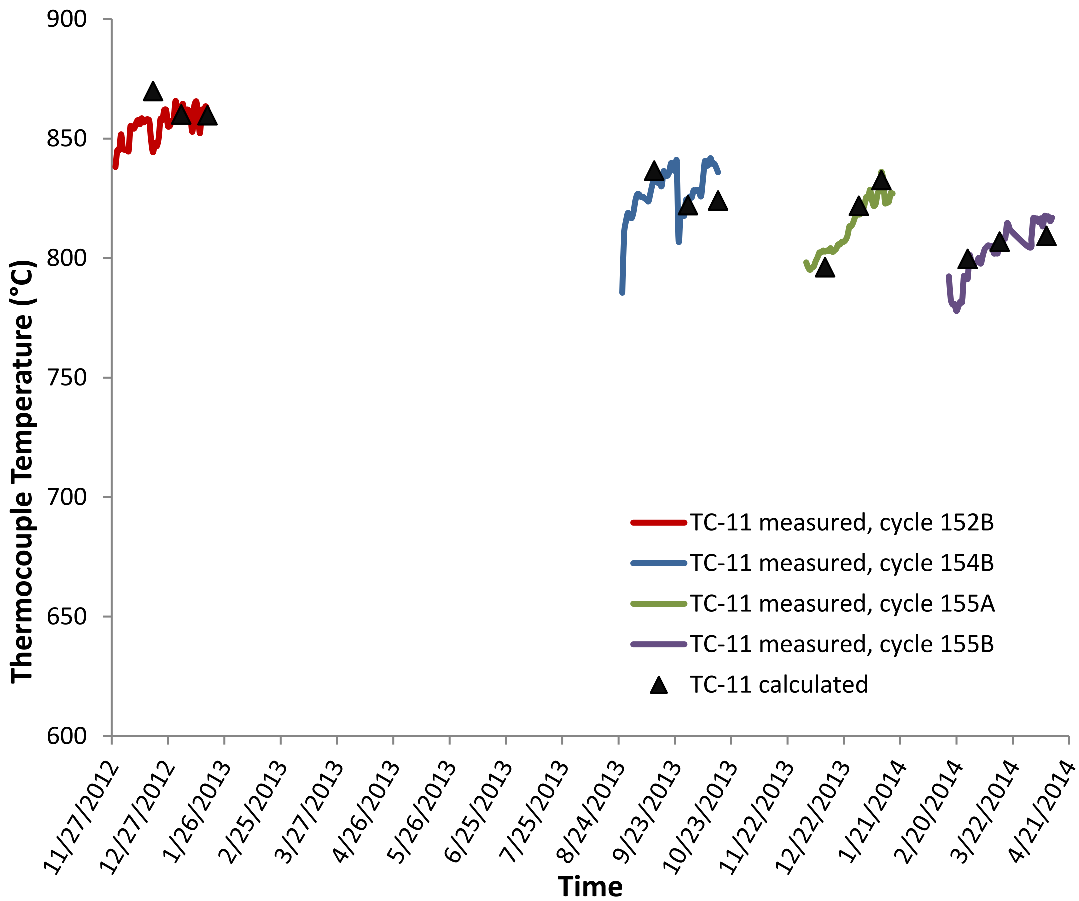

Figure 15. Measured and calculated temperature (°C) of TC-11 (18 inches below core mid-plane) during all irradiation cycles.

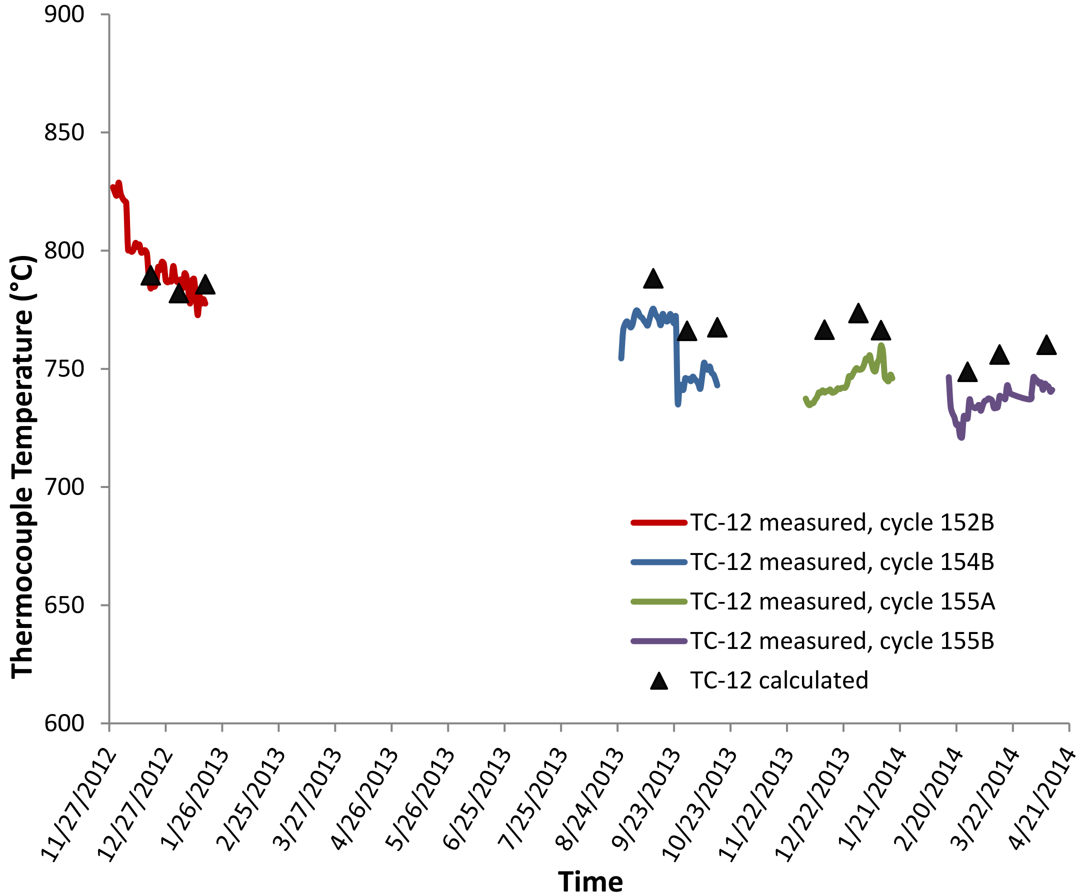

Figure 16. Measured and calculated temperature (°C) of TC-12 (11.25 inches below core mid-plane) during all irradiation cycles.

Plots of the axial distribution of volume-average temperature (ºC) of each specimen stack, during a selected day in each irradiation cycle, are shown in Figs. 17 – 20. Note that the highest temperature occurs in the center specimen stack which is significantly hotter than the peripheral stacks. Moreover, the specimen temperature varies with elevation because of the uncertainty in the variable gas gaps used to compensate for the axial heating profile. An abrupt change in the temperature gradient occurs at the top of the test train due to the presence of a tungsten heater that produces a localized hot spot at that location. The volume-average temperature of each specimen, during three selected days in each irradiation cycle, are stored in text files as described in the section entitled "Data Files."

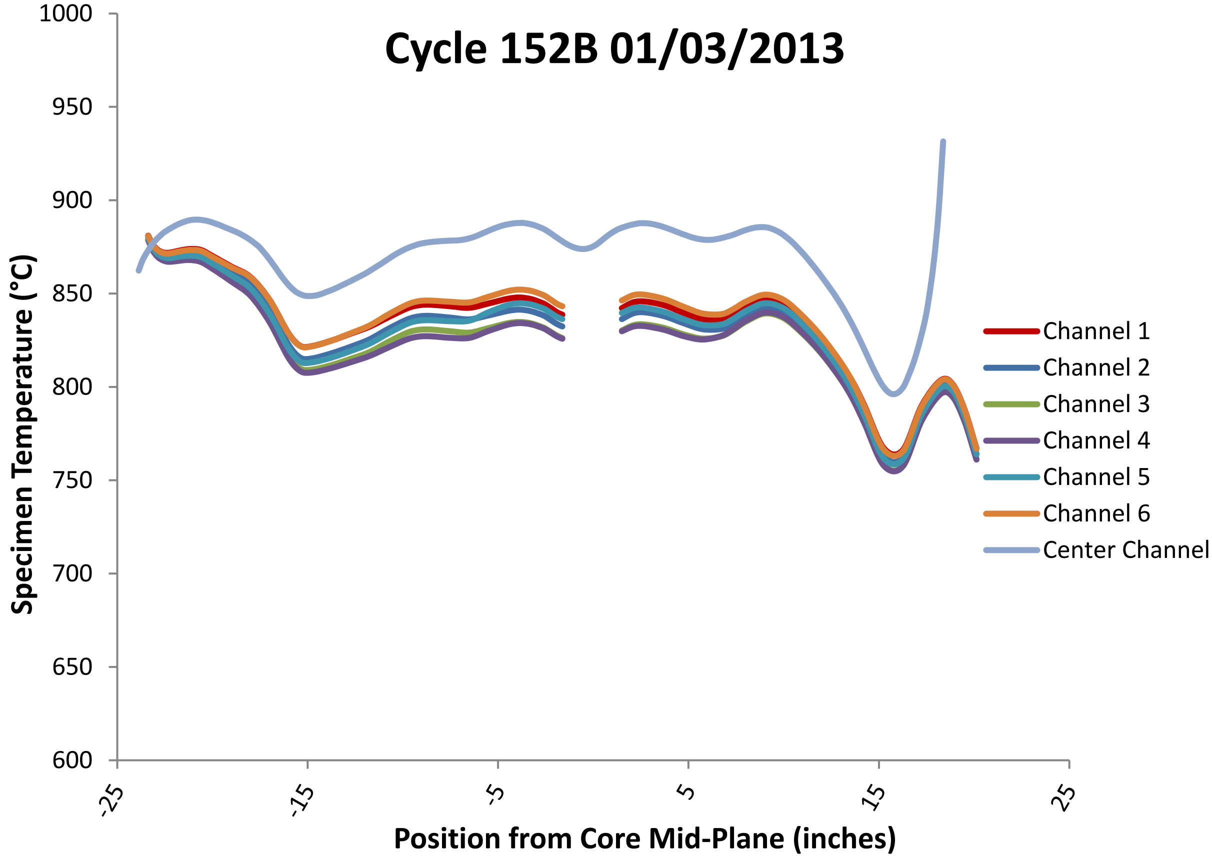

Figure 17. Distribution of specimen temperature (°C) during a selected day in cycle 152B.

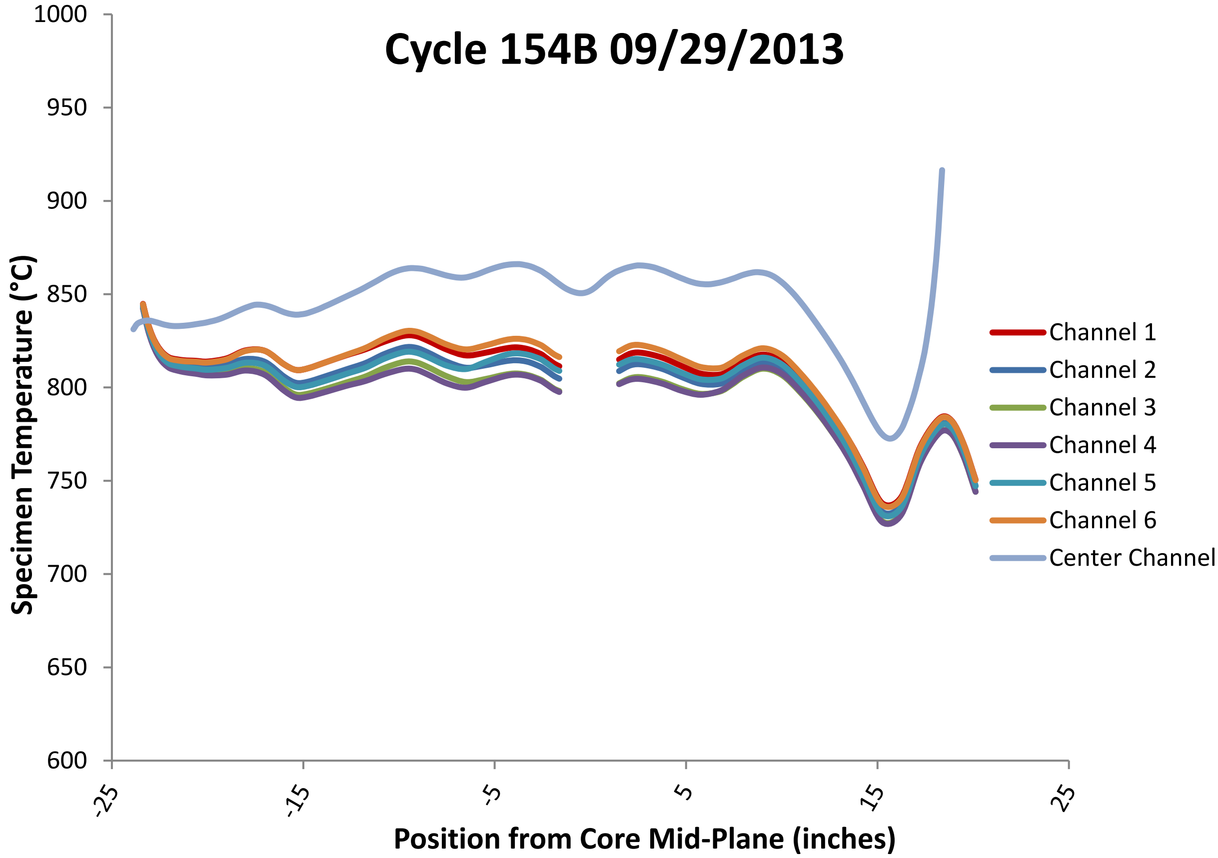

Figure 18. Distribution of specimen temperature (°C) during a selected day in cycle 154B.

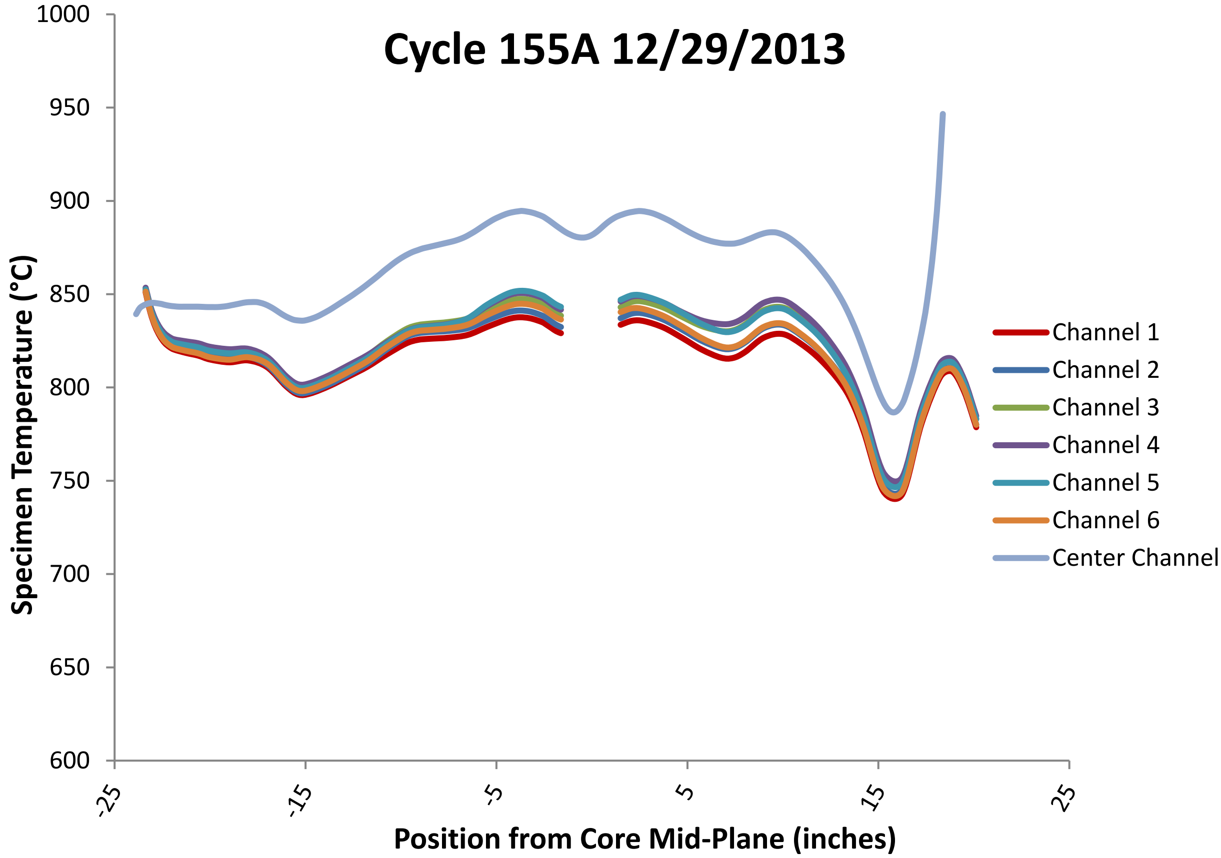

Figure 19. Distribution of specimen temperature (°C) during a selected day in cycle 155A.

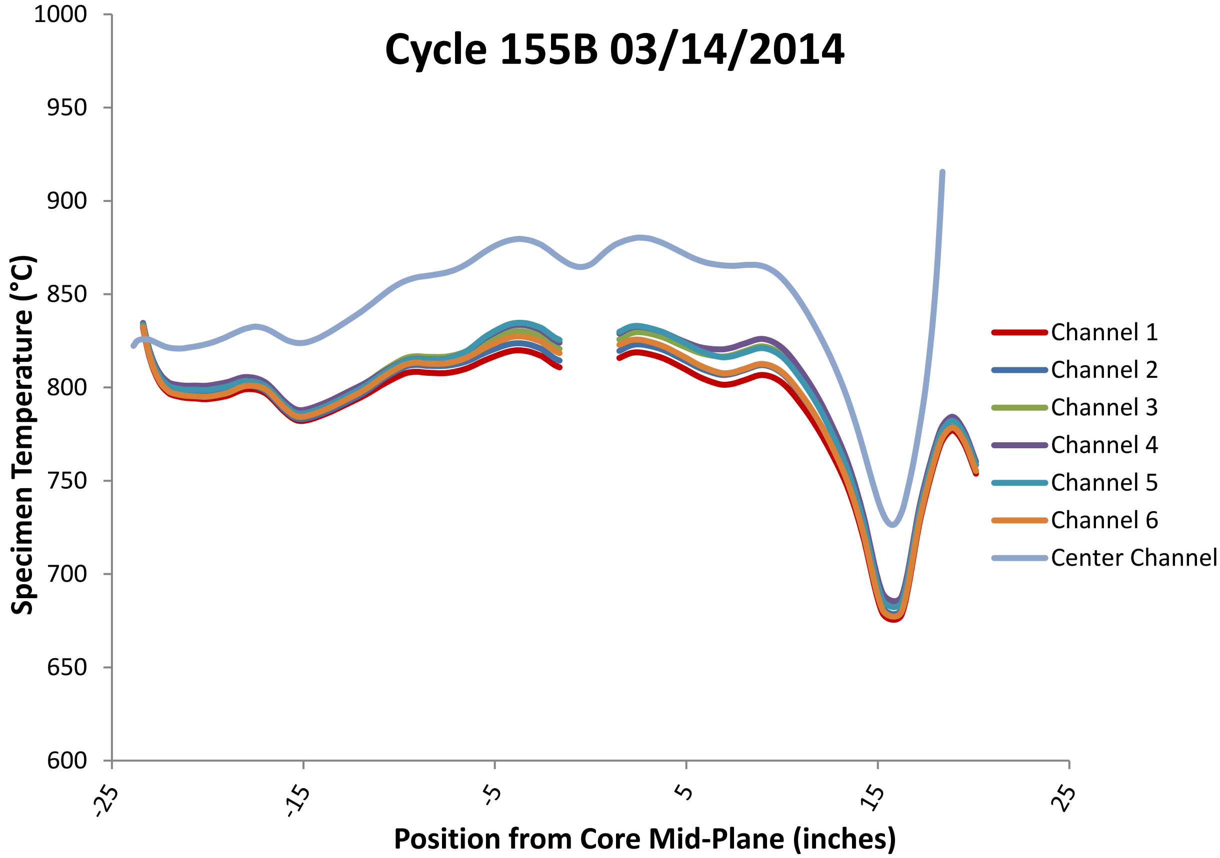

Figure 20. Distribution of specimen temperature (°C) during a selected day in cycle 155B.

CONCLUSIONS AND RECOMMENDATIONS

A finite element, steady-state heat transfer analysis of the entire AGC-3 test train was performed using ABAQUS. The analysis was performed at three selected days during each cycle, using the measured east source power, measured gas flows, as-run heating rates, and as-run graphite DPA, to obtain best-estimate temperatures of the specimens and thermocouples. In order to compensate for uncertainty in the gas gaps between heat shield and capsule, the model was adjusted in order to bring into agreement the measured and calculated thermocouple temperatures. The difference between the measured and calculated thermocouple temperature was used to estimate the mean and standard deviation of the error. Setting the uncertainty equal to the mean ± two standard deviations corresponding to a 95% confidence interval, the results indicate that the maximum uncertainty in the calculated thermocouple temperature is ±50°C.

The experiment requirements on temperature control are that the volume-average and time-average temperatures of each creep specimen shall be maintained at 900°C ±50°C (TFR-791, Section 3.3.3). However, the results of this analysis show that the temperature of the specimen stacks is outside the desired range at the top of the test train where the temperature is less than the desired temperature due to lower gamma heating at this location. In most cases, the temperature of the center specimen stack is approximately 900°C ±50°C while the temperature of the peripheral specimen stacks is approximately 850°C ±50°C. Moreover, specimen temperature varies with elevation because of the uncertainty in the variable gas gaps used to compensate for the axial heating profile.

DATA FILES

The ABAQUS files containing the models created for this analysis are stored on the HPC file server in directory “/projects/atr_exp/AGC-3.” The files created for each analysis case are listed in Table 1. ABAQUS Python scripts were created to read an ABAQUS output file and calculate the thermocouple temperature and volume average specimen temperature for each step in the analysis. The script “AbaqusTCData.py” calculates thermocouple temperature and writes the results to a file having the same name as the ABAQUS output file but with a “.txt” extension. The script “AbaqusSPData.py” calculates volume average specimen temperature and writes the results to a file having the same name as the ABAQUS output file but with a “.data” extension. The scripts and data files are stored in the same directory as the ABAQUS files.

Table 1. ABAQUS/CAE model files and ABAQUS input and output files.

File name	Description
AGC-3.cae, AGC-3.jnl	Model files for all cycles
AGC-3-152B-1.inp, AGC-3-152B-1.f, AGC-3-152B-1.odb	Analysis files for cycle 152B step 1
AGC-3-152B-2.inp, AGC-3-152B-2.f, AGC-3-152B-2.odb	Analysis files for cycle 152B step 2
AGC-3-152B-3.inp, AGC-3-152B-3.f, AGC-3-152B-3.odb	Analysis files for cycle 152B step 3
AGC-3-154B-1.inp, AGC-3-154B-1.f, AGC-3-154B-1.odb	Analysis files for cycle 154B step 1
AGC-3-154B-2.inp, AGC-3-154B-2.f, AGC-3-154B-2.odb	Analysis files for cycle 154B step 2
AGC-3-154B-3.inp, AGC-3-154B-3.f, AGC-3-154B-3.odb	Analysis files for cycle 154B step 3
AGC-3-155A-1.inp, AGC-3-155A-1.f, AGC-3-155A-1.odb	Analysis files for cycle 155A step 1
AGC-3-155A-2.inp, AGC-3-155A-2.f, AGC-3-155A-2.odb	Analysis files for cycle 155A step 2
AGC-3-155A-3.inp, AGC-3-155A-3.f, AGC-3-155A-3.odb	Analysis files for cycle 155A step 3
AGC-3-155B-1.inp, AGC-3-155B-1.f, AGC-3-155B-1.odb	Analysis files for cycle 155B step 1
AGC-3-155B-2.inp, AGC-3-155B-2.f, AGC-3-155B-2.odb	Analysis files for cycle 155B step 2
AGC-3-155B-3.inp, AGC-3-155B-3.f, AGC-3-155B-3.odb	Analysis files for cycle 155B step 3

REFERENCES

ABAQUS Standard, Version 6.14-2, SIMULIA, Inc., Providence, RI, 2014.

ASM Handbook Vol. 1: Properties and Selection: Irons, Steels, and High-Performance Alloys, 10th Edition, American Society of Metals, 1990.

ASM Handbook Vol. 2: Properties and Selection: Nonferrous Alloys and Special-Purpose Materials, 10th Edition, American Society of Metals, 1990.

Biasetto, L., Manzolaro, M., and Andrighetto, A., "Emissivity measurements of opaque gray bodies up to 2000°C by a dual-frequency pyrometer," The European Physics J. A 38, p. 167-171, 2008.

Barrie, S., "NGNP Advanced Graphite Capsule AGC-3 Experiment Test Train," TFR-791, Rev. 1, 2012.

Incropera, F. P. and DeWitt, D. P., *Fundamentals of Heat and Mass Transfer*, 5th ed., John Wiley & Sons, New York, 2002.

Marchenkov, E. I. and Shashkov, A. G., "Study of Thermal Conductivity of an He – Ar Mixture in the Temperature Range of 400 – 1500°K on an Installation With a Molybdenum Measuring Cell," Journal of Engineering Physics and Thermophysics 28(6), p. 725-731, 1975.

Maruyama, T. and Harayama, M., "Neutron irradiation effect on the thermal conductivity and dimensional change of graphite materials," J. Nuclear Materials 195, p. 44-50, 1992.

Mason, E. A. and von Ubisch, H., "Thermal Conductivities of Rare Gas Mixture," Physics of Fluids 3(3), p. 355-361, 1960.

Maynard, R. K., "Total Hemispherical Emissivity of Very High Temperature Reactor (VHTR) Candidate Materials: Hastelloy X, Haynes 230, and Alloy 617," Ph.D. Dissertation, University of Missouri, 2011.

Murray, P. E., "Validation of ABAQUS Standard 6.7-3 Heat Transfer," ECAR-131, Rev. 0, 2008.

Murray, P. E., "Thermal Analysis of the AGC Thermocouple Experiment," ECAR-2429, Rev. 0, 2014.

Murray, P. E., "As-Run Thermal Analysis of the AGC-1 Experiment," ECAR-2562, Rev. 0, 2014.

Murray, P. E., "As-Run Thermal Analysis of the AGC-2 Experiment," ECAR-2322, Rev. 0, 2014.

Murray, P. E., "Uncertainty Analysis of Temperature in the AGC-1 and AGC-2 Experiments," ECAR-3017, Rev. 0, 2016.

Oberg, E., Jones, F. D., Horton, H. L., Ryffell, H. H., *Machinery's Handbook*, 28th Edition, Industrial Press, 2008.

Parry, J. R., "As-Run Physics Analysis for the AGC-3 Experiment Irradiated in the ATR," ECAR-3051, Rev. 0, 2016.

Perry, R. H., and Green, D. W., *Perry's Chemical Engineers' Handbook*, 7th Edition, McGraw-Hill, 1997.

Price, R. J., "Thermal Conductivity of Neutron-Irradiated Reactor Graphites," Carbon 13, p. 201-204, 1975.

Vreeling, J. A., Wouters, O., and van der Lann, J. G., "Graphite irradiation testing for HTR technology at the High Flux Reactor in Petten," J. Nuclear Materials 381, p. 68-75, 2008.

Windes, W., "Data Report on Post-Irradiation Dimensional Change in AGC-1 Samples," INL/EXT-12-26255, 2012.

Windes, W. E., Winston, P. L., and Swank, W. D., "AGC-2 Disassembly Report," INL/EXT-14-32060, May, 2014.

DRAWINGS

603520, "ATR Advanced Graphite Capsule (AGC-3) Test Train Facility Assembly," Rev. 0.

603521, "ATR Advanced Graphite Capsule (AGC) Graphite Specimen Holder Machining Details," Rev. 2.

603522, "ATR Advanced Graphite Capsule (AGC) Hole Details and Upper and Lower Specimen Holders," Rev. 1.

603523, "ATR Advanced Graphite Capsule (AGC) Miscellaneous Graphite Component Assemblies and Details," Rev. 1.

603524, "ATR Advanced Graphite Capsule (AGC-3) Specimen Stack-Up Arrangements," Rev. 0.

603534, "ATR Advanced Graphite Capsule (AGC-3) Thermal Heat Shield Details," Rev. 1.

601501, "ATR Advanced Graphite Capsule (AGC) AGC-3 Graphite Specimen Cutout Diagrams," Rev. 4.

630434, "ATR Advanced Graphite Capsule (AGC) Capsule Facility In-Core Pressure Boundary Tube," Rev. 3.

443027, "ATR South and East Flux Trap Chopped Dummy In-Pile Tube Assembly," Rev. 7.

APPENDIX A

ECAR-3386 As-Run Thermal Analysis of the AGC-3 Experiment Page A1 of A62

Appendix A - Hydrodynamics, heat transfer, and nuclear heating

A.1 Thermophysical properties

Thermophysical properties of 304 and 304L austenitic stainless steel (Perry's Handbook, 7th edition, Table 2-375; Machinery's Handbook, 28th edition, p. 378):

$$T_S := \begin{pmatrix} 212 \\ 932 \end{pmatrix} {}^\circ F$$

$$\rho_{SST} := 0.29 \cdot \frac{lb}{in^3}$$

$$c_{p\_SST} := 0.12 \cdot \frac{BTU}{lb \cdot R}$$

$$k_{304\_SST} := \begin{pmatrix} 9.4 \\ 12.4 \end{pmatrix} \cdot \frac{BTU}{hr \cdot ft \cdot R} \qquad k_{304\_SST} = \begin{pmatrix} 0.783 \\ 1.033 \end{pmatrix} \cdot \frac{BTU}{hr \cdot in \cdot R}$$

Thermophysical properties of aluminum 6061 (Machinery's Handbook, p. 377):

$$\rho_{AL} := 0.098 \cdot \frac{lb}{in^3}$$

$$c_{p\_AL} := 0.23 \cdot \frac{BTU}{lb \cdot R}$$

$$k_{AL} := 104 \cdot \frac{BTU}{hr \cdot ft \cdot R} \qquad k_{AL} = 8.667 \cdot \frac{BTU}{hr \cdot in \cdot R}$$

ECAR-3386 As-Run Thermal Analysis of the AGC-3 Experiment Page A2 of A62

Thermophysical properties of tungsten (ASM Metals Handbook Vol. 2, Properties of Pure Metals - Tungsten, ASTM B777 Class 1):

$$\rho_W := 17.0 \cdot \frac{gm}{cm^3} \qquad \rho_W = 0.614 \cdot \frac{lb}{in^3}$$

$$c_{p\_W} := 0.131 \cdot \frac{J}{gm \cdot K} \qquad c_{p\_W} = 0.031 \cdot \frac{BTU}{lb \cdot R}$$

$$T_S := \begin{pmatrix} 500 \\ 1000 \\ 1500 \end{pmatrix} \cdot K \qquad T_S = \begin{pmatrix} 440 \\ 1340 \\ 2240 \end{pmatrix} \cdot {}^\circ F$$

$$k_W := \begin{pmatrix} 150 \\ 125 \\ 110 \end{pmatrix} \cdot \frac{W}{m \cdot K} \qquad k_W = \begin{pmatrix} 7.22 \\ 6.02 \\ 5.3 \end{pmatrix} \cdot \frac{BTU}{hr \cdot in \cdot R}$$

Thermophysical properties of Haynes 230 nickel alloy (ASM Metals Handbook Vol. 1, Wrought Nickel Alloys):

$$\rho_H := 8.8 \cdot \frac{gm}{cm^3} \qquad \rho_H = 0.318 \cdot \frac{lb}{in^3}$$

$$c_{p\_H} := 0.473 \cdot \frac{J}{gm \cdot K} \qquad c_{p\_H} = 0.113 \cdot \frac{BTU}{lb \cdot R}$$

$$T_S := \begin{pmatrix} 21 \\ 538 \\ 871 \end{pmatrix} {}^\circ C \qquad T_S = \begin{pmatrix} 70 \\ 1000 \\ 1600 \end{pmatrix} \cdot {}^\circ F$$

$$k_H := \begin{pmatrix} 8.9 \\ 18.4 \\ 24.4 \end{pmatrix} \cdot \frac{W}{m \cdot K} \qquad k_H = \begin{pmatrix} 0.43 \\ 0.89 \\ 1.17 \end{pmatrix} \cdot \frac{BTU}{hr \cdot in \cdot R}$$

Thermophysical properties of nuclear-grade graphite:

$\rho_g := 1.822 \dfrac{gm}{cm^3}$ $\rho_g = 0.0658 \cdot \dfrac{lb}{in^3}$ Density (Product Certification, NBG-25 graphite, SGL Group)

$c_{pg} := 5.66 \dfrac{cal}{mole \cdot K}$ $\dfrac{c_{pg}}{12 \cdot \dfrac{gm}{mole}} = 0.472 \cdot \dfrac{BTU}{lb \cdot R}$ Specific heat at 900 C (Perry's Handbook, 7th edition, Table 2-194)

Thermal conductivity of unirradiated fine-grained isotropic graphite (J. Nuclear Materials 381, p. 68-75, 2008):

$$T := \begin{pmatrix} 300 \\ 400 \\ 600 \\ 800 \\ 1000 \end{pmatrix} {}^\circ C \qquad T = \begin{pmatrix} 572 \\ 752 \\ 1112 \\ 1472 \\ 1832 \end{pmatrix} \cdot {}^\circ F$$

$$k_g := \begin{pmatrix} 95 \\ 85 \\ 72 \\ 65 \\ 60 \end{pmatrix} \frac{W}{m \cdot K} \qquad k_g = \begin{pmatrix} 4.574 \\ 4.093 \\ 3.467 \\ 3.13 \\ 2.889 \end{pmatrix} \cdot \frac{BTU}{in \cdot hr \cdot R}$$

Experimental data on effect of neutron fluence on thermal conductivity of fine-grained isotropic graphite (J. Nuclear Materials 381, p. 68-75, 2008; J. Nuclear Materials 195, p. 44-50, 1992; Carbon 13, p. 201-204, 1975); data is given at various values of temperature and dpa (displacemements per atom computed as a function of fast neutron fluence with energy > 0.1 MeV):

$dpa := 0.13$ $T_{irr} := 300\,{}^\circ C$ $k_{g\_irr} := 27.2 \dfrac{W}{m \cdot K}$

$dpa := 0.82$ $T_{irr} := 400\,{}^\circ C$ $k_{g\_irr} := 26.9 \dfrac{W}{m \cdot K}$

$dpa := 1.6$ $T_{irr} := 600\,{}^\circ C$ $k_{g\_irr} := 33 \dfrac{W}{m \cdot K}$

$dpa := 2.2$ $T_{irr} := 1000\,{}^\circ C$ $k_{g\_irr} := 39 \dfrac{W}{m \cdot K}$

$dpa := 9.0$ $T_{irr} := 800\,{}^\circ C$ $k_{g\_irr} := 37 \dfrac{W}{m \cdot K}$

$$dpa := \begin{pmatrix} 0.1 \\ 1.0 \\ 10 \end{pmatrix}$$ Displacemements per atom

$$T = \begin{pmatrix} 300 \\ 400 \\ 600 \\ 800 \\ 1000 \end{pmatrix} \cdot {}^{\circ}C$$ Temperature in degrees C

$$\varphi := \begin{pmatrix} 0.30 & 0.20 & 0.10 \\ 0.41 & 0.30 & 0.20 \\ 0.61 & 0.50 & 0.40 \\ 0.73 & 0.64 & 0.55 \\ 0.80 & 0.70 & 0.60 \end{pmatrix}$$

Ratio of irradiated to unirradiated thermal conductivity as a function of temperature (rows) and dpa (columns), evaluated using the experimental data given above

Thermal conductivity of irradiated graphite at various values of temperature and dpa:

$i := 0..4 \qquad j := 0..2$

$$\lambda_{i,j} := \varphi_{i,j} \cdot kg_i \qquad \lambda = \begin{pmatrix} 1.372 & 0.915 & 0.457 \\ 1.678 & 1.228 & 0.819 \\ 2.115 & 1.733 & 1.387 \\ 2.285 & 2.003 & 1.721 \\ 2.311 & 2.022 & 1.733 \end{pmatrix} \cdot \frac{BTU}{in \cdot hr \cdot R}$$

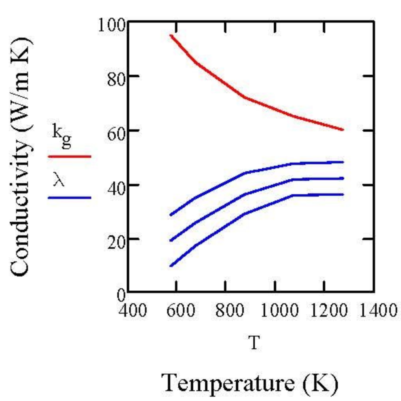

Thermophysical properties of compressed water (Perry's Handbook, Tables 2-355 and 2-356):

$P_L := 20\cdot bar = 290\cdot psi$

$$T_L := \begin{pmatrix} 300 \\ 350 \\ 400 \end{pmatrix}\cdot K \qquad T_L = \begin{pmatrix} 80 \\ 170 \\ 260 \end{pmatrix}\cdot {}^\circ F$$

$$\rho_{H2O} := \begin{pmatrix} 994.1 \\ 968.2 \\ 929.7 \end{pmatrix}\cdot\frac{kg}{m^3} \qquad \rho_{H2O} = \begin{pmatrix} 0.0359 \\ 0.035 \\ 0.0336 \end{pmatrix}\cdot\frac{lb}{in^3}$$

$$c_{p\_H2O} := \begin{pmatrix} 4.17 \\ 4.19 \\ 4.25 \end{pmatrix}\cdot\frac{J}{gm\cdot K} \qquad c_{p\_H2O} = \begin{pmatrix} 0.996 \\ 1.001 \\ 1.015 \end{pmatrix}\cdot\frac{BTU}{lb\cdot R}$$

$$k_{H2O} := \begin{pmatrix} 0.616 \\ 0.669 \\ 0.689 \end{pmatrix}\cdot\frac{W}{m\cdot K} \qquad k_{H2O} = \begin{pmatrix} 0.03 \\ 0.032 \\ 0.033 \end{pmatrix}\cdot\frac{BTU}{hr\cdot in\cdot R}$$

$$\mu_{H2O} := \begin{pmatrix} 0.000856 \\ 0.000371 \\ 0.000218 \end{pmatrix}\cdot\frac{N\cdot s}{m^2} \qquad \mu_{H2O} = \begin{pmatrix} 0.173 \\ 0.075 \\ 0.044 \end{pmatrix}\cdot\frac{lb}{hr\cdot in}$$

$$Pr_{H2O} := \begin{pmatrix} 5.80 \\ 2.32 \\ 1.34 \end{pmatrix}$$

$$\rho_w := 0.5\cdot\left(\rho_{H2O_0} + \rho_{H2O_1}\right) \qquad \rho_w = 0.0354\cdot\frac{lb}{in^3}$$

Density of compressed water at reactor primary coolant inlet temperature (125 deg F)

ECAR-3386 As-Run Thermal Analysis of the AGC-3 Experiment Page A6 of A62

Thermal conductivity of helium-argon gas mixtures (Physics of Fluids 3(3), p. 355-361, 1960; Journal of Engineering Physics and Thermophysics 28(6), p. 725-731, 1975):

$$T_{gas} := \begin{pmatrix} 302 \\ 793 \\ 1173 \end{pmatrix} \cdot K \qquad T_{gas} = \begin{pmatrix} 84 \\ 968 \\ 1652 \end{pmatrix} \cdot °F$$

$$k_{100Ar} := \begin{pmatrix} 0.0182 \\ 0.0383 \\ 0.0480 \end{pmatrix} \cdot \frac{W}{m \cdot K} \qquad k_{100Ar} = \begin{pmatrix} 0.00088 \\ 0.00184 \\ 0.00231 \end{pmatrix} \cdot \frac{BTU}{hr \cdot in \cdot R}$$

$$k_{10He90Ar} := \begin{pmatrix} 0.0234 \\ 0.0494 \\ 0.0590 \end{pmatrix} \cdot \frac{W}{m \cdot K} \qquad k_{10He90Ar} = \begin{pmatrix} 0.00113 \\ 0.00238 \\ 0.00284 \end{pmatrix} \cdot \frac{BTU}{hr \cdot in \cdot R}$$

$$k_{20He80Ar} := \begin{pmatrix} 0.0294 \\ 0.0622 \\ 0.0700 \end{pmatrix} \cdot \frac{W}{m \cdot K} \qquad k_{20He80Ar} = \begin{pmatrix} 0.00142 \\ 0.00299 \\ 0.00337 \end{pmatrix} \cdot \frac{BTU}{hr \cdot in \cdot R}$$

$$k_{30He70Ar} := \begin{pmatrix} 0.0364 \\ 0.0772 \\ 0.0880 \end{pmatrix} \cdot \frac{W}{m \cdot K} \qquad k_{30He70Ar} = \begin{pmatrix} 0.00175 \\ 0.00372 \\ 0.00424 \end{pmatrix} \cdot \frac{BTU}{hr \cdot in \cdot R}$$

$$k_{40He60Ar} := \begin{pmatrix} 0.0451 \\ 0.0957 \\ 0.106 \end{pmatrix} \cdot \frac{W}{m \cdot K} \qquad k_{40He60Ar} = \begin{pmatrix} 0.00217 \\ 0.00461 \\ 0.0051 \end{pmatrix} \cdot \frac{BTU}{hr \cdot in \cdot R}$$

$$k_{50He50Ar} := \begin{pmatrix} 0.0551 \\ 0.116 \\ 0.137 \end{pmatrix} \cdot \frac{W}{m \cdot K} \qquad k_{50He50Ar} = \begin{pmatrix} 0.00265 \\ 0.00559 \\ 0.0066 \end{pmatrix} \cdot \frac{BTU}{hr \cdot in \cdot R}$$

$$k_{60He40Ar} := \begin{pmatrix} 0.0667 \\ 0.140 \\ 0.167 \end{pmatrix} \cdot \frac{W}{m \cdot K} \qquad k_{60He40Ar} = \begin{pmatrix} 0.00321 \\ 0.00674 \\ 0.00804 \end{pmatrix} \cdot \frac{BTU}{hr \cdot in \cdot R}$$

$$k_{70He30Ar} := \begin{pmatrix} 0.0809 \\ 0.169 \\ 0.223 \end{pmatrix} \cdot \frac{W}{m \cdot K} \qquad k_{70He30Ar} = \begin{pmatrix} 0.0039 \\ 0.00814 \\ 0.01074 \end{pmatrix} \cdot \frac{BTU}{hr \cdot in \cdot R}$$

ECAR-3386 As-Run Thermal Analysis of the AGC-3 Experiment Page A7 of A62

$$k_{80He20Ar} := \begin{pmatrix} 0.0993 \\ 0.195 \\ 0.279 \end{pmatrix} \cdot \frac{W}{m \cdot K} \qquad k_{80He20Ar} = \begin{pmatrix} 0.00478 \\ 0.00939 \\ 0.01343 \end{pmatrix} \cdot \frac{BTU}{hr \cdot in \cdot R}$$

$$k_{90He10Ar} := \begin{pmatrix} 0.124 \\ 0.250 \\ 0.338 \end{pmatrix} \cdot \frac{W}{m \cdot K} \qquad k_{90He10Ar} = \begin{pmatrix} 0.00597 \\ 0.01204 \\ 0.01627 \end{pmatrix} \cdot \frac{BTU}{hr \cdot in \cdot R}$$

$$k_{100He} := \begin{pmatrix} 0.154 \\ 0.308 \\ 0.397 \end{pmatrix} \cdot \frac{W}{m \cdot K} \qquad k_{100He} = \begin{pmatrix} 0.00741 \\ 0.01483 \\ 0.01912 \end{pmatrix} \cdot \frac{BTU}{hr \cdot in \cdot R}$$

Thermal radiation properties of materials (for stainless steel and tungsten, Table A.11, "Fundamentals of Heat and Mass Transfer," 5th ed., F. Incropera and D. DeWitt, 2002; for graphite, European Physical J. A 38, p. 167-171, 2008; for Inconel 600 (TC sheath) and Haynes 230 (heat shield), CINDAS Thermophysical Properties of Matter Database; for stainless steel coated with graphite powder, "Total Hemispherical Emissivity of VHTR Candidate Materials," PhD Dissertation, 2011):

$\varepsilon_{SST\_lo} := 0.2$ Emissivity of clean stainless steel (304, Inconel 600, and Haynes 230)

$\varepsilon_{SST\_hi} := 0.4$ Emissivity of stainless steel coated with graphite powder

$\varepsilon_{W} := 0.10$ Emissivity of tungsten

$\varepsilon_{C} := 0.90$ Emissivity of graphite

$\sigma := 5.670 \cdot 10^{-8} \cdot \frac{W}{m^2 \cdot K^4}$ $\sigma = 1.189 \times 10^{-11} \cdot \frac{BTU}{hr \cdot in^2 \cdot R^4}$ Stefan-Boltzmann constant

ECAR-3386 As-Run Thermal Analysis of the AGC-3 Experiment Page A8 of A62

A.2 Gas gaps between capsule components

Calculate thermal expansion of capsule components:

$\alpha_g := 4.5\cdot 10^{-6}\cdot\frac{1}{K}$	Coefficient of thermal expansion of graphite (Perry's Handbook, Table 28-29)
$T_h := 800\,°C$	Irradiation temperature of graphite holder
$T_o := 25\,°C$	Reference temperature
$\Delta T_h := T_h - T_o = 775\cdot\Delta°C$	Temperature change of holder
$r_{o\_h} := 0.5\cdot 2.081\cdot in$	Outside radius of holder (Drawing 603521)
$u_{o\_h} := \alpha_g\cdot\Delta T_h\cdot r_{o\_h} = 0.0036\cdot in$	Radial thermal expansion at outside surface of holder
$r_{i\_h} := 0.5\cdot 0.510\cdot in$	Inside radius of channels in holder (Drawing 603522)
$u_{i\_h} := \alpha_g\cdot\Delta T_h\cdot r_{i\_h} = 0.0009\cdot in$	Radial thermal expansion at inside surface of channels in holder
$T_s := 900\,°C$	Irradiation temperature of specimens
$\Delta T_s := T_s - T_o = 875\cdot\Delta°C$	Temperature change of specimens
$r_{o\_s} := 0.5\cdot 0.491\cdot in$	Outside radius of specimens (Drawing 601501)
$u_{o\_s} := \alpha_g\cdot\Delta T_s\cdot r_{o\_s} = 0.001\cdot in$	Radial thermal expansion at outside surface of specimens
$u_{i\_h} - u_{o\_s} = -0.00008\cdot in$	Differential expansion between holder and specimens is negligible

ECAR-3386 As-Run Thermal Analysis of the AGC-3 Experiment Page A9 of A62

$\alpha_s := 17.3 \cdot 10^{-6} \cdot \frac{1}{K}$ Coefficient of thermal expansion of stainless steel (Perry's Handbook, Table 28-4)

$T_c := 150\,°C$ Irradiation temperature of capsule

$\Delta T_c := T_c - T_o = 125 \cdot \Delta °C$ Temperature change of capsule

$d_i := 2.13 \cdot in$ Inside diameter of capsule (drawing 630434)

$u_{i\_c} := \alpha_s \cdot \Delta T_c \cdot 0.5 \cdot d_i = 0.0023 \cdot in$ Radial thermal expansion at inside surface of capsule

Calculate location of heat shield assuming dimples on heat shield contact the inside surface of capsule:

$h_{dim} := 0.010 \cdot in$ Height of dimple on heat shield (drawing 603534)

$r_{o\_hs} := 0.5 \cdot d_i + u_{i\_c} - h_{dim} = 1.0573 \cdot in$ Outside radius of heat shield after contact with the inside surface of capsule

$t_{hs} := 0.004 in$ Thickness of heat shield (drawing 603534)

$r_{i\_hs} := r_{o\_hs} - t_{hs} = 1.0533 \cdot in$ Inside radius of heat shield

Calculate gas gaps between capsule and heat shield and between capsule and nubs on holder:

$d_c := 0.5 \cdot d_i + u_{i\_c} - r_{o\_hs} = 0.01 \cdot in$ Gas gap between capsule and heat shield

$d_{o\_n} := 2.121 \cdot in$ Outside diameter of nubs on holder (drawing 603522)

$d_n := 0.5 \cdot d_i + u_{i\_c} - 0.5 \cdot d_{o\_n} - u_{o\_h} = 0.0032 \cdot in$ Gas gap between capsule and nubs

Rings on holder separate gas zones; contact between heat shield and rings is assumed.

ECAR-3386 As-Run Thermal Analysis of the AGC-3 Experiment Page A10 of A62

Calculate gas gaps between capsule and graphite insulator at top of holder, and between heat shield and graphite insulator at top of holder:

$d_{o\_m} := 2.090 \cdot in$	Outside diameter of graphite insulator at top of holder (drawings 630428)
$d_m := 0.5 \cdot d_i + u_{i\_c} - 0.5 \cdot d_{o\_m} - u_{o\_h} = 0.019 \cdot in$	Gas gap between capsule and graphite insulator at top of holder
$d_e := r_{i\_hs} - 0.5 \cdot d_{o\_m} - u_{o\_h} = 0.0047 \cdot in$	Gas gap between heat shield and graphite insulator at top of holder

Calculate gas gaps between capsule and bottom end of holder, and between heat shield and bottom end of holder:

$d_{o\_b} := 1.991 \cdot in$	Outside diameter of bottom end of holder (drawing 603521)
$d_b := 0.5 \cdot d_i + u_{i\_c} - 0.5 \cdot d_{o\_b} - u_{o\_h} = 0.068 \cdot in$	Gas gap between capsule and bottom end of holder
$d_a := r_{i\_hs} - 0.5 \cdot d_{o\_b} - u_{o\_h} = 0.054 \cdot in$	Gas gap between heat shield and bottom end of holder

Calculate gas gaps between holder and specimens, holder and push rods, and holder and spacers:

$d_{i\_c} := 0.510 \cdot in$	Inside diameter of specimen channels in holder (drawing 603522)
$d_{i\_t} := 0.144 \cdot in$	Inside diameter of TC channels in holder (drawing 603522)
$d_{o\_s} := 0.491 \cdot in$	Outside diameter of specimens (drawing 601501)
$d_{o\_r} := 0.482 \cdot in$	Outside diameter of push rods and spacers (drawing 603523)
$d_{o\_t} := 0.125 \cdot in$	Outside diameter of thermocouples (drawing 603520)
$d_s := 0.5 \cdot \left(d_{i\_c} - d_{o\_s}\right) = 0.0095 \cdot in$	Gas gaps between specimens and holder
$d_p := 0.5 \cdot \left(d_{i\_c} - d_{o\_r}\right) = 0.014 \cdot in$	Gas gaps between spacer rod and holder, and push rod and holder

ECAR-3386 As-Run Thermal Analysis of the AGC-3 Experiment Page A11 of A62

Gas gap between thermocouples and holder is not known precisely due to the loose fit between these components; the minimum gap is assumed to be equal to 5% of the nominal gap corresponding to the case where the thermocouple is centered (ECAR-2429).

$$d_t := \begin{pmatrix} 0.05 \\ 1.95 \end{pmatrix} \cdot 0.0095\ \text{in} = \begin{pmatrix} 0.0005 \\ 0.0185 \end{pmatrix} \cdot \text{in}$$

Minimum and maximum gas gap between thermocouples and holder

Gas gap between heat shield and capsule is varied to account for uncertainty in the location of the heat shield and uncertainty in the gas mixture due to gas leakage around the rings separating gas zones; this gas gap is used to adjust the model in order to bring into agreement the measured and calculated temperatures.

$$d_c = 0.01 \cdot \text{in}$$

Nominal gas gap between capsule and heat shield

$$d_{v1} := \begin{pmatrix} 0.001 \\ 0.002 \\ 0.003 \\ 0.004 \\ 0.005 \\ 0.006 \\ 0.007 \\ 0.008 \end{pmatrix} \cdot \text{in}$$

Variable gas gaps between capsule and heat shield to account for uncertainties

$$d_{v2} := \begin{pmatrix} 0.009 \\ 0.010 \\ 0.011 \\ 0.012 \\ 0.013 \\ 0.014 \\ 0.015 \\ 0.016 \end{pmatrix} \cdot \text{in}$$

The following table shows the gas gaps between capsule and heat shield in each of five gas zones during each irradiation cycle; zone elevations are given relative to core mid-plane.

Zone Elevation (inches)		Gas Gap Between Heat Shield and Capsule (inches)		
Bottom	Top	Cycle 152B Step 1	Cycle 152B Step 2	Cycle 152B Step 3
-24.36	-16.02	0.009	0.009	0.013
-15.99	-8.02	0.014	0.013	0.012
-7.99	7.99	0.012	0.012	0.011
8.02	15.99	0.013	0.014	0.013
16.02	25	0.003	0.003	0.003
Zone Elevation (inches)		Gas Gap Between Heat Shield and Capsule (inches)		
Bottom	Top	Cycle 154B Step 1	Cycle 154B Step 2	Cycle 154B Step 3
-24.36	-16.02	0.013	0.016	0.016
-15.99	-8.02	0.010	0.011	0.011
-7.99	7.99	0.011	0.010	0.009
8.02	15.99	0.011	0.013	0.013
16.02	25	0.001	0.003	0.003
Zone Elevation (inches)		Gas Gap Between Heat Shield and Capsule (inches)		
Bottom	Top	Cycle 155A Step 1	Cycle 155A Step 2	Cycle 155A Step 3
-24.36	-16.02	0.012	0.014	0.016
-15.99	-8.02	0.012	0.012	0.011
-7.99	7.99	0.011	0.011	0.010
8.02	15.99	0.008	0.008	0.010
16.02	25	0.002	0.002	0.002
Zone Elevation (inches)		Gas Gap Between Heat Shield and Capsule (inches)		
Bottom	Top	Cycle 155B Step 1	Cycle 155B Step 2	Cycle 155B Step 3
-24.36	-16.02	0.016	0.016	0.016
-15.99	-8.02	0.010	0.010	0.010
-7.99	7.99	0.009	0.009	0.009
8.02	15.99	0.010	0.011	0.011
16.02	25	0.0005	0.0005	0.002

ECAR-3386 As-Run Thermal Analysis of the AGC-3 Experiment Page A13 of A62

Calculate temperature control gas gaps accounting for thermal expansion of heat shield, holder, and capsule:

$$d_h := \begin{pmatrix} 1.991 \\ 2.032 \\ 2.039 \\ 2.049 \\ 2.056 \\ 2.064 \\ 2.073 \\ 2.081 \end{pmatrix} \cdot in$$

Outside diameter of holder sections (drawing 603520)

$$d_g := r_{i\_hs} - 0.5 \cdot d_h - u_{o\_h} = \begin{pmatrix} 0.054 \\ 0.034 \\ 0.03 \\ 0.025 \\ 0.022 \\ 0.018 \\ 0.013 \\ 0.009 \end{pmatrix} \cdot in$$

Gas gaps between holder and heat shield after expansion

Include effect of change in diameter of graphite due to irradiation-induced shrinkage.

Effect of neutron fluence on graphite dimensions (INL/EXT-12-26255, Appendix A, 2012):

$$dpa = f(\Phi)$$

Displacemements per atom as a function of neutron fluence

$$\beta := 0.00191$$

$$\frac{\Delta D}{D} = \beta \cdot dpa$$

Diameter reduction, obtained from linear regression of data on NBG-25 specimens

Evaluate temperature control gas gaps at 3 dpa (exceeds the highest graphite dpa during irradiation):

$$d_h = \begin{pmatrix} 1.991 \\ 2.032 \\ 2.039 \\ 2.049 \\ 2.056 \\ 2.064 \\ 2.073 \\ 2.081 \end{pmatrix} \cdot in$$

Diameter of holder sections

$$d_g = \begin{pmatrix} 0.054 \\ 0.034 \\ 0.03 \\ 0.025 \\ 0.022 \\ 0.018 \\ 0.013 \\ 0.009 \end{pmatrix} \cdot in$$

Gas gaps between holder and heat shield (unirradiated)

$dpa := 3.0$

$$d_{g1} := d_g + 0.5 \cdot \beta \cdot dpa \cdot d_h = \begin{pmatrix} 0.06 \\ 0.039 \\ 0.036 \\ 0.031 \\ 0.028 \\ 0.024 \\ 0.019 \\ 0.015 \end{pmatrix} \cdot in$$

Gas gaps (irradiated at 3 dpa)

A.3 Heat transfer coefficients for conduction across gas gaps

Gas gaps (from Appendix A.2):

$$d_g = \begin{pmatrix} 0.054 \\ 0.034 \\ 0.03 \\ 0.025 \\ 0.022 \\ 0.018 \\ 0.013 \\ 0.009 \end{pmatrix} \cdot \mathrm{in}$$

Gas gaps between holder and heat shield at various segments of variable diameter holder

$d_s = 0.0095 \cdot \mathrm{in}$ Gas gaps between specimens and holder

$d_p = 0.014 \cdot \mathrm{in}$ Gas gaps between spacer rod and holder, and push rod and holder

$$d_{v1} = \begin{pmatrix} 0.001 \\ 0.002 \\ 0.003 \\ 0.004 \\ 0.005 \\ 0.006 \\ 0.007 \\ 0.008 \end{pmatrix} \cdot \mathrm{in} \qquad d_{v2} = \begin{pmatrix} 0.009 \\ 0.01 \\ 0.011 \\ 0.012 \\ 0.013 \\ 0.014 \\ 0.015 \\ 0.016 \end{pmatrix} \cdot \mathrm{in}$$

Gas gaps between capsule and heat shield

$$d_t = \begin{pmatrix} 0.0005 \\ 0.0185 \end{pmatrix} \cdot \mathrm{in}$$

Gas gaps between holder and thermocouple

$d_m = 0.0187 \cdot \mathrm{in}$ Gas gap between capsule and upper graphite insulator

$d_b = 0.0682 \cdot \mathrm{in}$ Gas gap between capsule and bottom end of holder

$d_a = 0.0542 \cdot \mathrm{in}$ Gas gap between heat shield and bottom end of holder

$d_n = 0.0032 \cdot \mathrm{in}$ Gas gap between capsule and nubs at bottom end of holder

$d_e = 0.0047 \cdot \mathrm{in}$ Gas gap between heat shield and upper graphite insulator

ECAR-3386 As-Run Thermal Analysis of the AGC-3 Experiment Page A16 of A62

Evaluate gas gap conductance using 50% helium 50% argon for all gas gaps other than temperature control gas gaps:

$$T_{gas} = \begin{pmatrix} 84 \\ 968 \\ 1652 \end{pmatrix} \cdot °F$$

$i := 0..2 \qquad m := 0..1 \qquad n := 0..7$

$$h_{s_i} := \frac{k_{50He50Ar_i}}{d_s} \qquad h_s = \begin{pmatrix} 0.279 \\ 0.588 \\ 0.694 \end{pmatrix} \cdot \frac{BTU}{in^2 \cdot hr \cdot R} \qquad h_{b_i} := \frac{k_{50He50Ar_i}}{d_b} \qquad h_b = \begin{pmatrix} 0.039 \\ 0.082 \\ 0.097 \end{pmatrix} \cdot \frac{BTU}{in^2 \cdot hr \cdot R}$$

$$h_{p_i} := \frac{k_{50He50Ar_i}}{d_p} \qquad h_p = \begin{pmatrix} 0.19 \\ 0.399 \\ 0.471 \end{pmatrix} \cdot \frac{BTU}{in^2 \cdot hr \cdot R} \qquad h_{n_i} := \frac{k_{50He50Ar_i}}{d_n} \qquad h_n = \begin{pmatrix} 0.836 \\ 1.76 \\ 2.078 \end{pmatrix} \cdot \frac{BTU}{in^2 \cdot hr \cdot R}$$

$$h_{v1_{i,n}} := \frac{k_{50He50Ar_i}}{d_{v1_n}} \qquad h_{v1} = \begin{pmatrix} 2.653 & 1.327 & 0.884 & 0.663 & 0.531 & 0.442 & 0.379 & 0.332 \\ 5.585 & 2.793 & 1.862 & 1.396 & 1.117 & 0.931 & 0.798 & 0.698 \\ 6.596 & 3.298 & 2.199 & 1.649 & 1.319 & 1.099 & 0.942 & 0.825 \end{pmatrix} \cdot \frac{BTU}{in^2 \cdot hr \cdot R}$$

$$h_{v2_{i,n}} := \frac{k_{50He50Ar_i}}{d_{v2_n}} \qquad h_{v2} = \begin{pmatrix} 0.295 & 0.265 & 0.241 & 0.221 & 0.204 & 0.19 & 0.177 & 0.166 \\ 0.621 & 0.559 & 0.508 & 0.465 & 0.43 & 0.399 & 0.372 & 0.349 \\ 0.733 & 0.66 & 0.6 & 0.55 & 0.507 & 0.471 & 0.44 & 0.412 \end{pmatrix} \cdot \frac{BTU}{in^2 \cdot hr \cdot R}$$

$$h_{m_i} := \frac{k_{50He50Ar_i}}{d_m} \qquad h_m = \begin{pmatrix} 0.142 \\ 0.299 \\ 0.353 \end{pmatrix} \cdot \frac{BTU}{in^2 \cdot hr \cdot R} \qquad h_{e_i} := \frac{k_{50He50Ar_i}}{d_e} \qquad h_e = \begin{pmatrix} 0.568 \\ 1.195 \\ 1.411 \end{pmatrix} \cdot \frac{BTU}{in^2 \cdot hr \cdot R}$$

$$h_{a_i} := \frac{k_{50He50Ar_i}}{d_a} \qquad h_a = \begin{pmatrix} 0.049 \\ 0.103 \\ 0.122 \end{pmatrix} \cdot \frac{BTU}{in^2 \cdot hr \cdot R}$$

$$h_{t_{i,m}} := \frac{k_{50He50Ar_i}}{d_{t_m}} \qquad h_t = \begin{pmatrix} 5.585 & 0.143 \\ 11.759 & 0.302 \\ 13.887 & 0.356 \end{pmatrix} \cdot \frac{BTU}{in^2 \cdot hr \cdot R}$$

Evaluate temperature control gas gap conductance using various gas mixtures:

$i := 0..2 \qquad j := 0..7 \qquad T_{gas} = \begin{pmatrix} 84 \\ 968 \\ 1652 \end{pmatrix} \cdot °F$

Evaluate gas gap conductance using 100% helium:

$$h_{g_{i,j}} := \frac{k_{100He_i}}{d_{g_j}} \qquad h_g = \begin{pmatrix} 0.137 & 0.22 & 0.246 & 0.295 & 0.342 & 0.42 & 0.563 & 0.808 \\ 0.274 & 0.44 & 0.491 & 0.589 & 0.684 & 0.839 & 1.126 & 1.616 \\ 0.353 & 0.568 & 0.633 & 0.759 & 0.882 & 1.082 & 1.451 & 2.084 \end{pmatrix} \cdot \frac{BTU}{in^2 \cdot hr \cdot R}$$

Evaluate gas gap conductance using 90% helium 10% argon:

$$h_{g_{i,j}} := \frac{k_{90He10Ar_i}}{d_{g_j}} \qquad h_g = \begin{pmatrix} 0.11 & 0.177 & 0.198 & 0.237 & 0.275 & 0.338 & 0.453 & 0.651 \\ 0.222 & 0.357 & 0.399 & 0.478 & 0.555 & 0.681 & 0.914 & 1.312 \\ 0.3 & 0.483 & 0.539 & 0.646 & 0.751 & 0.921 & 1.235 & 1.774 \end{pmatrix} \cdot \frac{BTU}{in^2 \cdot hr \cdot R}$$

Evaluate gas gap conductance using 80% helium 20% argon:

$$h_{g_{i,j}} := \frac{k_{80He20Ar_i}}{d_{g_j}} \qquad h_g = \begin{pmatrix} 0.088 & 0.142 & 0.158 & 0.19 & 0.221 & 0.271 & 0.363 & 0.521 \\ 0.173 & 0.279 & 0.311 & 0.373 & 0.433 & 0.531 & 0.713 & 1.023 \\ 0.248 & 0.399 & 0.445 & 0.534 & 0.62 & 0.76 & 1.02 & 1.464 \end{pmatrix} \cdot \frac{BTU}{in^2 \cdot hr \cdot R}$$

Evaluate gas gap conductance using 70% helium 30% argon:

$$h_{g_{i,j}} := \frac{k_{70He30Ar_i}}{d_{g_j}} \qquad h_g = \begin{pmatrix} 0.072 & 0.116 & 0.129 & 0.155 & 0.18 & 0.22 & 0.296 & 0.425 \\ 0.15 & 0.242 & 0.27 & 0.323 & 0.375 & 0.46 & 0.618 & 0.887 \\ 0.198 & 0.319 & 0.356 & 0.427 & 0.495 & 0.608 & 0.815 & 1.17 \end{pmatrix} \cdot \frac{BTU}{in^2 \cdot hr \cdot R}$$

Evaluate gas gap conductance using 60% helium 40 argon:

$$h_{g_{i,j}} := \frac{k_{60He40Ar_i}}{d_{g_j}} \qquad h_g = \begin{pmatrix} 0.059 & 0.095 & 0.106 & 0.128 & 0.148 & 0.182 & 0.244 & 0.35 \\ 0.124 & 0.2 & 0.223 & 0.268 & 0.311 & 0.381 & 0.512 & 0.735 \\ 0.148 & 0.239 & 0.266 & 0.319 & 0.371 & 0.455 & 0.61 & 0.876 \end{pmatrix} \cdot \frac{BTU}{in^2 \cdot hr \cdot R}$$

ECAR-3386 As-Run Thermal Analysis of the AGC-3 Experiment Page A18 of A62

Evaluate gas gap conductance using 50% helium 50% argon:

$$h_{g_{i,j}} := \frac{k_{50He50Ar_i}}{d_{g_j}} \qquad h_g = \begin{pmatrix} 0.049 & 0.079 & 0.088 & 0.105 & 0.122 & 0.15 & 0.201 & 0.289 \\ 0.103 & 0.166 & 0.185 & 0.222 & 0.258 & 0.316 & 0.424 & 0.609 \\ 0.122 & 0.196 & 0.219 & 0.262 & 0.304 & 0.373 & 0.501 & 0.719 \end{pmatrix} \cdot \frac{BTU}{in^2 \cdot hr \cdot R}$$

Evaluate gas gap conductance using 40% helium 60% argon:

$$h_{g_{i,j}} := \frac{k_{40He60Ar_i}}{d_{g_j}} \qquad h_g = \begin{pmatrix} 0.04 & 0.064 & 0.072 & 0.086 & 0.1 & 0.123 & 0.165 & 0.237 \\ 0.085 & 0.137 & 0.153 & 0.183 & 0.213 & 0.261 & 0.35 & 0.502 \\ 0.094 & 0.152 & 0.169 & 0.203 & 0.235 & 0.289 & 0.387 & 0.556 \end{pmatrix} \cdot \frac{BTU}{in^2 \cdot hr \cdot R}$$

Evaluate gas gap conductance using 30% helium 70% argon:

$$h_{g_{i,j}} := \frac{k_{30He70Ar_i}}{d_{g_j}} \qquad h_g = \begin{pmatrix} 0.032 & 0.052 & 0.058 & 0.07 & 0.081 & 0.099 & 0.133 & 0.191 \\ 0.069 & 0.11 & 0.123 & 0.148 & 0.171 & 0.21 & 0.282 & 0.405 \\ 0.078 & 0.126 & 0.14 & 0.168 & 0.195 & 0.24 & 0.322 & 0.462 \end{pmatrix} \cdot \frac{BTU}{in^2 \cdot hr \cdot R}$$

Evaluate gas gap conductance using 20% helium 80% argon:

$$h_{g_{i,j}} := \frac{k_{20He80Ar_i}}{d_{g_j}} \qquad h_g = \begin{pmatrix} 0.026 & 0.042 & 0.047 & 0.056 & 0.065 & 0.08 & 0.107 & 0.154 \\ 0.055 & 0.089 & 0.099 & 0.119 & 0.138 & 0.169 & 0.227 & 0.326 \\ 0.062 & 0.1 & 0.112 & 0.134 & 0.156 & 0.191 & 0.256 & 0.367 \end{pmatrix} \cdot \frac{BTU}{in^2 \cdot hr \cdot R}$$

Evaluate gas gap conductance using 10% helium 90% argon:

$$h_{g_{i,j}} := \frac{k_{10He90Ar_i}}{d_{g_j}} \qquad h_g = \begin{pmatrix} 0.021 & 0.033 & 0.037 & 0.045 & 0.052 & 0.064 & 0.086 & 0.123 \\ 0.044 & 0.071 & 0.079 & 0.094 & 0.11 & 0.135 & 0.181 & 0.259 \\ 0.052 & 0.084 & 0.094 & 0.113 & 0.131 & 0.161 & 0.216 & 0.31 \end{pmatrix} \cdot \frac{BTU}{in^2 \cdot hr \cdot R}$$

Evaluate gas gap conductance using 100% argon:

$$h_{g_{i,j}} := \frac{k_{100Ar_i}}{d_{g_j}} \qquad h_g = \begin{pmatrix} 0.016 & 0.026 & 0.029 & 0.035 & 0.04 & 0.05 & 0.067 & 0.096 \\ 0.034 & 0.055 & 0.061 & 0.073 & 0.085 & 0.104 & 0.14 & 0.201 \\ 0.043 & 0.069 & 0.077 & 0.092 & 0.107 & 0.131 & 0.175 & 0.252 \end{pmatrix} \cdot \frac{BTU}{in^2 \cdot hr \cdot R}$$

ECAR-3386 As-Run Thermal Analysis of the AGC-3 Experiment Page A19 of A62

Evaluate temperature control gas gap conductance including the effect of irradiation-induced shrinkage of graphite (calculation performed at 3 dpa):

$i := 0..2 \qquad j := 0..7 \qquad T_{gas} = \begin{pmatrix} 84 \\ 968 \\ 1652 \end{pmatrix} \cdot °F$

Evaluate gas gap conductance using 100% helium:

$$h_{g_{i,j}} := \frac{k_{100He_i}}{d_{g1_j}} \qquad h_g = \begin{pmatrix} 0.124 & 0.188 & 0.206 & 0.239 & 0.269 & 0.314 & 0.388 & 0.49 \\ 0.248 & 0.375 & 0.412 & 0.478 & 0.538 & 0.629 & 0.776 & 0.98 \\ 0.319 & 0.484 & 0.531 & 0.616 & 0.693 & 0.81 & 1 & 1.263 \end{pmatrix} \cdot \frac{BTU}{in^2 \cdot hr \cdot R}$$

Evaluate gas gap conductance using 90% helium 10% argon:

$$h_{g_{i,j}} := \frac{k_{90He10Ar_i}}{d_{g1_j}} \qquad h_g = \begin{pmatrix} 0.1 & 0.151 & 0.166 & 0.192 & 0.217 & 0.253 & 0.312 & 0.394 \\ 0.201 & 0.305 & 0.334 & 0.388 & 0.437 & 0.51 & 0.63 & 0.795 \\ 0.272 & 0.412 & 0.452 & 0.524 & 0.59 & 0.69 & 0.851 & 1.075 \end{pmatrix} \cdot \frac{BTU}{in^2 \cdot hr \cdot R}$$

Evaluate gas gap conductance using 80% helium 20% argon:

$$h_{g_{i,j}} := \frac{k_{80He20Ar_i}}{d_{g1_j}} \qquad h_g = \begin{pmatrix} 0.08 & 0.121 & 0.133 & 0.154 & 0.173 & 0.203 & 0.25 & 0.316 \\ 0.157 & 0.238 & 0.261 & 0.302 & 0.341 & 0.398 & 0.491 & 0.62 \\ 0.224 & 0.34 & 0.373 & 0.433 & 0.487 & 0.57 & 0.703 & 0.888 \end{pmatrix} \cdot \frac{BTU}{in^2 \cdot hr \cdot R}$$

Evaluate gas gap conductance using 70% helium 30% argon:

$$h_{g_{i,j}} := \frac{k_{70He30Ar_i}}{d_{g1_j}} \qquad h_g = \begin{pmatrix} 0.065 & 0.099 & 0.108 & 0.125 & 0.141 & 0.165 & 0.204 & 0.257 \\ 0.136 & 0.206 & 0.226 & 0.262 & 0.295 & 0.345 & 0.426 & 0.538 \\ 0.179 & 0.272 & 0.298 & 0.346 & 0.39 & 0.455 & 0.562 & 0.709 \end{pmatrix} \cdot \frac{BTU}{in^2 \cdot hr \cdot R}$$

Evaluate gas gap conductance using 60% helium 40% argon:

$$h_{g_{i,j}} := \frac{k_{60He40Ar_i}}{d_{g1_j}} \qquad h_g = \begin{pmatrix} 0.054 & 0.081 & 0.089 & 0.103 & 0.117 & 0.136 & 0.168 & 0.212 \\ 0.113 & 0.171 & 0.187 & 0.217 & 0.245 & 0.286 & 0.353 & 0.445 \\ 0.134 & 0.204 & 0.223 & 0.259 & 0.292 & 0.341 & 0.421 & 0.531 \end{pmatrix} \cdot \frac{BTU}{in^2 \cdot hr \cdot R}$$

Evaluate gas gap conductance using 50% helium 50% argon:

$$h_{g_{i,j}} := \frac{k_{50He50Ar_i}}{d_{g1_j}} \qquad h_g = \begin{pmatrix} 0.044 & 0.067 & 0.074 & 0.085 & 0.096 & 0.112 & 0.139 & 0.175 \\ 0.093 & 0.141 & 0.155 & 0.18 & 0.203 & 0.237 & 0.292 & 0.369 \\ 0.11 & 0.167 & 0.183 & 0.212 & 0.239 & 0.28 & 0.345 & 0.436 \end{pmatrix} \cdot \frac{BTU}{in^2 \cdot hr \cdot R}$$

Evaluate gas gap conductance using 40% helium 60% argon:

$$h_{g_{i,j}} := \frac{k_{40He60Ar_i}}{d_{g1_j}} \qquad h_g = \begin{pmatrix} 0.036 & 0.055 & 0.06 & 0.07 & 0.079 & 0.092 & 0.114 & 0.143 \\ 0.077 & 0.117 & 0.128 & 0.148 & 0.167 & 0.195 & 0.241 & 0.304 \\ 0.085 & 0.129 & 0.142 & 0.164 & 0.185 & 0.216 & 0.267 & 0.337 \end{pmatrix} \cdot \frac{BTU}{in^2 \cdot hr \cdot R}$$

Evaluate gas gap conductance using 30% helium 70% argon:

$$h_{g_{i,j}} := \frac{k_{30He70Ar_i}}{d_{g1_j}} \qquad h_g = \begin{pmatrix} 0.029 & 0.044 & 0.049 & 0.056 & 0.064 & 0.074 & 0.092 & 0.116 \\ 0.062 & 0.094 & 0.103 & 0.12 & 0.135 & 0.158 & 0.194 & 0.246 \\ 0.071 & 0.107 & 0.118 & 0.136 & 0.154 & 0.18 & 0.222 & 0.28 \end{pmatrix} \cdot \frac{BTU}{in^2 \cdot hr \cdot R}$$

Evaluate gas gap conductance using 20% helium 80% argon:

$$h_{g_{i,j}} := \frac{k_{20He80Ar_i}}{d_{g1_j}} \qquad h_g = \begin{pmatrix} 0.024 & 0.036 & 0.039 & 0.046 & 0.051 & 0.06 & 0.074 & 0.094 \\ 0.05 & 0.076 & 0.083 & 0.096 & 0.109 & 0.127 & 0.157 & 0.198 \\ 0.056 & 0.085 & 0.094 & 0.109 & 0.122 & 0.143 & 0.176 & 0.223 \end{pmatrix} \cdot \frac{BTU}{in^2 \cdot hr \cdot R}$$

Evaluate gas gap conductance using 10% helium 90% argon:

$$h_{g_{i,j}} := \frac{k_{10He90Ar_i}}{d_{g1_j}} \qquad h_g = \begin{pmatrix} 0.019 & 0.029 & 0.031 & 0.036 & 0.041 & 0.048 & 0.059 & 0.074 \\ 0.04 & 0.06 & 0.066 & 0.077 & 0.086 & 0.101 & 0.124 & 0.157 \\ 0.047 & 0.072 & 0.079 & 0.092 & 0.103 & 0.12 & 0.149 & 0.188 \end{pmatrix} \cdot \frac{BTU}{in^2 \cdot hr \cdot R}$$

Evaluate gas gap conductance using 100% argon:

$$h_{g_{i,j}} := \frac{k_{100Ar_i}}{d_{g1_j}} \qquad h_g = \begin{pmatrix} 0.015 & 0.022 & 0.024 & 0.028 & 0.032 & 0.037 & 0.046 & 0.058 \\ 0.031 & 0.047 & 0.051 & 0.059 & 0.067 & 0.078 & 0.096 & 0.122 \\ 0.039 & 0.059 & 0.064 & 0.074 & 0.084 & 0.098 & 0.121 & 0.153 \end{pmatrix} \cdot \frac{BTU}{in^2 \cdot hr \cdot R}$$

ECAR-3386 As-Run Thermal Analysis of the AGC-3 Experiment Page A21 of A62

A.4 Turbulent forced convection in the annulus between capsule and chopped dummy in-pile tube

$T_{inlet} := 125\,°F$ $\quad P_{inlet} := 360 \cdot psi$ Primary coolant inlet temperature and pressure

$\Delta p := 77 \cdot psi$ Core pressure drop for 2-pump operation

$T_{film} := \begin{pmatrix} 125 \\ 170 \\ 260 \end{pmatrix} °F$ Assumed range of film temperature

Interpolated thermophysical property values at film temperature:

$$\rho := \begin{bmatrix} 0.5 \cdot \left(\rho_{H2O_0} + \rho_{H2O_1}\right) \\ \rho_{H2O_1} \\ \rho_{H2O_2} \end{bmatrix} \qquad \rho = \begin{pmatrix} 0.0354 \\ 0.035 \\ 0.0336 \end{pmatrix} \cdot \frac{lb}{in^3}$$

$$c_p := \begin{bmatrix} 0.5 \cdot \left(c_{p\_H2O_0} + c_{p\_H2O_1}\right) \\ c_{p\_H2O_1} \\ c_{p\_H2O_2} \end{bmatrix} \qquad c_p = \begin{pmatrix} 0.998 \\ 1.001 \\ 1.015 \end{pmatrix} \cdot \frac{BTU}{lb \cdot R}$$

$$k := \begin{bmatrix} 0.5 \cdot \left(k_{H2O_0} + k_{H2O_1}\right) \\ k_{H2O_1} \\ k_{H2O_2} \end{bmatrix} \qquad k = \begin{pmatrix} 0.031 \\ 0.032 \\ 0.033 \end{pmatrix} \cdot \frac{BTU}{hr \cdot in \cdot R}$$

$$\mu := \begin{bmatrix} 0.5 \cdot \left(\mu_{H2O_0} + \mu_{H2O_1}\right) \\ \mu_{H2O_1} \\ \mu_{H2O_2} \end{bmatrix} \qquad \mu = \begin{pmatrix} 0.124 \\ 0.075 \\ 0.044 \end{pmatrix} \cdot \frac{lb}{hr \cdot in}$$

$$Pr := \begin{bmatrix} 0.5 \cdot \left(Pr_{H2O_0} + Pr_{H2O_1}\right) \\ Pr_{H2O_1} \\ Pr_{H2O_2} \end{bmatrix} \qquad Pr = \begin{pmatrix} 4.06 \\ 2.32 \\ 1.34 \end{pmatrix}$$

ECAR-3386 As-Run Thermal Analysis of the AGC-3 Experiment Page A22 of A62

Hydrodynamics in the annulus between capsule and chopped dummy in-pile tube:

$D_i := 2.50 \cdot in$		Outside diameter of capsule (drawing 630434)
$D_o := 2.624 \cdot in$		Inside diameter of chopped dummy in-pile tube (drawing 443027)
$D_{hy} := D_o - D_i$	$D_{hy} = 0.124 \cdot in$	Hydraulic diameter of annulus
$A_f := \frac{\pi}{4} \cdot (D_o + D_i) \cdot D_{hy}$	$A_f = 0.499 \cdot in^2$	Flow area of annulus
$L_f := 145 \cdot in$		Length of annulus (Drawings 603520 and 443027)
$V_f := 218.7 \cdot \frac{in}{s}$		Flow velocity (initially assumed due to nonlinear f-Re dependence)
$Re := \frac{\rho_0 \cdot D_{hy} \cdot V_f}{\mu_0}$	$Re = 27981$	
$\varepsilon := 250 \times 10^{-6}\ in$		Wall roughness (Perry's Handbook, Table 6-1)
$f := \left[-4 \cdot \log\left[\frac{0.27 \cdot \varepsilon}{D_{hy}} + \left(\frac{7}{Re}\right)^{0.9}\right]\right]^{-2}$		Turbulent Fanning friction factor for rough tubes (Perry's Handbook, Eq. 6-39)
$f = 0.00717$		
$K_c := 0.5$		Maximum loss coefficient for sudden contraction (Perry's Handbook, Eq. 6-91)
$K_e := 1.0$		Maximum loss coefficient for sudden enlargement (Perry's Handbook, Eq. 6-95)
$K_f := \frac{4 \cdot f \cdot L_f}{D_{hy}}$	$K_f = 33.554$	Loss coefficient for pipe friction (Perry's Handbook, Eq. 6-32)

ECAR-3386 As-Run Thermal Analysis of the AGC-3 Experiment Page A23 of A62

Bernoulli equation (Perry's Handbook, Eq. 6-90):

$$V_f := \sqrt{\frac{2 \cdot \Delta p}{\rho_0 \cdot (K_c + K_e + K_f)}} \qquad V_f = 218.7 \cdot \frac{in}{s}$$

Checks (equal to velocity assumed in Re)

$$Q_f := V_f \cdot A_f \qquad Q_f = 28.4 \cdot \frac{gal}{min}$$

$$m_f := \rho_0 \cdot V_f \qquad m_f = 27914 \cdot \frac{lb}{in^2 \cdot hr}$$

Heat transfer coefficient for turbulent forced convection in an annulus:

Colburn correlation (Perry's Handbook, Eq. 5-50c, using film temperature method to account for fluid property variation):

$$i := 0..1$$

$$Re_{i_i} := \frac{\rho_i \cdot D_{hy} \cdot V_f}{\mu_i} \qquad Re_i = \begin{pmatrix} 27987 \\ 45670 \end{pmatrix}$$

Reynolds number

Nusselt number (applies to both surfaces of annulus):

$$Nu_i := 0.023 \cdot \left(Re_{i_i}\right)^{0.8} \cdot \left(Pr_i\right)^{0.33} \qquad Nu = \begin{pmatrix} 131.858 \\ 162.196 \end{pmatrix}$$

$$h_i := \frac{Nu_i \cdot k_i}{D_{hy}} \qquad h = \begin{pmatrix} 32.9 \\ 42.13 \end{pmatrix} \cdot \frac{BTU}{hr \cdot in^2 \cdot R}$$

ECAR-3386 As-Run Thermal Analysis of the AGC-3 Experiment Page A24 of A62

A.5 Nuclear heating rates

Heating rates at 20.4 MW east source power (ECAR-3051 Tables 3 through 9). A cosine function is used to represent the axial heating profile. In some cases, the heating rates are averaged over azimuthal segments.

Heating rates of stainless steel capsule, averaged over azimuthal segments:

$$x := \begin{pmatrix} -24.12 \\ -23.125 \\ -22.125 \\ -21.125 \\ -20.125 \\ -19.125 \\ -18.125 \\ -17.125 \\ -15.125 \\ -13.125 \\ -11.125 \\ -9.125 \\ -7.125 \\ -5.125 \\ -3.125 \\ -1.125 \\ 1.125 \\ 3.125 \\ 5.125 \\ 7.125 \\ 9.125 \\ 11.125 \\ 13.125 \\ 15.125 \\ 17.125 \\ 18.125 \\ 19.125 \\ 20.125 \\ 21.125 \\ 22.125 \\ 23.125 \\ 24.125 \end{pmatrix} \cdot in \qquad q_{capsule} := \begin{pmatrix} 1.92 \\ 2.36 \\ 2.77 \\ 3.15 \\ 3.51 \\ 3.90 \\ 4.27 \\ 4.61 \\ 5.26 \\ 5.83 \\ 6.29 \\ 6.70 \\ 7.03 \\ 7.26 \\ 7.36 \\ 7.43 \\ 7.40 \\ 7.27 \\ 7.06 \\ 6.75 \\ 6.35 \\ 5.86 \\ 5.30 \\ 4.62 \\ 3.94 \\ 3.53 \\ 3.08 \\ 2.66 \\ 2.21 \\ 1.74 \\ 1.36 \\ 1.06 \end{pmatrix} \cdot \frac{W}{gm}$$

ECAR-3386 As-Run Thermal Analysis of the AGC-3 Experiment Page A25 of A62

$f(x,a,b,c) := a \cdot \cos[b \cdot (x + c)]$ Axial heating profile

$g_s := \begin{pmatrix} 10 \\ 0.05 \\ 1 \end{pmatrix}$ Inital guess of regression coefficients

$s_f := \text{genfit}\left(\frac{x}{in}, \frac{q_{capsule}}{\frac{W}{gm}}, g_s, f\right)$ Calculate regression coefficients for heating profile

$s_f = \begin{pmatrix} 7.505 \\ 0.057 \\ 1.065 \end{pmatrix}$

$F_f(x) := f\left(x, s_{f_0}, s_{f_1}, s_{f_2}\right)$ Axial heating profile

$\rho_{SST} \cdot s_{f_0} \cdot \frac{W}{gm} = 3369 \cdot \frac{BTU}{hr \cdot in^3}$ Peak heating

Plot comparing calculated heating data to heating data fitted to a cosine function:

$z := \frac{x}{in}$

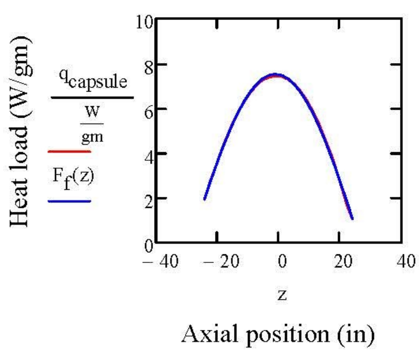

ECAR-3386 As-Run Thermal Analysis of the AGC-3 Experiment Page A26 of A62

Heating rates of stainless steel heat shield, averaged over azimuthal segments:

$$x = \begin{pmatrix} -24.12 \\ -23.125 \\ -22.125 \\ -21.125 \\ -20.125 \\ -19.125 \\ -18.125 \\ -17.125 \\ -15.125 \\ -13.125 \\ -11.125 \\ -9.125 \\ -7.125 \\ -5.125 \\ -3.125 \\ -1.125 \\ 1.125 \\ 3.125 \\ 5.125 \\ 7.125 \\ 9.125 \\ 11.125 \\ 13.125 \\ 15.125 \\ 17.125 \\ 18.125 \\ 19.125 \\ 20.125 \\ 21.125 \\ 22.125 \\ 23.125 \\ 24.125 \end{pmatrix} \cdot in \qquad q_{shield} := \begin{pmatrix} 2.58 \\ 3.43 \\ 4.13 \\ 4.69 \\ 5.28 \\ 5.89 \\ 6.41 \\ 6.92 \\ 7.91 \\ 8.78 \\ 9.37 \\ 9.98 \\ 10.51 \\ 10.74 \\ 10.96 \\ 11.03 \\ 11.01 \\ 10.78 \\ 10.36 \\ 9.94 \\ 9.33 \\ 8.60 \\ 7.74 \\ 6.76 \\ 5.71 \\ 5.06 \\ 4.36 \\ 3.73 \\ 3.07 \\ 2.33 \\ 1.81 \\ 1.41 \end{pmatrix} \cdot \frac{W}{gm}$$

ECAR-3386 As-Run Thermal Analysis of the AGC-3 Experiment Page A27 of A62

$f(x,a,b,c) := a \cdot \cos[b \cdot (x + c)]$ Axial heating profile

$g_s := \begin{pmatrix} 10 \\ 0.05 \\ 1 \end{pmatrix}$ Inital guess of regression coefficients

$s_f := \text{genfit}\left(\frac{x}{in}, \frac{q_{shield}}{\frac{W}{gm}}, g_s, f\right)$ Calculate regression coefficients for heating profile

$s_f = \begin{pmatrix} 11.162 \\ 0.057 \\ 1.228 \end{pmatrix}$

$F_f(x) := f\left(x, s_{f_0}, s_{f_1}, s_{f_2}\right)$ Axial heating profile

$\rho_H \cdot s_{f_0} \cdot \frac{W}{gm} = 5492 \cdot \frac{BTU}{hr \cdot in^3}$ Peak heating

Plot comparing calculated heating data to heating data fitted to a cosine function:

$z := \frac{x}{in}$

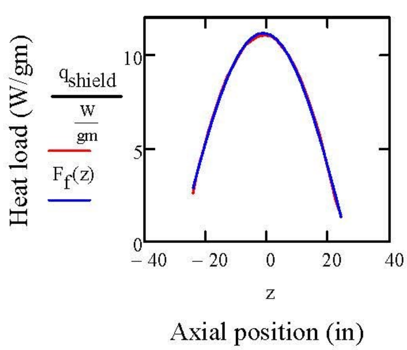

ECAR-3386 As-Run Thermal Analysis of the AGC-3 Experiment Page A28 of A62

Heating rates of graphite holder, averaged over azimuthal segments:

$$x = \begin{pmatrix} -24.12 \\ -23.125 \\ -22.125 \\ -21.125 \\ -20.125 \\ -19.125 \\ -18.125 \\ -17.125 \\ -15.125 \\ -13.125 \\ -11.125 \\ -9.125 \\ -7.125 \\ -5.125 \\ -3.125 \\ -1.125 \\ 1.125 \\ 3.125 \\ 5.125 \\ 7.125 \\ 9.125 \\ 11.125 \\ 13.125 \\ 15.125 \\ 17.125 \\ 18.125 \\ 19.125 \\ 20.125 \\ 21.125 \\ 22.125 \\ 23.125 \\ 24.125 \end{pmatrix} \cdot in \qquad q_{holder} := \begin{pmatrix} 1.53 \\ 2.01 \\ 2.29 \\ 2.61 \\ 2.92 \\ 3.22 \\ 3.53 \\ 3.83 \\ 4.35 \\ 4.82 \\ 5.20 \\ 5.53 \\ 5.79 \\ 5.98 \\ 6.09 \\ 6.16 \\ 6.12 \\ 6.01 \\ 5.86 \\ 5.60 \\ 5.27 \\ 4.87 \\ 4.42 \\ 3.87 \\ 3.29 \\ 2.99 \\ 2.61 \\ 2.30 \\ 2.01 \\ 1.66 \\ 1.34 \\ 1.07 \end{pmatrix} \cdot \frac{W}{gm}$$

ECAR-3386 As-Run Thermal Analysis of the AGC-3 Experiment Page A29 of A62

$f(x,a,b,c) := a\cdot\cos[b\cdot(x+c)]$ Axial heating profile

$g_s := \begin{pmatrix} 10 \\ 0.05 \\ 1 \end{pmatrix}$ Inital guess of regression coefficients

$s_f := \mathrm{genfit}\left(\frac{x}{in}, \frac{q_{holder}}{\frac{W}{gm}}, g_s, f\right)$ Calculate regression coefficients for heating profile

$s_f = \begin{pmatrix} 6.19 \\ 0.056 \\ 0.901 \end{pmatrix}$

$F_f(x) := f\left(x, s_{f_0}, s_{f_1}, s_{f_2}\right)$ Axial heating profile

$\rho_g \cdot s_{f_0} \cdot \frac{W}{gm} = 631 \cdot \frac{BTU}{hr \cdot in^3}$ Peak heating

Plot comparing calculated heating data to heating data fitted to a cosine function:

$z := \frac{x}{in}$

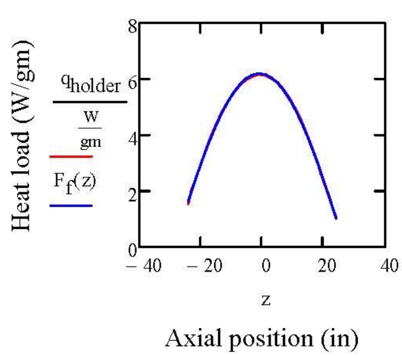

Heating rates of graphite samples in the center channel, during the first two cycles of irradiation (152B and 154B):

$$x = \begin{pmatrix} -24.12 \\ -23.125 \\ -22.125 \\ -21.125 \\ -20.125 \\ -19.125 \\ -18.125 \\ -17.125 \\ -15.125 \\ -13.125 \\ -11.125 \\ -9.125 \\ -7.125 \\ -5.125 \\ -3.125 \\ -1.125 \\ 1.125 \\ 3.125 \\ 5.125 \\ 7.125 \\ 9.125 \\ 11.125 \\ 13.125 \\ 15.125 \\ 17.125 \\ 18.125 \\ 19.125 \\ 20.125 \\ 21.125 \\ 22.125 \\ 23.125 \\ 24.125 \end{pmatrix} \cdot in \qquad q_{sample} := \begin{pmatrix} 1.49 \\ 2.03 \\ 2.32 \\ 2.61 \\ 2.9 \\ 3.24 \\ 3.49 \\ 3.8 \\ 4.35 \\ 4.8 \\ 5.19 \\ 5.52 \\ 5.81 \\ 5.97 \\ 6.03 \\ 6.11 \\ 6.11 \\ 6.1 \\ 5.87 \\ 5.62 \\ 5.21 \\ 4.88 \\ 4.4 \\ 3.86 \\ 3.27 \\ 3.02 \\ 3.69 \\ 2.23 \\ 2.03 \\ 1.68 \\ 1.39 \\ 1.1 \end{pmatrix} \cdot \frac{W}{gm}$$

ECAR-3386 As-Run Thermal Analysis of the AGC-3 Experiment Page A31 of A62

$$f(x,a,b,c) := a\cdot\cos[b\cdot(x+c)]$$ Axial heating profile

$$g_s := \begin{pmatrix} 10 \\ 0.05 \\ 1 \end{pmatrix}$$ Inital guess of regression coefficients

$$s_f := \mathrm{genfit}\left(\frac{x}{in}, \frac{q_{sample}}{\frac{W}{gm}}, g_s, f\right)$$ Calculate regression coefficients for heating profile

$$s_f = \begin{pmatrix} 6.18 \\ 0.056 \\ 0.73 \end{pmatrix}$$

$$F_f(x) := f\left(x, s_{f_0}, s_{f_1}, s_{f_2}\right)$$ Axial heating profile

$$q_{channel\_center} := \rho_g \cdot s_{f_0} \cdot \frac{W}{gm} = 630\cdot\frac{BTU}{hr\cdot in^3}$$ Peak heating

Plot comparing calculated heating data to heating data fitted to a cosine function:

$$z := \frac{x}{in}$$

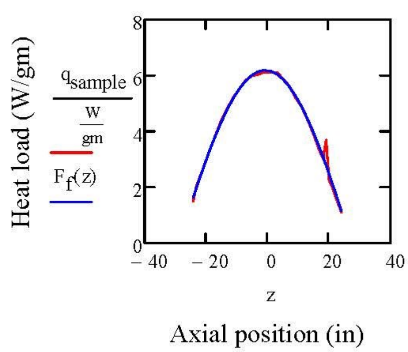

Heating rates of graphite samples in channel 1, during the first two cycles of irradiation (152B and 154B):

$$x = \begin{pmatrix} -24.12 \\ -23.125 \\ -22.125 \\ -21.125 \\ -20.125 \\ -19.125 \\ -18.125 \\ -17.125 \\ -15.125 \\ -13.125 \\ -11.125 \\ -9.125 \\ -7.125 \\ -5.125 \\ -3.125 \\ -1.125 \\ 1.125 \\ 3.125 \\ 5.125 \\ 7.125 \\ 9.125 \\ 11.125 \\ 13.125 \\ 15.125 \\ 17.125 \\ 18.125 \\ 19.125 \\ 20.125 \\ 21.125 \\ 22.125 \\ 23.125 \\ 24.125 \end{pmatrix} \cdot in \qquad q_{sample} := \begin{pmatrix} 1.65 \\ 2.19 \\ 2.53 \\ 2.89 \\ 3.16 \\ 3.48 \\ 3.84 \\ 4.17 \\ 4.71 \\ 5.32 \\ 5.67 \\ 6.04 \\ 6.27 \\ 6.51 \\ 6.63 \\ 6.67 \\ 6.64 \\ 6.58 \\ 6.36 \\ 6.02 \\ 5.77 \\ 5.32 \\ 4.75 \\ 4.26 \\ 3.6 \\ 3.26 \\ 2.94 \\ 2.59 \\ 2.19 \\ 1.81 \\ 1.45 \\ 1.15 \end{pmatrix} \cdot \frac{W}{gm}$$

ECAR-3386 As-Run Thermal Analysis of the AGC-3 Experiment Page A33 of A62

$f(x,a,b,c) := a \cdot \cos[b \cdot (x + c)]$ Axial heating profile

$g_s := \begin{pmatrix} 10 \\ 0.05 \\ 1 \end{pmatrix}$ Inital guess of regression coefficients

$s_f := \text{genfit}\left(\frac{x}{in}, \frac{q_{sample}}{\frac{W}{gm}}, g_s, f\right)$ Calculate regression coefficients for heating profile

$s_f = \begin{pmatrix} 6.733 \\ 0.056 \\ 0.889 \end{pmatrix}$

$F_f(x) := f\left(x, s_{f_0}, s_{f_1}, s_{f_2}\right)$ Axial heating profile

$q_{channel\_1} := \rho_g \cdot s_{f_0} \cdot \frac{W}{gm} = 686 \cdot \frac{BTU}{hr \cdot in^3}$ Peak heating

Plot comparing calculated heating data to heating data fitted to a cosine function:

$z := \frac{x}{in}$

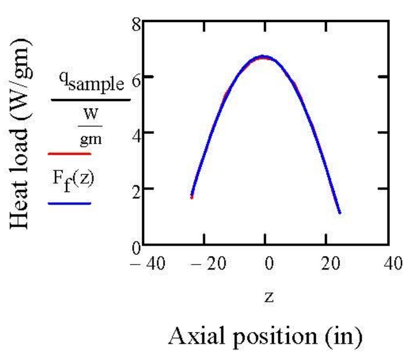

Heating rates of graphite samples in channel 2, during the first two cycles of irradiation (152B and 154B):

$$x = \begin{pmatrix} -24.12 \\ -23.125 \\ -22.125 \\ -21.125 \\ -20.125 \\ -19.125 \\ -18.125 \\ -17.125 \\ -15.125 \\ -13.125 \\ -11.125 \\ -9.125 \\ -7.125 \\ -5.125 \\ -3.125 \\ -1.125 \\ 1.125 \\ 3.125 \\ 5.125 \\ 7.125 \\ 9.125 \\ 11.125 \\ 13.125 \\ 15.125 \\ 17.125 \\ 18.125 \\ 19.125 \\ 20.125 \\ 21.125 \\ 22.125 \\ 23.125 \\ 24.125 \end{pmatrix} \cdot in \qquad q_{sample} := \begin{pmatrix} 1.57 \\ 2.14 \\ 2.42 \\ 2.75 \\ 3.07 \\ 3.34 \\ 3.66 \\ 3.97 \\ 4.52 \\ 5 \\ 5.4 \\ 5.74 \\ 6.06 \\ 6.14 \\ 6.33 \\ 6.39 \\ 6.28 \\ 6.23 \\ 6.04 \\ 5.83 \\ 5.45 \\ 5.12 \\ 4.56 \\ 4 \\ 3.44 \\ 3.08 \\ 2.76 \\ 2.42 \\ 2.14 \\ 1.78 \\ 1.43 \\ 1.11 \end{pmatrix} \cdot \frac{W}{gm}$$

Title: As-Run Thermal Analysis of the AGC-3 Experiment

ECAR No.: 3386 Rev. No.: 0 Project No.: 23747 Date: 10/11/2016

ECAR-3386 As-Run Thermal Analysis of the AGC-3 Experiment Page A35 of A62

$f(x,a,b,c) := a\cdot\cos[b\cdot(x + c)]$ Axial heating profile

$g_s := \begin{pmatrix} 10 \\ 0.05 \\ 1 \end{pmatrix}$ Inital guess of regression coefficients

$s_f := \mathrm{genfit}\left(\frac{x}{in}, \frac{q_{sample}}{\frac{W}{gm}}, g_s, f\right)$ Calculate regression coefficients for heating profile

$s_f = \begin{pmatrix} 6.409 \\ 0.056 \\ 0.9 \end{pmatrix}$

$F_f(x) := f\left(x, s_{f_0}, s_{f_1}, s_{f_2}\right)$ Axial heating profile

$q_{channel\_2} := \rho_g \cdot s_{f_0} \cdot \frac{W}{gm} = 653 \cdot \frac{BTU}{hr \cdot in^3}$ Peak heating

Plot comparing calculated heating data to heating data fitted to a cosine function:

$z := \frac{x}{in}$

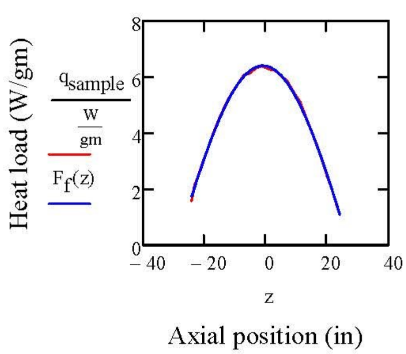

ECAR-3386 As-Run Thermal Analysis of the AGC-3 Experiment Page A36 of A62

Heating rates of graphite samples in channel 3, during the first two cycles of irradiation (152B and 154B):

$$x = \begin{pmatrix} -24.12 \\ -23.125 \\ -22.125 \\ -21.125 \\ -20.125 \\ -19.125 \\ -18.125 \\ -17.125 \\ -15.125 \\ -13.125 \\ -11.125 \\ -9.125 \\ -7.125 \\ -5.125 \\ -3.125 \\ -1.125 \\ 1.125 \\ 3.125 \\ 5.125 \\ 7.125 \\ 9.125 \\ 11.125 \\ 13.125 \\ 15.125 \\ 17.125 \\ 18.125 \\ 19.125 \\ 20.125 \\ 21.125 \\ 22.125 \\ 23.125 \\ 24.125 \end{pmatrix} \cdot in \qquad q_{sample} := \begin{pmatrix} 1.42 \\ 1.93 \\ 2.24 \\ 2.54 \\ 2.85 \\ 3.11 \\ 3.4 \\ 3.63 \\ 4.18 \\ 4.66 \\ 4.99 \\ 5.29 \\ 5.51 \\ 5.69 \\ 5.77 \\ 5.81 \\ 5.78 \\ 5.7 \\ 5.6 \\ 5.31 \\ 5.01 \\ 4.63 \\ 4.27 \\ 3.73 \\ 3.15 \\ 2.87 \\ 2.5 \\ 2.21 \\ 1.94 \\ 1.65 \\ 1.35 \\ 1.07 \end{pmatrix} \cdot \frac{W}{gm}$$

$f(x, a, b, c) := a \cdot \cos[b \cdot (x + c)]$ Axial heating profile

$g_s := \begin{pmatrix} 10 \\ 0.05 \\ 1 \end{pmatrix}$ Inital guess of regression coefficients

$s_f := \text{genfit}\left(\frac{x}{in}, \frac{q_{sample}}{\frac{W}{gm}}, g_s, f\right)$ Calculate regression coefficients for heating profile

$s_f = \begin{pmatrix} 5.884 \\ 0.056 \\ 0.907 \end{pmatrix}$

$F_f(x) := f\left(x, s_{f_0}, s_{f_1}, s_{f_2}\right)$ Axial heating profile

$q_{channel\_3} := \rho_g \cdot s_{f_0} \cdot \frac{W}{gm} = 599 \cdot \frac{BTU}{hr \cdot in^3}$ Peak heating

Plot comparing calculated heating data to heating data fitted to a cosine function:

$z := \frac{x}{in}$

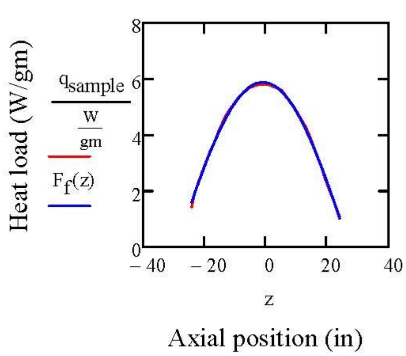

Heating rates of graphite samples in channel 4, during the first two cycles of irradiation (152B and 154B):

$$x = \begin{pmatrix} -24.12 \\ -23.125 \\ -22.125 \\ -21.125 \\ -20.125 \\ -19.125 \\ -18.125 \\ -17.125 \\ -15.125 \\ -13.125 \\ -11.125 \\ -9.125 \\ -7.125 \\ -5.125 \\ -3.125 \\ -1.125 \\ 1.125 \\ 3.125 \\ 5.125 \\ 7.125 \\ 9.125 \\ 11.125 \\ 13.125 \\ 15.125 \\ 17.125 \\ 18.125 \\ 19.125 \\ 20.125 \\ 21.125 \\ 22.125 \\ 23.125 \\ 24.125 \end{pmatrix} \cdot in \qquad q_{sample} := \begin{pmatrix} 1.38 \\ 1.83 \\ 2.12 \\ 2.43 \\ 2.67 \\ 2.99 \\ 3.27 \\ 3.49 \\ 4.02 \\ 4.46 \\ 4.79 \\ 5.09 \\ 5.38 \\ 5.48 \\ 5.59 \\ 5.63 \\ 5.6 \\ 5.52 \\ 5.4 \\ 5.19 \\ 4.82 \\ 4.45 \\ 4.04 \\ 3.55 \\ 3.05 \\ 2.79 \\ 2.36 \\ 2.13 \\ 1.89 \\ 1.56 \\ 1.25 \\ 1.04 \end{pmatrix} \cdot \frac{W}{gm}$$

ECAR-3386 As-Run Thermal Analysis of the AGC-3 Experiment Page A39 of A62

$f(x,a,b,c) := a \cdot \cos[b \cdot (x + c)]$ Axial heating profile

$g_s := \begin{pmatrix} 10 \\ 0.05 \\ 1 \end{pmatrix}$ Inital guess of regression coefficients

$s_f := \mathrm{genfit}\left(\frac{x}{in}, \frac{q_{sample}}{\frac{W}{gm}}, g_s, f\right)$ Calculate regression coefficients for heating profile

$s_f = \begin{pmatrix} 5.687 \\ 0.056 \\ 0.89 \end{pmatrix}$

$F_f(x) := f\left(x, s_{f_0}, s_{f_1}, s_{f_2}\right)$ Axial heating profile

$q_{channel\_4} := \rho_g \cdot s_{f_0} \cdot \frac{W}{gm} = 579 \cdot \frac{BTU}{hr \cdot in^3}$ Peak heating

Plot comparing calculated heating data to heating data fitted to a cosine function:

$z := \frac{x}{in}$

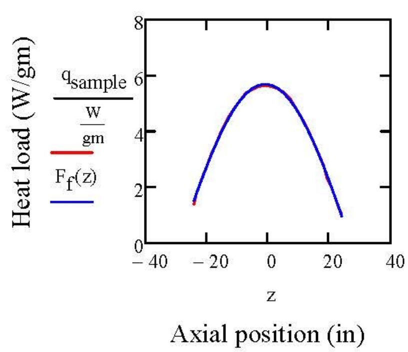

ECAR-3386 As-Run Thermal Analysis of the AGC-3 Experiment Page A40 of A62

Heating rates of graphite samples in channel 5, during the first two cycles of irradiation (152B and 154B):

$$x = \begin{pmatrix} -24.12 \\ -23.125 \\ -22.125 \\ -21.125 \\ -20.125 \\ -19.125 \\ -18.125 \\ -17.125 \\ -15.125 \\ -13.125 \\ -11.125 \\ -9.125 \\ -7.125 \\ -5.125 \\ -3.125 \\ -1.125 \\ 1.125 \\ 3.125 \\ 5.125 \\ 7.125 \\ 9.125 \\ 11.125 \\ 13.125 \\ 15.125 \\ 17.125 \\ 18.125 \\ 19.125 \\ 20.125 \\ 21.125 \\ 22.125 \\ 23.125 \\ 24.125 \end{pmatrix} \cdot in \qquad q_{sample} := \begin{pmatrix} 1.47 \\ 1.95 \\ 2.29 \\ 2.59 \\ 2.86 \\ 3.18 \\ 3.47 \\ 3.72 \\ 4.29 \\ 4.71 \\ 5.13 \\ 5.52 \\ 5.77 \\ 5.84 \\ 6.1 \\ 6.1 \\ 6.14 \\ 5.94 \\ 5.79 \\ 5.54 \\ 5.15 \\ 4.83 \\ 4.36 \\ 3.8 \\ 3.26 \\ 2.94 \\ 2.59 \\ 2.25 \\ 2.01 \\ 1.63 \\ 1.33 \\ 1.07 \end{pmatrix} \cdot \frac{W}{gm}$$

ECAR-3386 As-Run Thermal Analysis of the AGC-3 Experiment Page A41 of A62

$f(x,a,b,c) := a\cdot\cos[b\cdot(x+c)]$ Axial heating profile

$g_s := \begin{pmatrix} 10 \\ 0.05 \\ 1 \end{pmatrix}$ Inital guess of regression coefficients

$s_f := \text{genfit}\left(\frac{x}{in}, \frac{q_{sample}}{\frac{W}{gm}}, g_s, f\right)$ Calculate regression coefficients for heating profile

$s_f = \begin{pmatrix} 6.129 \\ 0.056 \\ 0.875 \end{pmatrix}$

$F_f(x) := f\left(x, s_{f_0}, s_{f_1}, s_{f_2}\right)$ Axial heating profile

$q_{channel\_5} := \rho_g \cdot s_{f_0} \cdot \frac{W}{gm} = 624 \cdot \frac{BTU}{hr \cdot in^3}$ Peak heating

Plot comparing calculated heating data to heating data fitted to a cosine function:

$z := \frac{x}{in}$

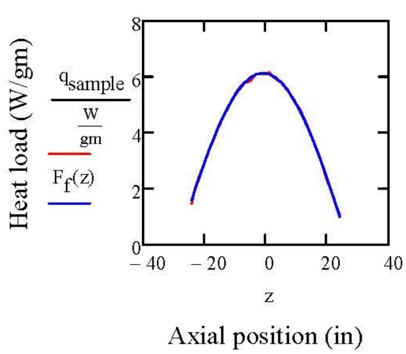

Heating rates of graphite samples in channel 6, during the first two cycles of irradiation (152B and 154B):

$$x = \begin{pmatrix} -24.12 \\ -23.125 \\ -22.125 \\ -21.125 \\ -20.125 \\ -19.125 \\ -18.125 \\ -17.125 \\ -15.125 \\ -13.125 \\ -11.125 \\ -9.125 \\ -7.125 \\ -5.125 \\ -3.125 \\ -1.125 \\ 1.125 \\ 3.125 \\ 5.125 \\ 7.125 \\ 9.125 \\ 11.125 \\ 13.125 \\ 15.125 \\ 17.125 \\ 18.125 \\ 19.125 \\ 20.125 \\ 21.125 \\ 22.125 \\ 23.125 \\ 24.125 \end{pmatrix} \cdot in \qquad q_{sample} := \begin{pmatrix} 1.6 \\ 2.14 \\ 2.44 \\ 2.81 \\ 3.16 \\ 3.46 \\ 3.77 \\ 4.1 \\ 4.7 \\ 5.16 \\ 5.64 \\ 6 \\ 6.25 \\ 6.45 \\ 6.6 \\ 6.64 \\ 6.63 \\ 6.48 \\ 6.27 \\ 6 \\ 5.68 \\ 5.17 \\ 4.72 \\ 4.18 \\ 3.54 \\ 3.22 \\ 2.83 \\ 2.47 \\ 2.14 \\ 1.78 \\ 1.44 \\ 1.13 \end{pmatrix} \cdot \frac{W}{gm}$$

$f(x,a,b,c) := a\cdot\cos[b\cdot(x+c)]$ Axial heating profile

$g_s := \begin{pmatrix} 10 \\ 0.05 \\ 1 \end{pmatrix}$ Inital guess of regression coefficients

$s_f := \mathrm{genfit}\left(\frac{x}{in}, \frac{q_{sample}}{\frac{W}{gm}}, g_s, f\right)$ Calculate regression coefficients for heating profile

$s_f = \begin{pmatrix} 6.674 \\ 0.056 \\ 0.903 \end{pmatrix}$

$F_f(x) := f\left(x, s_{f_0}, s_{f_1}, s_{f_2}\right)$ Axial heating profile

$q_{channel\_6} := \rho_g \cdot s_{f_0} \cdot \frac{W}{gm} = 680 \cdot \frac{BTU}{hr \cdot in^3}$ Peak heating

Plot comparing calculated heating data to heating data fitted to a cosine function:

$z := \frac{x}{in}$

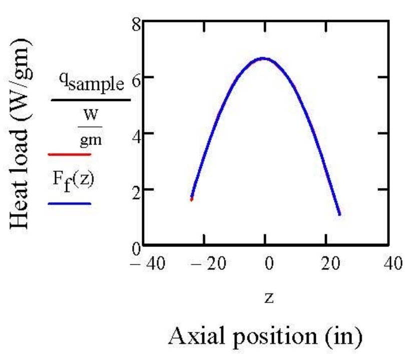

The test train was rotated 180 degrees after the first two cycles of irradiation.

Effect of 180 degree test train rotation on the azimuthal position of the graphite samples (the symbol <-> indicates that the heating rates in these channels are interchanged):

channel 1 <-> channel 4

channel 2 <-> channel 5

channel 3 <-> channel 6

Peak heating rate of each channel of graphite samples during the second two cycles of irradiation (155A and 155B):

$$q_{channel\_center} := 630 \frac{BTU}{hr \cdot in^3}$$

$$q_{channel\_1} := 579 \frac{BTU}{hr \cdot in^3}$$

$$q_{channel\_2} := 624 \frac{BTU}{hr \cdot in^3}$$

$$q_{channel\_3} := 680 \frac{BTU}{hr \cdot in^3}$$

$$q_{channel\_4} := 686 \frac{BTU}{hr \cdot in^3}$$

$$q_{channel\_5} := 653 \frac{BTU}{hr \cdot in^3}$$

$$q_{channel\_6} := 599 \frac{BTU}{hr \cdot in^3}$$

ECAR-3386 As-Run Thermal Analysis of the AGC-3 Experiment Page A45 of A62

Heating rates of coolant:

$$x = \begin{pmatrix} -24.12 \\ -23.125 \\ -22.125 \\ -21.125 \\ -20.125 \\ -19.125 \\ -18.125 \\ -17.125 \\ -15.125 \\ -13.125 \\ -11.125 \\ -9.125 \\ -7.125 \\ -5.125 \\ -3.125 \\ -1.125 \\ 1.125 \\ 3.125 \\ 5.125 \\ 7.125 \\ 9.125 \\ 11.125 \\ 13.125 \\ 15.125 \\ 17.125 \\ 18.125 \\ 19.125 \\ 20.125 \\ 21.125 \\ 22.125 \\ 23.125 \\ 24.125 \end{pmatrix} \cdot in \qquad q_{coolant} := \begin{pmatrix} 3.27 \\ 4.12 \\ 4.88 \\ 5.56 \\ 6.24 \\ 6.92 \\ 7.58 \\ 8.23 \\ 9.38 \\ 10.38 \\ 11.24 \\ 11.93 \\ 12.44 \\ 12.85 \\ 13.08 \\ 13.13 \\ 13.16 \\ 12.96 \\ 12.57 \\ 11.99 \\ 11.34 \\ 10.47 \\ 9.47 \\ 8.36 \\ 7.11 \\ 6.37 \\ 5.63 \\ 4.93 \\ 4.25 \\ 3.55 \\ 2.86 \\ 2.22 \end{pmatrix} \cdot \frac{W}{gm}$$

$f(x,a,b,c) := a \cdot \cos[b \cdot (x + c)]$ Axial heating profile

$g_s := \begin{pmatrix} 10 \\ 0.05 \\ 1 \end{pmatrix}$ Inital guess of regression coefficients

$s_f := \text{genfit}\left(\frac{x}{in}, \frac{q_{coolant}}{\frac{W}{gm}}, g_s, f\right)$ Calculate regression coefficients for heating profile

$s_f = \begin{pmatrix} 13.315 \\ 0.056 \\ 0.891 \end{pmatrix}$

$F_f(x) := f\left(x, s_{f_0}, s_{f_1}, s_{f_2}\right)$ Axial heating profile

$\rho_0 \cdot s_{f_0} \cdot \frac{W}{gm} = 730 \cdot \frac{BTU}{hr \cdot in^3}$ Peak heating

Plot comparing calculated heating data to heating data fitted to a cosine function:

$z := \frac{x}{in}$

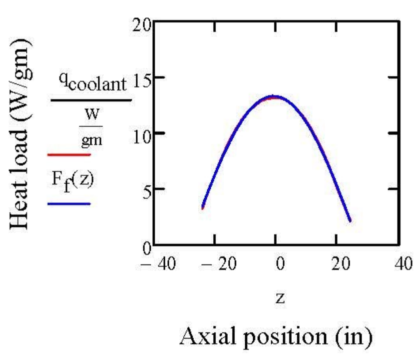

Calculate average density of thermocouple:

$D_{o\_tc} := 0.125 \cdot in$ Outside diameter of thermocouple sheath

$D_{i\_tc} := 0.093 \cdot in$ Inside diameter of thermocouple sheath

$D_{wire} := 0.025 \cdot in$ Diameter of thermocouple wire

$A_{wire} := 2 \cdot \frac{\pi}{4} \cdot D_{wire}^{2}$ Cross sectional area of 2 wires

$D_{i\_ins} := \sqrt{\frac{4}{\pi} \cdot A_{wire}} = 0.0354 \cdot in$ Inside diameter of insulation

$A_{sheath} := \frac{\pi}{4} \cdot \left(D_{o\_tc}^{2} - D_{i\_tc}^{2}\right) = 0.0055 \cdot in^{2}$ Cross sectional area of sheath

$A_{ins} := \frac{\pi}{4} \cdot \left(D_{i\_tc}^{2} - D_{i\_ins}^{2}\right) = 0.0375 \cdot cm^{2}$ Cross sectional area of insulation

$\rho_{metal} := 8.4 \frac{gm}{cm^{3}}$ Density of sheath and wires

$\rho_{MgO} := 3.65 \frac{gm}{cm^{3}}$ Density of insulation

Density of thermocouple (composite material consisting of inconel sheath, MgO insulation, and wires)

$$\rho_{tc} := \frac{\rho_{metal} \cdot \left(A_{sheath} + A_{wire}\right) + \rho_{MgO} \cdot A_{ins}}{A_{sheath} + A_{wire} + A_{ins}} = 6.2 \cdot \frac{gm}{cm^{3}}$$

ECAR-3386 As-Run Thermal Analysis of the AGC-3 Experiment Page A48 of A62

Heating rates of thermocouples (average of thermocouples TC-10 and TC-11 spanning an elevation from 18 inches below core to the top of core), during the first two cycles of irradiation (152B and 154B):

$$x := \begin{pmatrix} -18.125 \\ -17.125 \\ -15.125 \\ -13.125 \\ -11.125 \\ -9.125 \\ -7.125 \\ -5.125 \\ -3.125 \\ -1.125 \\ 1.125 \\ 3.125 \\ 5.125 \\ 7.125 \\ 9.125 \\ 11.125 \\ 13.125 \\ 15.125 \\ 17.125 \\ 18.125 \\ 19.125 \\ 20.125 \\ 21.125 \\ 22.125 \\ 23.125 \\ 24.125 \end{pmatrix} \cdot in \qquad q_{tc} := \begin{pmatrix} 3.81 \\ 5.76 \\ 6.41 \\ 7.18 \\ 7.71 \\ 8.42 \\ 8.60 \\ 8.64 \\ 9.19 \\ 9.08 \\ 9.23 \\ 8.93 \\ 8.84 \\ 8.40 \\ 7.85 \\ 7.18 \\ 6.51 \\ 5.65 \\ 4.82 \\ 4.32 \\ 3.73 \\ 3.16 \\ 2.60 \\ 2.05 \\ 1.60 \\ 1.27 \end{pmatrix} \cdot \frac{W}{gm}$$

$f(x,a,b,c) := a\cdot\cos[b\cdot(x+c)]$ Axial heating profile

$g_s := \begin{pmatrix} 10 \\ 0.05 \\ 1 \end{pmatrix}$ Inital guess of regression coefficients

$s_f := \text{genfit}\left(\frac{x}{in}, \frac{q_{tc}}{\frac{W}{gm}}, g_s, f\right)$ Calculate regression coefficients for heating profile

$s_f = \begin{pmatrix} 9.298 \\ 0.059 \\ 0.596 \end{pmatrix}$

$F_f(x) := f\left(x, s_{f_0}, s_{f_1}, s_{f_2}\right)$ Axial heating profile

$q_{TC\_profile} := \rho_{tc}\cdot s_{f_0}\cdot\frac{W}{gm} = 3198\cdot\frac{BTU}{hr\cdot in^3}$ Peak heating

Plot comparing calculated heating data to heating data fitted to a cosine function:

$z := \frac{x}{in}$

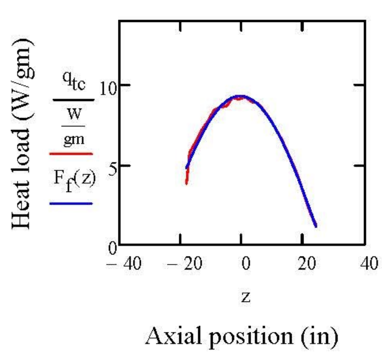

ECAR-3386 As-Run Thermal Analysis of the AGC-3 Experiment Page A50 of A62

Ratio of the heating rate of each TC to the heating rate obtained from the heating profile at an elevation of 18.125 inches above core mid-plane (the location closest to core-mid-plane at which the TC heating rates can be compared):

$$\gamma_{TC01} := \frac{4.15}{4.32} = 0.961 \qquad \gamma_{TC07} := \frac{3.93}{4.32} = 0.91$$

$$\gamma_{TC02} := \frac{4.29}{4.32} = 0.993 \qquad \gamma_{TC08} := \frac{3.61}{4.32} = 0.836$$

$$\gamma_{TC03} := \frac{4.27}{4.32} = 0.988 \qquad \gamma_{TC09} := \frac{4.16}{4.32} = 0.963$$

$$\gamma_{TC04} := \frac{3.84}{4.32} = 0.889 \qquad \gamma_{TC10} := \frac{4.38}{4.32} = 1.014$$

$$\gamma_{TC05} := \frac{3.66}{4.32} = 0.847 \qquad \gamma_{TC11} := \frac{4.26}{4.32} = 0.986$$

$$\gamma_{TC06} := \frac{4.09}{4.32} = 0.947 \qquad \gamma_{TC12} := \frac{3.89}{4.32} = 0.9$$

Peak heating rate of each TC during the first two cycles of irradiation (152B and 154B):

$$q_{TC01} := \gamma_{TC01} \cdot q_{TC\_profile} = 3072 \cdot \frac{BTU}{hr \cdot in^3} \qquad q_{TC07} := \gamma_{TC07} \cdot q_{TC\_profile} = 2909 \cdot \frac{BTU}{hr \cdot in^3}$$

$$q_{TC02} := \gamma_{TC02} \cdot q_{TC\_profile} = 3176 \cdot \frac{BTU}{hr \cdot in^3} \qquad q_{TC08} := \gamma_{TC08} \cdot q_{TC\_profile} = 2672 \cdot \frac{BTU}{hr \cdot in^3}$$

$$q_{TC03} := \gamma_{TC03} \cdot q_{TC\_profile} = 3161 \cdot \frac{BTU}{hr \cdot in^3} \qquad q_{TC09} := \gamma_{TC09} \cdot q_{TC\_profile} = 3079 \cdot \frac{BTU}{hr \cdot in^3}$$

$$q_{TC04} := \gamma_{TC04} \cdot q_{TC\_profile} = 2843 \cdot \frac{BTU}{hr \cdot in^3} \qquad q_{TC10} := \gamma_{TC10} \cdot q_{TC\_profile} = 3242 \cdot \frac{BTU}{hr \cdot in^3}$$

$$q_{TC05} := \gamma_{TC05} \cdot q_{TC\_profile} = 2709 \cdot \frac{BTU}{hr \cdot in^3} \qquad q_{TC11} := \gamma_{TC11} \cdot q_{TC\_profile} = 3153 \cdot \frac{BTU}{hr \cdot in^3}$$

$$q_{TC06} := \gamma_{TC06} \cdot q_{TC\_profile} = 3028 \cdot \frac{BTU}{hr \cdot in^3} \qquad q_{TC12} := \gamma_{TC12} \cdot q_{TC\_profile} = 2880 \cdot \frac{BTU}{hr \cdot in^3}$$

ECAR-3386 As-Run Thermal Analysis of the AGC-3 Experiment Page A51 of A62

The test train was rotated 180 degrees after the first two cycles of irradiation.

Effect of 180 degree test train rotation on the azimuthal position of the thermocouples (the symbol <-> indicates that the heating rates in these channels are interchanged):

TC 1 <-> TC 6

TC 2 <-> TC 7

TC 3 <-> TC 8

TC 4 <-> TC 11

TC 5 <-> TC 10

TC 9 <-> TC 12

Peak heating rate of each TC during the second two cycles of irradiation (155A and 155B):

$$q_{TC01} := \gamma_{TC06} \cdot q_{TC\_profile} = 3028 \cdot \frac{BTU}{hr \cdot in^3} \qquad q_{TC07} := \gamma_{TC02} \cdot q_{TC\_profile} = 3176 \cdot \frac{BTU}{hr \cdot in^3}$$

$$q_{TC02} := \gamma_{TC07} \cdot q_{TC\_profile} = 2909 \cdot \frac{BTU}{hr \cdot in^3} \qquad q_{TC08} := \gamma_{TC03} \cdot q_{TC\_profile} = 3161 \cdot \frac{BTU}{hr \cdot in^3}$$

$$q_{TC03} := \gamma_{TC08} \cdot q_{TC\_profile} = 2672 \cdot \frac{BTU}{hr \cdot in^3} \qquad q_{TC09} := \gamma_{TC12} \cdot q_{TC\_profile} = 2880 \cdot \frac{BTU}{hr \cdot in^3}$$

$$q_{TC04} := \gamma_{TC11} \cdot q_{TC\_profile} = 3153 \cdot \frac{BTU}{hr \cdot in^3} \qquad q_{TC10} := \gamma_{TC05} \cdot q_{TC\_profile} = 2709 \cdot \frac{BTU}{hr \cdot in^3}$$

$$q_{TC05} := \gamma_{TC10} \cdot q_{TC\_profile} = 3242 \cdot \frac{BTU}{hr \cdot in^3} \qquad q_{TC11} := \gamma_{TC04} \cdot q_{TC\_profile} = 2843 \cdot \frac{BTU}{hr \cdot in^3}$$

$$q_{TC06} := \gamma_{TC01} \cdot q_{TC\_profile} = 3072 \cdot \frac{BTU}{hr \cdot in^3} \qquad q_{TC12} := \gamma_{TC09} \cdot q_{TC\_profile} = 3079 \cdot \frac{BTU}{hr \cdot in^3}$$

Adjust heating profile by splitting into separate profiles below and above core mid-plane.

Normalized heating profile obtained by fitting heating data to a cosine function:

$$P_{norm}(x) := \cos[0.056\cdot(x + 0.9)]$$

Integrate normalized heating profile:

$$I := \int_{-27.5}^{25.5} P_{norm}(x)\, dx\cdot in = 35.6\cdot in$$

$L := 25.5\cdot in - (-27.5\cdot in) = 53\cdot in$ Length of integral of integration

$\gamma := \frac{I}{L} = 0.671$ Ratio of average heating to maximum heating

Split into separate profiles below and above core mid-plane:

$$P_{norm\_below}(x) := \cos[0.053\cdot(x + 0.9)]$$

$$I_{below} := \int_{-27.5}^{0} P_{norm\_below}(x)\, dx\cdot in = 19.5\cdot in$$

$$P_{norm\_above}(x) := \cos[0.059\cdot(x + 0.9)]$$

$$I_{above} := \int_{0}^{25.5} P_{norm\_above}(x)\, dx\cdot in = 16\cdot in$$

Integrate normalized heating profiles to check that total core heating is unchanged:

$$I_{below} + I_{above} = 35.6\cdot in$$

ECAR-3386 As-Run Thermal Analysis of the AGC-3 Experiment Page A53 of A62

Define array of coordinates:

$i := 0..24$

$\zeta_i := -24 + 2 \cdot i$

Define arrays of normalized heating values:

$i := 0..24$ $\quad P := P_{norm}(\zeta)$

$j := 0..12$ $\quad P_{adj_j} := P_{norm\_below}(\zeta_j)$

$k := 13..24$ $\quad P_{adj_k} := P_{norm\_above}(\zeta_k)$

Plot symmetric and unsymmetric heating profiles:

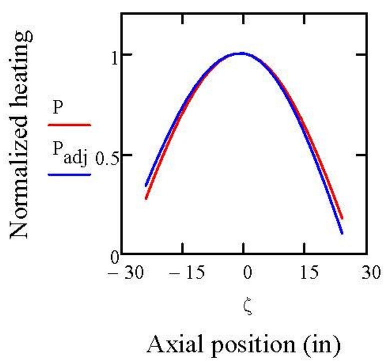

Note: The unsymmetric heating profile (blue trace) was shown to improve temperature calculations in the AGC tests as compared to using the symmetric heating profile (red trace); see ECAR-2562 and ECAR-2322.

Heating rates of other components with uniform heating rather than an axial heating profile:

Tungsten at top of center stack and bottom of lower stacks (ECAR-3051 Table 10):

$q_{W\_bot} := 2.71 \cdot \frac{W}{gm}$ Heating rate of tungsten at the bottom of lower stacks

$x_1 := -23.75$ Axial position of bottom of lower stacks

$\beta_1 := \frac{P_{norm\_below}(x_1)}{P_{norm}(x_1)} = 1.226$ Adjustment to heating profile

$\beta_1 \cdot \rho_W \cdot q_{W\_bot} = 3159 \cdot \frac{BTU}{hr \cdot in^3}$ Adjusted heating rate

$q_{W\_top} := 3.75 \cdot \frac{W}{gm}$ Heating rate of tungsten at the top of center stack

$x_2 := 19.25$ Axial position of top of center stack

$\beta_2 := \frac{P_{norm\_above}(x_2)}{P_{norm}(x_2)} = 0.871$ Adjustment to heating profile

$\beta_2 \cdot \rho_W \cdot q_{W\_top} = 3103 \cdot \frac{BTU}{hr \cdot in^3}$ Adjusted heating rate

ECAR-3386 As-Run Thermal Analysis of the AGC-3 Experiment Page A55 of A62

A.6 Source power, gas flows, and DPA

Graphite DPA as a function of irradiation time:

$$t := \begin{pmatrix} 0 \\ 51.0 \\ 104.4 \\ 159.5 \\ 209.4 \end{pmatrix} \cdot \text{day}$$

Effective full power days accumulated at the start of cycles 152B, 154B, 155A and 155B ("Advanced Test Reactor Power History Through Cycle 155B-1," Interoffice Memorandum DEH-02-14)

$$DPA := \begin{pmatrix} 0 \\ 0.84 \\ 1.76 \\ 2.72 \\ 3.60 \end{pmatrix}$$

Maximum DPA accumulated at the start of each cycle, averaged over the specimen stacks (ECAR-3051 Table 19)

$$i := 0 .. 3$$

$$\beta_i := \frac{DPA_{i+1} - DPA_i}{t_{i+1} - t_i} \qquad \beta = \begin{pmatrix} 0.016 \\ 0.017 \\ 0.017 \\ 0.018 \end{pmatrix} \cdot \text{day}^{-1}$$

DPA accumulated per day in each cycle

$$\text{time} := \frac{t}{\text{day}}$$

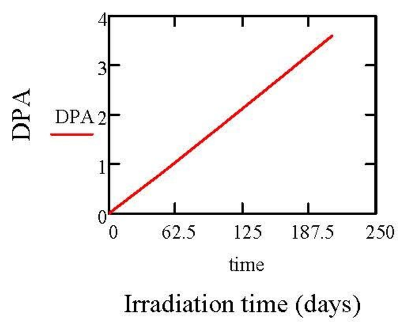

ECAR-3386 As-Run Thermal Analysis of the AGC-3 Experiment Page A56 of A62

DPA at selected days during each cycle is calculated using the DPA rate and EFPD at that day:

$$\mathrm{EFPD} := \begin{pmatrix} 21 \\ 36 \\ 50 \end{pmatrix} \mathrm{day}$$

Effective full power days in cycle 152B at 12/19/2012, 1/03/2013 and 1/17/2013

$$\beta_0 \cdot (\mathrm{EFPD} - t_0) = \begin{pmatrix} 0.35 \\ 0.59 \\ 0.82 \end{pmatrix}$$

DPA

$$\Delta\mathrm{day} := \begin{pmatrix} 18.5 \\ 36.5 \\ 52.5 \end{pmatrix} \cdot \mathrm{day}$$

Effective full power days in cycle 154B at 09/11/2013, 09/29/2013 and 10/15/2013

$$\mathrm{EFPD} := t_1 + \Delta\mathrm{day} = \begin{pmatrix} 69.5 \\ 87.5 \\ 103.5 \end{pmatrix} \cdot \mathrm{day}$$

Total effective full power days

$$\beta_0 \cdot t_1 + \beta_1 \cdot (\mathrm{EFPD} - t_1) = \begin{pmatrix} 1.16 \\ 1.47 \\ 1.74 \end{pmatrix}$$

DPA

$$\Delta\mathrm{day} := \begin{pmatrix} 18 \\ 36 \\ 48 \end{pmatrix} \cdot \mathrm{day}$$

Effective full power days in cycle 155A at 12/11/2013, 12/29/2013 and 01/10/2014

$$\mathrm{EFPD} := t_2 + \Delta\mathrm{day} = \begin{pmatrix} 122.4 \\ 140.4 \\ 152.4 \end{pmatrix} \cdot \mathrm{day}$$

Total effective full power days

$$\beta_0 \cdot t_1 + \beta_1 \cdot (t_2 - t_1) + \beta_2 \cdot (\mathrm{EFPD} - t_2) = \begin{pmatrix} 2.07 \\ 2.39 \\ 2.6 \end{pmatrix}$$

DPA

$$\Delta\mathrm{day} := \begin{pmatrix} 13 \\ 30 \\ 46 \end{pmatrix} \cdot \mathrm{day}$$

Effective full power days in cycle 155B at 02/25/2014, 03/14/2014 and 04/08/2014

$$\mathrm{EFPD} := t_3 + \Delta\mathrm{day} = \begin{pmatrix} 172.5 \\ 189.5 \\ 205.5 \end{pmatrix} \cdot \mathrm{day}$$

Total effective full power days

$$\beta_0 \cdot t_1 + \beta_1 \cdot (t_2 - t_1) + \beta_2 \cdot (t_3 - t_2) + \beta_3 \cdot (\mathrm{EFPD} - t_3) = \begin{pmatrix} 2.95 \\ 3.25 \\ 3.53 \end{pmatrix}$$

DPA

ECAR-3386 As-Run Thermal Analysis of the AGC-3 Experiment Page A57 of A62

East source power and gas flows are obtained from the NDMAS system; spreadsheets containing data recorded at 10 minute intervals are stored in NDMAS (https://htgr.inl.gov); values given here are for selected days during the cycle and are computed by averaging the data over the entire day:

Cycle: 152B, Date: 12/19/2012, Power: 20.25 MW, DPA: 0.35

Temperature control gas: zone 1: 0.501 Ar

Temperature control gas: zone 2: 0.052 Ar

Temperature control gas: zone 3: 0.069 Ar

Temperature control gas: zone 4: 0.201 Ar

Temperature control gas: zone 5: 0.967 Ar

Temperature control gas: zone 6: 0.500 Ar

Cycle: 152B, Date: 1/03/2013, Power: 20.48 MW, DPA: 0.59

Temperature control gas: zone 1: 0.464 Ar

Temperature control gas: zone 2: 0.068 Ar

Temperature control gas: zone 3: 0.065 Ar

Temperature control gas: zone 4: 0.168 Ar

Temperature control gas: zone 5: 0.967 Ar

Temperature control gas: zone 6: 0.500 Ar

Cycle: 152B, Date: 1/17/2013, Power: 20.66 MW, DPA: 0.82

Temperature control gas: zone 1: 0.328 Ar

Temperature control gas: zone 2: 0.131 Ar

Temperature control gas: zone 3: 0.082 Ar

Temperature control gas: zone 4: 0.198 Ar

Temperature control gas: zone 5: 0.981 Ar

Temperature control gas: zone 6: 0.500 Ar

ECAR-3386 As-Run Thermal Analysis of the AGC-3 Experiment Page A58 of A62

Cycle: 154B, Date: 09/11/2013, Power: 21.13 MW, DPA: 1.16

Temperature control gas: zone 1: 0.211 Ar

Temperature control gas: zone 2: 0.212 Ar

Temperature control gas: zone 3: 0.0056 Ar

Temperature control gas: zone 4: 0.212 Ar

Temperature control gas: zone 5: 0.915 Ar

Temperature control gas: zone 6: 0.500 Ar

Cycle: 154B, Date: 09/29/2013, Power: 21.21 MW, DPA: 1.47

Temperature control gas: zone 1: 0.068 Ar

Temperature control gas: zone 2: 0.068 Ar

Temperature control gas: zone 3: 0.0053 Ar

Temperature control gas: zone 4: 0.0012 Ar

Temperature control gas: zone 5: 0.801 Ar

Temperature control gas: zone 6: 0.500 Ar

Cycle: 154B, Date: 10/15/2013, Power: 21.19 MW, DPA: 1.74

Temperature control gas: zone 1: 0.068 Ar

Temperature control gas: zone 2: 0.068 Ar

Temperature control gas: zone 3: 0.0054 Ar

Temperature control gas: zone 4: 0.0014 Ar

Temperature control gas: zone 5: 0.801 Ar

Temperature control gas: zone 6: 0.500 Ar

ECAR-3386 As-Run Thermal Analysis of the AGC-3 Experiment Page A59 of A62

Cycle: 155A, Date: 12/11/2013, Power: 20.61 MW, DPA: 2.07

Temperature control gas: zone 1: 0.168 Ar

Temperature control gas: zone 2: 0.000 Ar

Temperature control gas: zone 3: 0.0051 Ar

Temperature control gas: zone 4: 0.768 Ar

Temperature control gas: zone 5: 1.000 Ar

Temperature control gas: zone 6: 0.500 Ar

Cycle: 155A, Date: 12/29/2013, Power: 20.67 MW, DPA: 2.39

Temperature control gas: zone 1: 0.168 Ar

Temperature control gas: zone 2: 0.000 Ar

Temperature control gas: zone 3: 0.0045 Ar

Temperature control gas: zone 4: 0.775 Ar

Temperature control gas: zone 5: 1.000 Ar

Temperature control gas: zone 6: 0.500 Ar

Cycle: 155A, Date: 01/10/2014, Power: 21.19 MW, DPA: 2.60

Temperature control gas: zone 1: 0.107 Ar

Temperature control gas: zone 2: 0.000 Ar

Temperature control gas: zone 3: 0.0048 Ar

Temperature control gas: zone 4: 0.575 Ar

Temperature control gas: zone 5: 1.000 Ar

Temperature control gas: zone 6: 0.500 Ar

ECAR-3386 As-Run Thermal Analysis of the AGC-3 Experiment Page A60 of A62

Cycle: 155B, Date: 02/25/2014, Power: 21.07 MW, DPA: 2.95

Temperature control gas: zone 1: 0.000 Ar

Temperature control gas: zone 2: 0.016 Ar

Temperature control gas: zone 3: 0.005 Ar

Temperature control gas: zone 4: 0.402 Ar

Temperature control gas: zone 5: 0.999 Ar

Temperature control gas: zone 6: 0.500 Ar

Cycle: 155B, Date: 03/14/2014, Power: 21.32 MW, DPA: 3.25

Temperature control gas: zone 1: 0.000 Ar

Temperature control gas: zone 2: 0.001 Ar

Temperature control gas: zone 3: 0.005 Ar

Temperature control gas: zone 4: 0.069 Ar

Temperature control gas: zone 5: 0.928 Ar

Temperature control gas: zone 6: 0.483 Ar

Cycle: 155B, Date: 04/08/2014, Power: 21.34 MW, DPA: 3.53

Temperature control gas: zone 1: 0.000 Ar

Temperature control gas: zone 2: 0.000 Ar

Temperature control gas: zone 3: 0.005 Ar

Temperature control gas: zone 4: 0.001 Ar

Temperature control gas: zone 5: 0.721 Ar

Temperature control gas: zone 6: 0.466 Ar

Adjustments to gas flows:

The control gas in zone 6 (gas between heat shield and capsule, normally set to 50% argon) is assumed to flow into zone 5 (top of test train) and dilute the argon-rich control gas in zone 5 since there is no seal between these zones. The argon gas flow in zone 5 is assumed to be equal to the average of the argon gas flows in zones 5 and 6.

In some cases, the gases in adjacent zones may mix since the seals between zones are not gas-tight. The gas flow data shows that zone 4 contained a helium-rich mixture during most of the irradiation except for cycle 155A and the early part of cycle 155B when an argon-rich gas mixture was used. Since the reactor power and the temperature of the TCs in zone 4 did not change significantly when an argon-rich mixture was introduced, the argon-rich gas in zone 4 may have been diluted by gas leakage from the helium-rich gas in zone 3. During cycle 155A and the early part of cycle 155B, the argon gas flow in zone 4 is assumed to be equal to the average of the argon gas flows in zones 3 and 4.

Adjust argon gas flows using the assumptions given above:

Cycle: 152B, Date: 12/19/2012

$$Ar_{zone\_5} := \frac{0.967 + 0.500}{2} = 0.734$$

Cycle: 152B, Date: 1/03/2013

$$Ar_{zone\_5} := \frac{0.967 + 0.500}{2} = 0.734$$

Cycle: 152B, Date: 1/17/2013

$$Ar_{zone\_5} := \frac{0.981 + 0.500}{2} = 0.74$$

Cycle: 154B, Date: 09/11/2013

$$Ar_{zone\_5} := \frac{0.915 + 0.500}{2} = 0.708$$

Cycle: 154B, Date: 09/29/2013

$$Ar_{zone\_5} := \frac{0.801 + 0.500}{2} = 0.651$$

Cycle: 154B, Date: 10/15/2013

$$Ar_{zone\_5} := \frac{0.801 + 0.500}{2} = 0.651$$

Title: As-Run Thermal Analysis of the AGC-3 Experiment

ECAR No.: 3386 Rev. No.: 0 Project No.: 23747 Date: 10/11/2016

Cycle: 155A, Date: 12/11/2013

$$Ar_{zone\_4} := \frac{0.0051 + 0.768}{2} = 0.387$$

$$Ar_{zone\_5} := \frac{1.000 + 0.500}{2} = 0.75$$

Cycle: 155A, Date: 12/29/2013

$$Ar_{zone\_4} := \frac{0.0045 + 0.775}{2} = 0.39$$

$$Ar_{zone\_5} := \frac{1.000 + 0.500}{2} = 0.75$$

Cycle: 155A, Date: 01/10/2014

$$Ar_{zone\_4} := \frac{0.0048 + 0.575}{2} = 0.29$$

$$Ar_{zone\_5} := \frac{1.000 + 0.500}{2} = 0.75$$

Cycle: 155B, Date: 02/25/2014

$$Ar_{zone\_4} := \frac{0.005 + 0.402}{2} = 0.204$$

$$Ar_{zone\_5} := \frac{0.999 + 0.500}{2} = 0.75$$

Cycle: 155B, Date: 03/14/2014

$$Ar_{zone\_5} := \frac{0.928 + 0.483}{2} = 0.705$$

Cycle: 155B, Date: 04/08/2014

$$Ar_{zone\_5} := \frac{0.721 + 0.466}{2} = 0.594$$

APPENDIX B

Appendix B – Report file containing results of ABAQUS validation

```
ABQ EXE: abq6142
COMPUTER: service0_ice_inl_gov
OS: Linux
OS TYPE: 3.0.101-0.46-default
t1
=====================================================================
ODB: Test-1
dictTest[Test-1].Keys:  ['Grp1']
          NT11-n325
Max error: 1.20% <----------
    Max1:  37.3320     Min1:  10.5200 Range:  26.8120
Abq Max2:  37.7813 Abq Min2:  10.6362 Range:  27.1451
          NT11-n281
Max error: 1.48% <----------
    Max1:  55.1070     Min1:  13.9970 Range:  41.1100
Abq Max2:  54.7760 Abq Min2:  14.2043 Range:  40.5717
=====================================================================

t2
=====================================================================
ODB: Test-2
dictTest[Test-2].Keys:  ['Grp2', 'Grp1']
          NT15-n61
Max error: 1.34% <----------
    Max1:  37.3320     Min1:  10.5200 Range:  26.8120
Abq Max2:  37.7366 Abq Min2:  10.6609 Range:  27.0756
          NT11-n61
Max error: 1.54% <----------
    Max1:  55.1070     Min1:  13.9970 Range:  41.1100
Abq Max2:  54.7444 Abq Min2:  14.2131 Range:  40.5313
=====================================================================

t3
=====================================================================
ODB: Test-3
dictTest[Test-3].Keys:  ['Grp1']
          NT11-n130
Max error: 1.65% <----------
    Max1:  44.5920     Min1:  12.5210 Range:  32.0710
Abq Max2:  44.7825 Abq Min2:  12.7270 Range:  32.0555
          NT11-n59
Max error: 1.85% <----------
    Max1:  55.3390     Min1:  14.7770 Range:  40.5620
Abq Max2:  55.0396 Abq Min2:  15.0511 Range:  39.9885
=====================================================================

t4
=====================================================================
ODB: Test-4
```

ECAR-3386 As-Run Thermal Analysis of the AGC-3 Experiment Page B2 of B4

```
dictTest[Test-4].Keys:  ['Grp1']
          NT11-n281
Error: 0.00%     <----------
Ans:       13.7600     Abq:       13.7600
          NT11-n303
Error: 0.00%     <----------
Ans:       11.3200     Abq:       11.3200
          NT11-n325
Error: 0.00%     <----------
Ans:        4.0000     Abq:        4.0000
          NT11-n314
Error: 0.00%     <----------
Ans:        8.2700     Abq:        8.2700
          NT11-n292
Error: 0.00%     <----------
Ans:       13.1500     Abq:       13.1500
=====================================================================

t5
=====================================================================
ODB: Test-5
dictTest[Test-5].Keys:  ['Grp3', 'Grp2', 'Grp1', 'Grp5', 'Grp4']
          NT13-n62
Error: 0.00%     <----------
Ans:       11.3200     Abq:       11.3200
          NT12-n62
Error: 0.00%     <----------
Ans:       13.1500     Abq:       13.1500
          NT11-n62
Error: 0.00%     <----------
Ans:       13.7600     Abq:       13.7600
          NT15-n62
Error: 0.00%     <----------
Ans:        4.0000     Abq:        4.0000
          NT14-n62
Error: 0.00%     <----------
Ans:        8.2700     Abq:        8.2700
=====================================================================

t6
=====================================================================
ODB: Test-6
dictTest[Test-6].Keys:  ['Grp1']
          NT11-n533
Max error: 0.39% <----------
    Max1:  80.7640     Min1:  61.8970 Range:  18.8670
Abq Max2:  80.4914 Abq Min2:  61.7364 Range:  18.7551
          NT11-n803
Max error: 0.38% <----------
    Max1:  94.5930     Min1:  71.5310 Range:  23.0620
Abq Max2:  94.3007 Abq Min2:  71.2781 Range:  23.0226
=====================================================================
```

ECAR-3386 As-Run Thermal Analysis of the AGC-3 Experiment Page B3 of B4

```
t7
======================================================================
ODB: Test-7
dictTest[Test-7].Keys:  ['Grp1']
          HFL-e56
Error: 0.19%     <----------
Ans:        -0.1700     Abq:        -0.1697
======================================================================

t8
======================================================================
ODB: Test-8
dictTest[Test-8].Keys:  ['Grp1']
          HFL-e1121
Error: 1.74%     <----------
Ans:         0.1710     Abq:         0.1740
          HFL-e3678
Error: 2.25%     <----------
Ans:        -0.1620     Abq:        -0.1656
======================================================================

t9
======================================================================
ODB: Test-9
dictTest[Test-9].Keys:  ['Grp1']
          NT11-n13
Error: 0.01%     <----------
Ans:        50.0010     Abq:        50.0036
          NT11-n17
Error: 0.00%     <----------
Ans:        55.5500     Abq:        55.5500
          NT11-n328
Error: 0.20%     <----------
Ans:        51.6040     Abq:        51.7074
          NT11-n38
Error: 0.05%     <----------
Ans:        50.0890     Abq:        50.1148
          NT11-n28
Error: 0.11%     <----------
Ans:        50.7010     Abq:        50.7550
          NT11-n218
Error: 0.01%     <----------
Ans:        50.0110     Abq:        50.0176
          NT11-n32
Error: 0.10%     <----------
Ans:        50.3060     Abq:        50.3555
          NT11-n324
Error: 0.20%     <----------
Ans:        52.4260     Abq:        52.5321
          NT11-n4
Error: 0.08%     <----------
```

ECAR-3386 As-Run Thermal Analysis of the AGC-3 Experiment Page B4 of B4

```
Ans:        51.0600     Abq:        51.1006
          NT11-n320
Error: 0.16%      <----------
Ans:        53.6690     Abq:        53.7552
=====================================================================

t10
=====================================================================
ODB: Test-10
dictTest[Test-10].Keys:  ['Grp1']
          NT11-n325
Error: 0.15%      <----------
Ans:       215.7130     Abq:       216.0345
=====================================================================

t11
=====================================================================
ODB: Test-11
dictTest[Test-11].Keys:  ['Grp1']
          HFL-e55
Error: 0.02%      <----------
Ans:        -5.5000     Abq:        -5.4989
=====================================================================

t12
=====================================================================
ODB: Test-12
dictTest[Test-12].Keys:  ['Grp1']
          NT11-n336
Error: 0.00%      <----------
Ans:       406.6667     Abq:       406.6667
=====================================================================
```